DESIGN, DEVELOPMENT AND FABRICATION OF A HIGH REDUNDANCY LINEAR ELECTROMECHANICAL ACTUATOR FOR FAULT TOLERANCE

A thesis submitted in partial fulfillment of the requirements

for the award of the degree of

DOCTOR OF PHILOSOPHY

By

GOLLAPUDI ARUN MANOHAR

(ROLL NO: 715037)

DEPARTMENT OF MECHANICAL ENGINEERING

NATIONAL INSTITUTE OF TECHNOLOGY

WARANGAL (T.S.) - 506 004

JANUARY – 2021

DESIGN, DEVELOPMENT AND FABRICATION OF A HIGH REDUNDANCY LINEAR ELECTROMECHANICAL ACTUATOR FOR FAULT TOLERANCE

A thesis submitted in partial fulfillment of the requirements

for the award of the degree of

DOCTOR OF PHILOSOPHY

By

GOLLAPUDI ARUN MANOHAR

(ROLL NO: 715037)

Under the Guidance of

Dr. V. VASU
(Supervisor)
Department of Mechanical Engineering

Dr. K. SRIKANTH
(Co-Supervisor)
Department of Mechanical Engineering

DEPARTMENT OF MECHANICAL ENGINEERING
NATIONAL INSTITUTE OF TECHNOLOGY
WARANGAL (T.S.) - 506 004

JANUARY - 2021

THESIS APPROVAL FOR Ph.D.

This thesis entitled **"DESIGN, DEVELOPMENT AND FABRICATION OF A HIGH REDUNDANCY LINEAR ELECTROMECHANICAL ACTUATOR FOR FAULT TOLERANCE"** by **Mr. Gollapudi Arun Manohar** is approved for the degree of Doctor of Philosophy.

Examiners

_____

_____

_____

Supervisor(s)

Dr. V. Vasu
(Supervisor)

Associate Professor, Mechanical Engineering Department, NIT Warangal

for **Dr. K. Srikanth**
(Co-Supervisor)

Associate Professor, Mechanical Engineering Department, NIT Warangal

Chairman

Prof. Adepu Kumar

Head, Mechanical Engineering Department, NIT Warangal

DEPARTMENT OF MECHANICAL ENGINEERING
NATIONAL INSTITUTE OF TECHNOLOGY
WARANGAL (T.S)

CERTIFICATE

This is to certify the thesis entitled **"Design, Development and Fabrication of a High Redundancy Linear Electromechanical Actuator for Fault Tolerance"** submitted by **Mr. Gollapudi Arun Manohar** for the award of the degree of **Doctor of Philosophy in Mechanical Engineering**, in the Faculty of Engineering of **National Institute of Technology, Warangal** is a bonafide research work carried out by him under our guidance in the **National Institute of Technology, Warangal, Telangana.**

Place: Warangal.
Date: 13/01/2021

Dr. V. VASU
Associate Professor
(Supervisor)
Department of Mechanical Engineering

for **Dr. K. SRIKANTH**
Associate Professor
(Co-Supervisor)
Department of Mechanical Engineering

Dr. Adepu Kumar
(Professor & Head, MED)
(Chairman, DSC)

DEPARTMENT OF MECHANICAL ENGINEERING
NATIONAL INSTITUTE OF TECHNOLOGY
WARANGAL (T.S.)

DECLARATION

I, hereby declare that the matter embodied in this thesis titled **"Design, Development and Fabrication of a High Redundancy Linear Electromechanical Actuator for Fault Tolerance"** is the result of research carried out by me under the guidance of **Dr. V. Vasu** Department of Mechanical Engineering and **Dr. K. Srikanth**, Department of Mechanical Engineering, National Institute of Technology (Deemed University), Warangal, Telangana. This work or any part of this work has not been submitted to any other University or Institute for the award of any other degree or diploma.

Place: Warangal

Date: 13/01/2021

Gollapudi Arun Manohar
Research Scholar,
Department of Mechanical Engineering,
National Institute of Technology, Warangal,
Telangana.

Dedicated to

My Parents

and

My Wife

ACKNOWLEDGEMENTS

I express my sincere thanks and profound gratitude to my supervisors **Dr. V. Vasu** and **Dr. K. Srikanth,** for their continuous guidance, help, and support during all the stages of the work to bring up the research to this conclusive end of my dissertation.

I extend my sincere gratitude to **Prof. N. V. Ramana Rao,** Director, National Institute of Technology Warangal, India, for providing the necessary facilities and encouragement throughout my work. I am thankful to **Prof. A. Kumar**, Head, Department of Mechanical Engineering, NIT Warangal, and other faculty members for their encouragement and support extended during this period.

It's my great opportunity to express my deepest gratitude to the Doctorial Scrutiny Committee (DSC) members, **Prof. N. Selvaraj**, Professor and **Dr. V. Hari Kumar**, Associate Professor, Department of Mechanical Engineering, and **Prof. L. Anjaneyulu**, Professor, Department of Electronics and Communication Engineering for their adeptness and many discussions during the research period. I express my sincere thanks to **Prof. C. S. P. Rao**, Director, National Institute of Technology Andhra Pradesh, India, for his support at the initial stage of the work.

It's my great opportunity to express my deepest gratitude to Ministry of Electronics & Information Technology (**MeitY**), Government of India, for sponsoring this research work under the Visvesvaraya PhD scheme for Electronics & IT.

I am grateful to my senior researchers Dr. M. Sandeep, Dr. N. Shiva Kumar, Dr. V. Narayana (Nathan), and Dr. G. Suresh for their unconditional support, help, and inspiration during my work. I express my special thanks to my co-scholars Mr. Ch. Satish, Mr. Ch. Naresh, Mr. K. Raja Sekhar, Mr. T. Nikhil, and Mr. M. Upendra for their support, help, and advice during my entire project.

I thank Mrs. M. Dharani, technical staff of Mechatronics Lab, and Mr. M. V. Vijay Kumar, office staff of Mechanical Engineering Department, NIT Warangal for their constant help and encouragement.

I express my sincere gratitude to the God, my parents, family members and my wife for their unceasing sacrifices, endeavors, and encouragement.

Finally, I would also like to acknowledge the help given by all the persons who have directly or indirectly supported the work.

Gollapudi Arun Manohar

RESEARCH PUBLICATIONS

1. Arun Manohar Gollapudi, Vasu Velagapudi, Srikanth Korla, Modeling and simulation of a high-redundancy direct-driven linear electromechanical actuator for fault-tolerance under various fault conditions. Engineering Science and Technology, an International Journal, 2020, volume 23, issue 5 (1171-1181). https://www.sciencedirect.com/science/article/pii/S2215098619319512

2. G. Arun Manohar, V. Vasu and K. Srikanth, Modeling and Simulation of High Redundancy Linear Electromechanical Actuator for Fault Tolerance, Springer, 2019. https://link.springer.com/chapter/10.1007/978-981-13-1903-7_9

3. G Arun Manohara, V Vasu, K Srikanth, Development of a high redundancy actuator with direct driven linear electromechanical actuators for fault-tolerance, Elsevier, Procedia Computer Science, 2018, Volume 133, (932–939). https://www.sciencedirect.com/science/article/pii/S187705091831041X

4. G Arun Manohara, V Vasu, K Srikanth, Modeling and simulation of high redundancy actuator for fault-tolerance, Elsevier, Materials Today: Proceedings, 2018, volume 5, issue 9. (18867-18873) https://www.sciencedirect.com/science/article/pii/S2214785318313579

ABSTRACT

This thesis is concerned with the design, development, and fabrication of the system for a class of fault-tolerant actuators with high levels of redundancy. The high-redundancy actuator (HRA) is a linear displacement actuation system, which consists of a large number of small electromechanical actuation elements arranged in a series and parallel configuration. Each actuation element of the HRA provides only a small contribution to the required force and travel of the actuation system. Since the capability of each actuation element is small, the effect of faults within the individual actuation elements on the overall system is also small, and faults in elements can be intrinsically accommodated. So, in the presence of faults, the HRA will gracefully degrade instead of total failure. The main objective of the present work is focused on the HRA based on compact size direct driven electromechanical actuators. The performance analysis of the HRA is a study under various faults in the simulation environment and the same is validated with the experimental results. Firstly, the work was focused on the selection of a suitable configuration for a particular application, because it has a significant influence on the reliability of HRA. The reliability of the system will vary even with the same number of elements in the same two-dimensional arrangement. So, the reliability of different configurations was studied based on the fault probabilities method with limited actuation elements (like 2×2 series-in-parallel, 2×2 parallel-in-series, 3×3 series-in-parallel, 3×3 parallel-in-series). It was observed that the travel capability of a series-in-parallel structure is superior to a parallel-in-series configuration for low fault probabilities. Based on the reliability results, the mathematical and the 3D model of a Direct Driven Electromechanical Actuator (DDEMA) and a HRA with 3×3 Series-in-Parallel configuration was developed and simulated with the aid of MATLAB software. The performance of the HRA with nine actuators was analyzed under different fault conditions in the simulation environment and the results showed, up to three faults the HRA can provide nearly 100% inherent fault-tolerance. Hence, the sudden failure of the system in the presence of fault was avoided. However, the capability of the actuator was found to be reduced gradually depending upon the number of faults introduced in the HRA system. Based on the simulation model, the HRA with nine

actuation elements in the 3×3 Series-in-Parallel configuration was developed to validate the simulation results. The experimental setup was made by assembling the individual EMAs, the custom-made aluminum blocks, and the steel rods with linear bearings. An LVDT connected to the LABVIEW module (NI USB-6008) was used to measure the linear displacement of the HRA and an Arduino Mega 2560 was used to measure the linear displacement of the individual actuators form the encoders. From the results, it was found that the 3×3 HRA can achieve the desired capability of up to three actuator's failure. Hence, there is no sudden failure of the system under any type of actuation faults. All the results have been validated with the simulation results and it was found to be nearly the same.

CONTENTS

LIST OF TABLES

LIST OF FIGURES

ABBREVIATIONS

Abbreviation	Description
EMA	Electromechanical Actuator
DDEMA	Direct Driven Electromechanical Actuator
FT	Fault Tolerance
ACE	Actuator Control Electronics
ECU	Electronic Control Unit
CPU	Central Processing Unit
HRA	High Redundancy Actuator
SP	Series-in-Parallel
PS	Parallel-in-Series
LVDT	Linear Variable Differential Transformer/Transistor
emf	Electromotive force
FSC	Flight control system
FDI	Fault detection and identification/isolation
SISO	Single input single output
MIMO	Multiple input multiple output
P	Proportional
PI	Proportional-integral
PID	Proportional-integral-derivative
DC	Direct current

CHAPTER - 1

INTRODUCTION

Sensors and actuators are the necessary elements in any of the modern engineering systems. Sensors perform a broad range of functions which include, measuring force, motion, acceleration, temperature, and several other characteristics of the physical systems in real-time. In contrast, the actuator converts one form of energy like hydraulic, pneumatic, electrical, or chemical energy into mechanical movement. In most applications, the signal from the sensors will be sent to the system and cause the actuators to execute the preferred action. For example, to perform a spot welding task on a vehicle in an automobile assembly plant, a sensor will be responsible for giving the input signal to the controller. The controller energies the actuator to cause a robotic arm to move [1]. The presence of any malfunction in the sensor or actuator will lead to imperfect welding or even failure of the welding process. Faulty elements in any engineering system can be a huge hassle. Sometimes, they might cause irrevocable damage to the industries. Particularly, a fault in the safety-critical system can lead to disasters of unimaginable magnitude. So, designing modern engineering systems with a high level of reliability is of utmost importance to avoid any unexpected failures [2].

One important way to achieve reliability is by having a fault-tolerance design that can tolerate any malfunctions of the individual components of the system. In general, fault-tolerance can be achieved by adopting a redundancy technique which includes the addition of resources, time, or information beyond the normal requirements of the system being operated. In recent years, fault-tolerance has become one of the greatest tools for providing safety to any mechatronic system. The aircraft actuation, railway track switching [3], and nuclear power systems are some of the most important systems that need redundancy to ensure reliability [4].

More recently, the aerospace field significantly increased the use of multi redundant-actuation systems to avoid unexpected failures [5]. Modern aircraft adopted quadruplex flight control computers and quadruplex redundant actuators as primary flight

controls to make the fly-by-wire systems highly reliable [6]. In the occurrence of a fault, it is still feasible to make the aircraft fly safely even if a single computer is active.

Railway track switches are safety-critical resources, which provide flexibility to railway networks but they exhibit single points of failure. Failure of switch within a high traffic passenger rail system causes an inconsistent level of delay. Subsystem redundancy is one of the approaches, which can be used to confirm a suitable safety integrity or/and operational reliability level. By successful adoption of redundancy, a significant enhancement in the availability and reliability of the switches can be achieved [3].

In the nuclear power plant, one of the important parts of it was the control rods [7]. The reaction inside the nuclear reactor is controlled by the control rods which are inserted and removed into and from the reactor. The control system which is responsible for the insertion and removal of the control rods is called the control rods control system (CRCS). It is essential to maintain the high reliability of the CRCS because its malfunction can cause a sudden shutdown of the power plant. Therefore, a duplex hardware redundancy of CRCS is implemented to ensure the high reliability of the nuclear power system. Since actuators and sensors are vital to the control system, it is essential to preserve the actuators and sensors at the requisite reliability to ensure the system can attain the essential performance.

1.1 Linear Actuators

A linear actuator is a device that produces movement in a straight line. In general, linear actuators are of three types: Hydraulic, Pneumatic, and Electromechanical actuators. For moving very heavy loads, hydraulic actuators are primarily used and for extremely fast applications, pneumatic actuators are good. Electromechanical actuators provide the strength of hydraulic actuators with more precise movement and motion control.

1.1.1 Hydraulic actuators: A hydraulic actuator consists of a hollow cylindrical tube with a sliding piston inside and a fluid pump that uses hydraulic power to enable mechanical action. As the fluids are almost impossible to compress, a hydraulic actuator can employ significant force. In general hydraulic cylinders are of two types, single acting, and double-acting cylinders. In the case of a single-acting cylinder, the fluid pressure is applied to only one side of the piston then the piston can move in the only forward direction and the reverse

stroke is possible with the help of a spring. In the case of a double-acting cylinder, the fluid pressure is applied to both sides of the piston then the piston can move in forward and backward directions depending on the difference in pressure between the two sides. However, the major disadvantage of hydraulic systems is the requirement to have a power pack, contamination of oil, the noise made by the hydraulic systems, and low maximum torque to power ratios [8].

1.1.2 Pneumatic actuators: A pneumatic actuator is a device that converts compressed air energy into mechanical movement. In the industries, these pneumatic actuators are also known as air actuators, pneumatic cylinders, and air cylinders. A pneumatic actuator consists of a cylinder, piston, and valves. These actuators can convert the energy into linear as well as rotary motion. Linear pneumatic actuators have extensive use as the drive element for a limited function like pick and place motion of the robots, end stops in mechanical systems [8, 9], and more broadly utilized as actuation in special-purpose machinery.

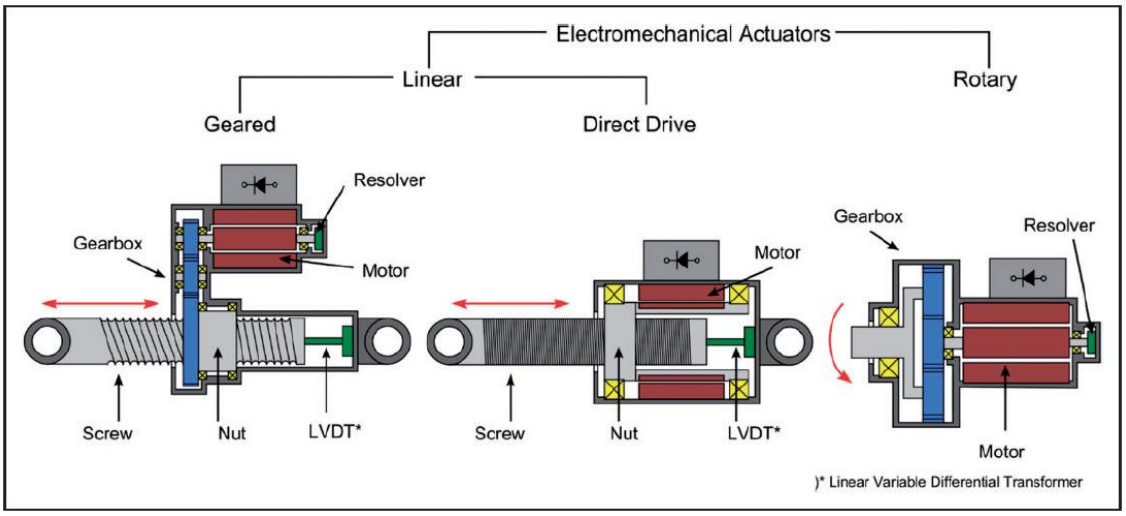

Figure 1.1 Classification of different EMA types [10].

1.1.3 Electrical actuators: The most common form of an electrical drive is an electric motor which is used for machine tools and robotic applications. Even though solenoids and linear motors have been investigated and proved as possible means for generating controlled linear motion [10]. Enhancements in the design of the motors have enabled the power to weight ratio of electric motors. In recent years, the efficiency and reliability of

the actuation system have also increased significantly. The easiness of the motion control systems compared to pneumatics and hydraulic drives is an additional key influential factor in the increasing usage of electric drives for machine applications [10]. The significant enhancements in the permanent magnetic DC servo-motors have become the most commonly used rotary electric drives. These electric drives offer better low-speed torque capability and higher power to weight ratios than the stepper and other traditional AC motors [11].

In general, the electric drives produce rotary motion but the linear motion using electric drives is attained by using rotary to linear transmission systems like lead-screws, rack, and pinion, etc. The linear actuators are further classified into geared and direct-driven linear EMAs as shown in figure 1.1. In general, the geared linear electromechanical actuator consists of a DC motor with a lead-screw or ball-screw or roller-screw and a nut assembly [10]. The linear motion of the actuator screw is measured by a linear variable differential transducer (LVDT) which is attached between the movable and the fixed ends. The distribution of required power and receiving the feedback signals from the actuator is done by an Electronic Control Unit (ECU). The architecture of a gear-driven Electromechanical Actuator (EMA) is as shown in the figure below.

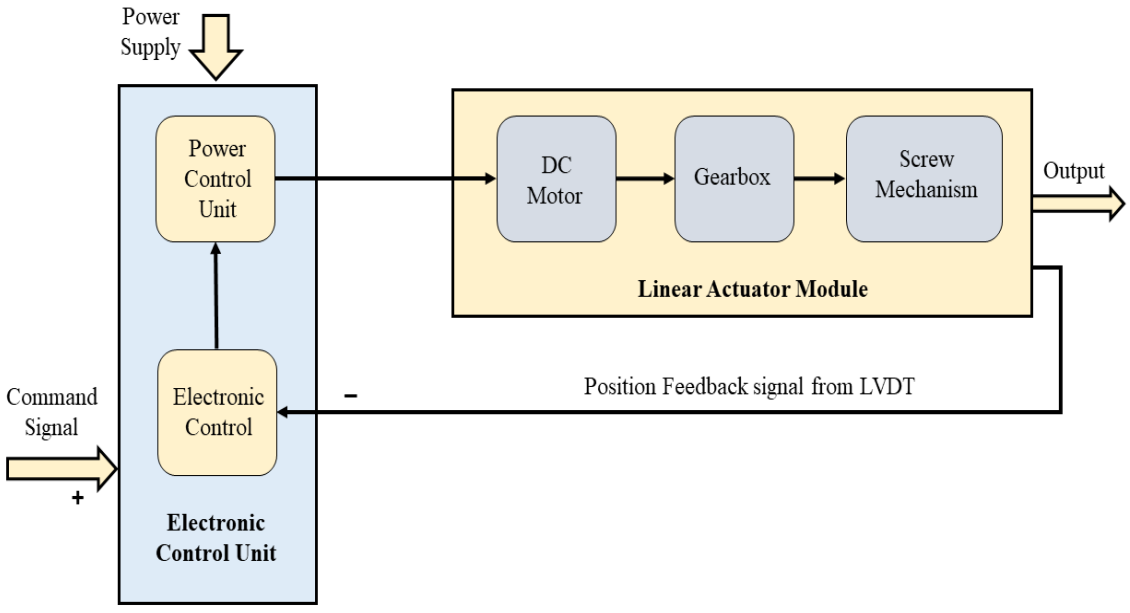

Figure 1.2 The architecture of a gear-driven EMA

Traditionally, the redundancy of both sensors and actuators can be attained by connecting two or more of these devices in parallel. For sensor redundancy, the output is combined through voting as shown in figure 1.3, whereas, for actuator redundancy, the output is the mechanical consolidation as shown in figure 1.4. This method works fine for sensors, however, for actuators, this strategy does not apply because sensors deal with information whereas actuators deal with the energy conversion.

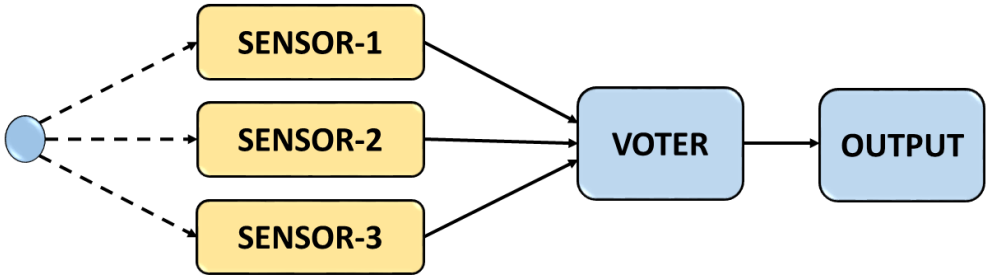

Figure 1.3 Traditional redundancy of sensors

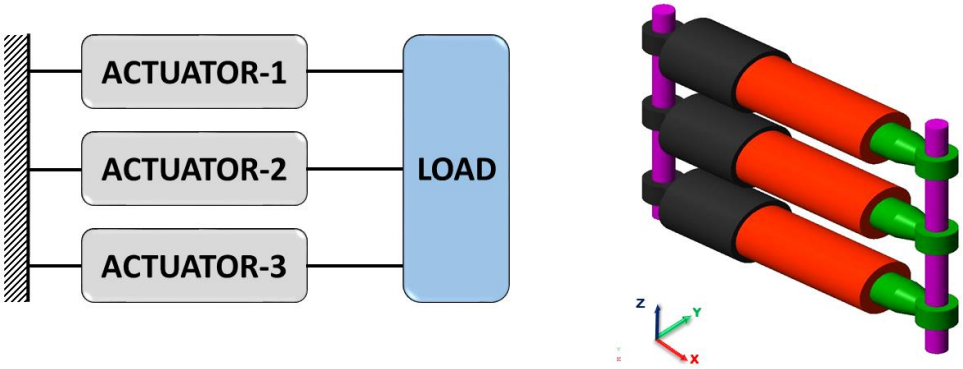

(a) (b)

Figure 1.4. Traditional redundancy of the actuators, (a) Block diagram (b) 3D model

The task to be completed by this group of actuators in parallel is carried out by any one of the individual actuators from the same group. The fact that each of these actuators can perform the required task alone enables them to override any faulty actuators [12]. However, these actuators in parallel increase the size, weight, and cost of the system and eventually, reduces the efficiency of the system. Moreover, the use of pure parallel configuration holds no value in the event of jamming/lock-up of an actuator within it. Considering these problems associated with the traditional pure parallel redundancy, the

concept of a high redundancy actuator (HRA) with a grid (both in series and in parallel) configuration was put forward to achieve inherent fault-tolerance.

1.2 High Redundancy Actuator

The basic idea behind HRA (based on Electromagnetic or Electromechanical) comes from the behavior of human musculature [13]. The musculature has many individual cells that work in a very typical and ingenious way and the motion provided by each muscle cell contributes very minutely to the entire travel and force of the overall muscle system. This is what makes the muscular system highly robust in spite of occasional damage to the individual cells. By implementing the same concept, the HRA has been designed with many small individual actuation elements that are connected in both series and parallel configuration to form a single actuation system [14]. The displacement and force provided by each actuation element in the HRA are very small compared to the overall output of the actuation system. The schematic diagram of a HRA with 30 actuation elements is shown in figure 1.5. Here, each one of the rectangular blocks represents a linear actuation element. X_1 to X_5 are the displacements of the individual actuators, and X_L is the overall displacement of the load due to HRA. The base of the actuators that are connected to the fixed support remains immovable while the bases of the other actuators are moveable. This HRA is having 5 actuation elements in each row and 6 actuation elements in column-wise so it is denoted as a 6×5 High Redundancy Actuation system.

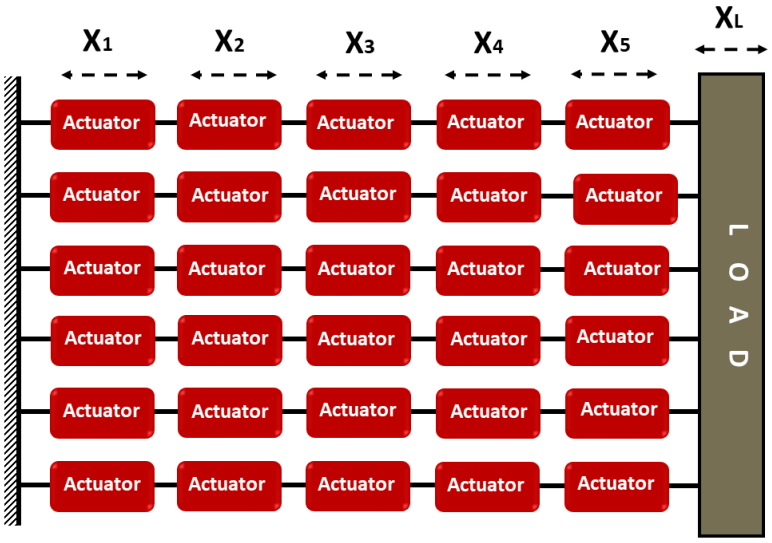

Figure 1.5 Schematic diagram of a HRA

The HRA reduces the complications experienced by traditional redundancy structures, as the degree of over-engineering is reduced. For example, a HRA may employ 100 actuation elements, but the specified action may require only 80 actuation elements. Thus, the HRA, in this case, is only 20% over-engineered, whereas in the triplex and quadruplex cases it is 200% and 300% over-engineered respectively. By the attachment of actuation elements in serial, the problems of the lock-up fault of the actuators are resolved as the HRAs are inherently tolerated [15]. One additional benefit is that instead of large changes of capability only the reduction in actuation of the HRA will occur. It can be observed the system may change from fully operational to total failure within a short period in the case of parallel redundancy systems. The capability of the high redundancy actuator will decrease gradually instead of sudden failure. Hence, in this particular area of research, the primarily focused was to compensate for the actuator faults in the subsystem level and to avoid complete failure due to lock-up or loose fault and make the system to complete the task with reduced capability.

1.3 High Redundancy Actuator Configurations

The arrangement of actuation elements can be done in many ways to form a HRA. The effectiveness of the fault tolerance to particular faults depends on how the actuation elements in the HRA are configured. The common faults that an EMA may undergo are: electrical faults like short circuit and open circuit faults and mechanical faults like lock-up are loose faults [16, 17]. The actuation elements of a HRA in four different configurations are shown in figure 1.6.

These four configurations of the HRA under both electrical and mechanical faults are presented within this thesis. The pure parallel configuration is intolerant to lock-up faults but it can tolerate loose faults, on the other hand, the pure series configuration can tolerate lock-up faults but it is intolerant to the loose fault. Hence, the arrangements of parallel and serial actuation elements will provide tolerance to both loose fault and lock-up fault. When these faults are considered, the two major configuration types emerged are series elements connected in parallel (series-in-parallel) and parallel elements connected in series (parallel-in-series). These configurations provide superior tolerance to lock-up faults and a degree of tolerance to loose faults. The Parallel-in-series configurations provide greater tolerance to loose faults and a degree of tolerance to lock-up faults. The

choice of configuration, and the number of elements therein, will be dictated by the likelihood of each fault mode in the actuator technology and the requirements of the application, hence, no definitive configuration can be made. The details of the configurations and configurations under faults were addressed in chapter-3.

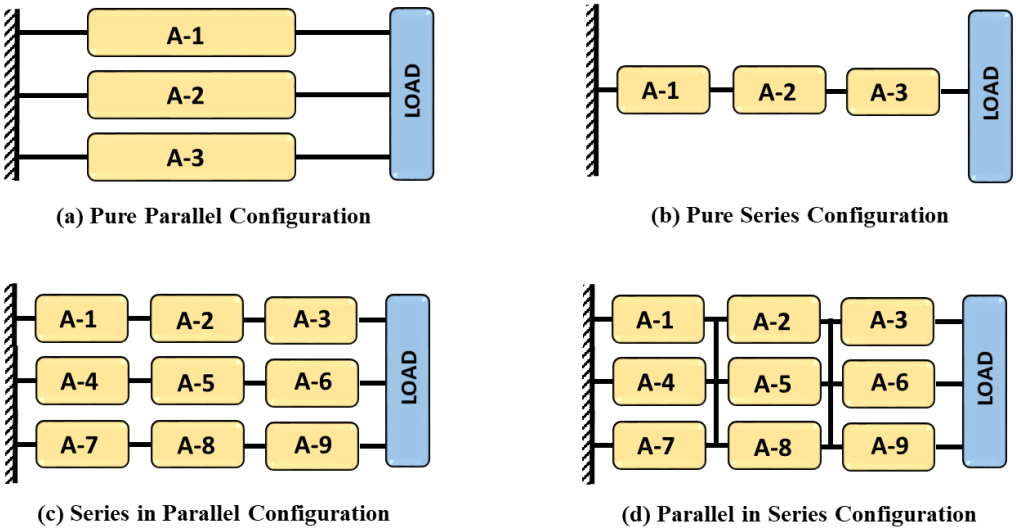

Figure 1.6 Different configurations of the HRA

1.4 Research Aim and Objectives

The main aim of this research work is to exhibit the concept of a High Redundancy Actuation system with 9-element actuation based on direct driven electromechanical actuators (DDEMAs). The specific objectives of this research work are:

- To analyze the reliability of series-in-parallel and parallel-in-series configurations of the high redundancy actuation system.
- To design and develop the mathematical and 3D model of a single EMA and a HRA having nine actuation elements.
- To analyze the performance of the designed 3×3 HRA under specified fault conditions in the simulation environment.
- To design and develop a lab-scale experimental setup to validate the simulation results.

1.5 Thesis Overview

The entire thesis is presented in six chapters.

- **Chapter 1:** A brief introduction of actuators and various types of linear actuators are given, and the concept of the high redundancy actuation system based on electromechanical actuators has been introduced. Research objectives and thesis overview are explained in this chapter.
- **Chapter 2:** The literature survey related to high redundancy actuation system, electromechanical actuator faults, and fault tolerance concepts are summarized and gap analysis, and overall research work plan are provided.
- **Chapter 3:** The reliability analysis of series-in-parallel and parallel-in-series configurations of the high redundancy actuation system was derived and based on the results the high redundancy actuation configuration was selected for further analysis.
- **Chapter 4:** Based on the reliability results obtained from the previous chapter, a 3×3 series-in-parallel high redundancy actuator mathematical and 3D model was designed. The results of the model were analyzed under both healthy and faulty conditions.
- **Chapter 5:** This chapter gives the fabrication of a single electromechanical actuator and a 3×3 high redundancy actuator. The experimental setup with all the individual electrical and mechanical elements is explained in detail and the results obtained were validated with the simulation results.
- **Chapter 6:** This thesis ends with the scope for future work and conclusions drawn from the reliability analysis of configurations of high redundancy actuator, simulation, and experimental results.

CHAPTER - 2

LITERATURE REVIEW

2.1 Introduction

This chapter describes the main concepts of the work presented in this thesis like a fault, failure and graceful degradation, EMA faults, actuator redundancy, fault-tolerance, HRA, configurations of HRA, and controller design. So, the literature review begins with an overview of the extensive research publications associated with those areas. Different failure modes in electromechanical actuators are discussed in this section. These failure modes have been established as the most common types of failures in systems performance and include a wide extension of the common types of failure in electromechanical actuators. However, the main concern of actuator failure is mechanical jamming.

As already discussed in the previous chapter, the electromechanical actuators (EMAs) are a combination of an electrical (electric motor) and a mechanical system (mechanical gear-box). For linear EMAs, the rotational motion of the motor is converted into linear motion with the aid of a mechanical assembly, such as a lead screw or ball screw, or roller screw [18]. The jamming of the actuator may occur due to the failure of these mechanical components. The details regarding the failures are discussed in this chapter and the working of the EMAs are described in chapter-4.

This chapter ends with a discussion on the previous work related to the High Redundancy Actuator, the research gaps, and the flow chart of the work plan.

2.2 Fault, Failure, and Graceful Degradation

Any fault in the system will deviate that system from its normal performance or behavior. Fault can be expressed as the occurrence of an unpredictable defect in the software or hardware of the system. On the other hand, failure is expressed as a permanent interruption to the ability of the system to carry out a required function. According to [19], the term fault is used to represent a malfunction of the system rather than a disaster, while

the term failure is used to represent a complete breakdown. The concept of fault, graceful degradation, and failure can be represented by a simple diagram as shown in figure 2.1.

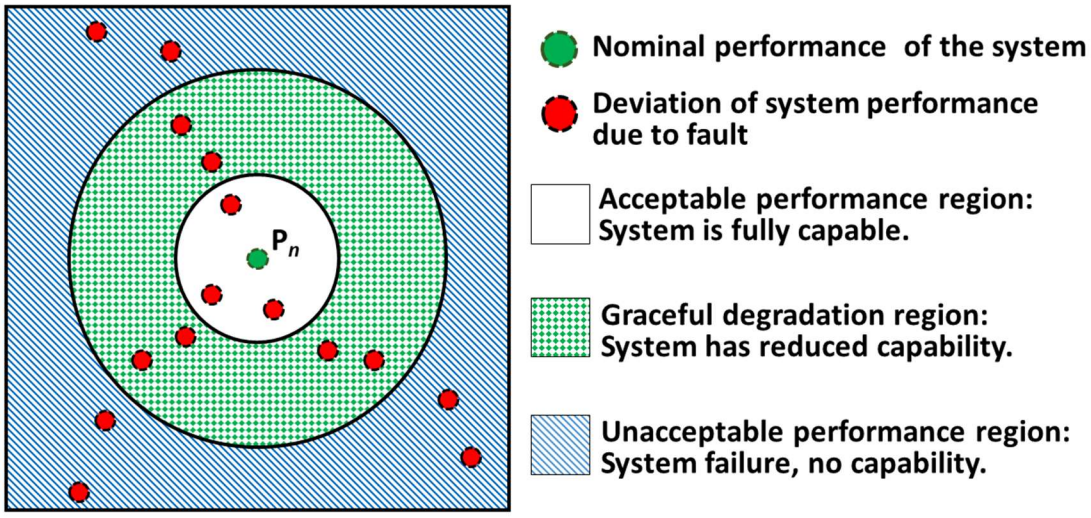

Figure 2.1. Concept of fault, failure, and graceful degradation

The performance value of the system that is operational can lie within the acceptable or graceful degradation or unacceptable regions and this is determined by the degree of fault. The innermost point (P_n, shown in green) represents a system without any faults, showing nominal performance. As evident from the diagram when the degree of fault is minimum, the deviation of the system will also be minimum and the performance of the system will remain in the acceptable region (represented in white). Under these circumstances, the system withstands these faults and achieves complete fault tolerance. A system that attains complete fault-tolerance will fall under the acceptable region. If the system is able to perform without a complete breakdown in spite of an increased degree of faults, then the system is said to be within the graceful degradation region. So, the system that attains the partial fault-tolerance will lie within the graceful degradation region. When the performance values of the system deviate beyond the graceful degradation value then the system will collapse and is considered to be in the unacceptable region.

2.3 Actuator Faults

A fault in an actuation system is defined as “a defect that occurs in the hardware or software of a system, which may be located in the controller, power supply, actuators or

sensors of the system, or indeed in the plant itself. Faults often result in unexpected or undesirable behavior changes of the system, and where faults result in the system being unable to complete an expected action, the system is said to have failed" [20].

2.3.1 Classification of Faults

In general, faults are classified based on several criteria, such as physical locations in the system, time characteristics of the faults, and the effect of faults on the performance of the system [21]. According to their physical locations the faults are classified into, plant/process faults actuator faults, and sensor faults shown in Figure 2.2.

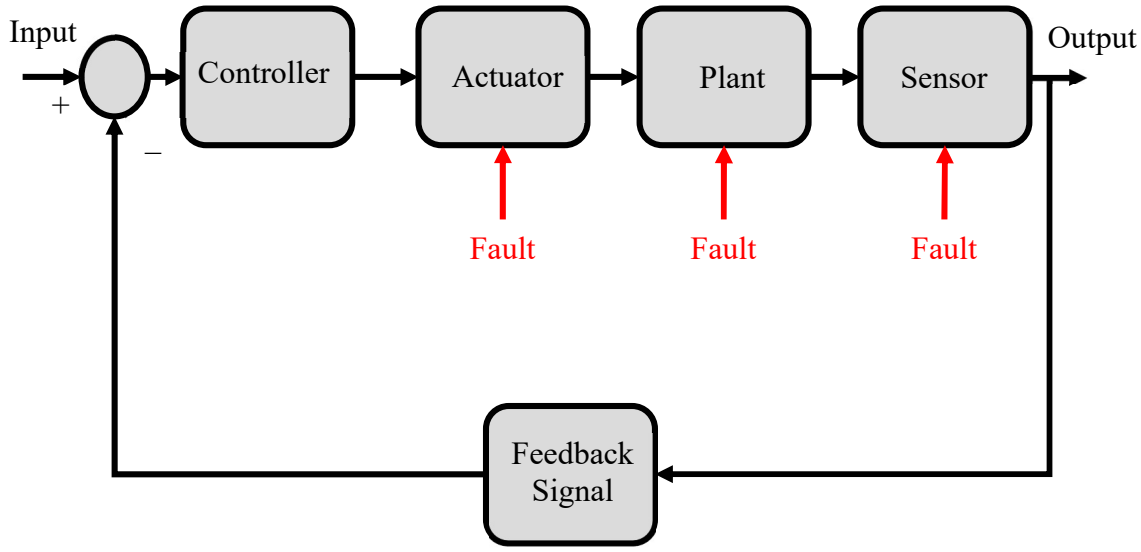

Figure 2.2: Types of faults based on their physical locations.

2.3.1.1. Plant/Process Faults

The physical parameters of the system are directly affected due to this type of fault and as a result dynamics of the input/output properties of the system will change [21]. An extensive variety of faults will occur due to the wear and tear, environmental conduction and aging of the components, etc. So, plant/process faults are also recognized as component faults [22].

2.3.1.2 Sensor Faults

Sensors are devices that detect and react to the signals from any physical system or environment. Some of the main functions of these instruments are to take measurements or

readings from a system such as potentiometers, current sensors, load cells, etc. Sensor faults will lead to incorrect measurements or readings from the real dynamic systems [22]. The sensing devices, transducers, signal processors, or data acquisition equipment are some of the sensor network components where the sensor faults are likely to occur [23]. There may be a number of reasons for these sensor faults like power failure, joint or connection failure, physical damage, and miscalibration [24]. Nowadays the fault-tolerant control research has mainly focused on sensor faults. The sensors that deal with information and measurements are the main reasons for the advancement of fault tolerance in this particular area.

2.3.1.3. Actuator Faults

The faults that occurred in the actuator can cause a partial degradation of the actuator or complete loss of control. The partial degradation of the actuator is due to partial actuator faults and loss of control of the actuator is due to the complete actuator faults of the system [25].

If an actuator is subjected to partial actuator fault then the response of the actuator becomes slow or less effective and provides a part of the normal actuation signal, On the other hand, the actuator produces no signal if it is subjected to complete actuation faults [22]. Partial or complete actuator faults can take place in the actuation system due to the equipment aging or malfunction or wear and tear leading to degradation in the performance. The main focus of the studies presented in this thesis is the actuator faults related to EMA. It is composed of both mechanical and electrical subsystems which makes an interesting research problem. However, the current research was interested in two major fault modes which are described in figure 2.3.

The movement of the actuation element subjected to the lock-up fault will become zero and it will act as a rigid element between the two supports [26, 27]. In general, it is known as jamming of the actuator. “This might occur due to excessive wear of the ball screw that creates mechanical interference within the mechanism and thus causes the actuator to jam in place” [28]. Under this fault, the actuation element will become very rigid and results in the loss of travel capability. Loose faults in the actuation element will

lead to zero applied force. This is due to the loss of proper connection between the mechanical elements of the actuation system.

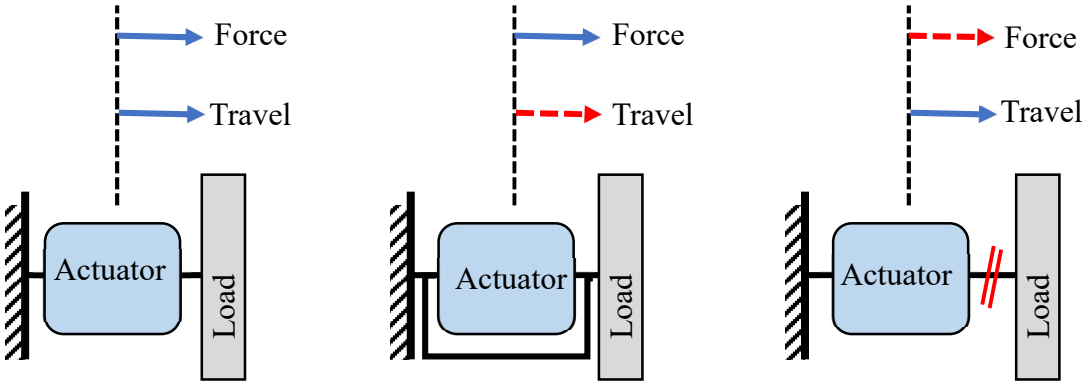

(a) Normal (b) Lock-up fault (c) Loose fault

Figure 2.3: Normal, Lock-up, and loose faults of an actuator.

The fault tolerance strategy that has been generally applied to sensor fault tolerance is not applicable for actuator faults. This is because the sensors deal with the transfer of information whereas the actuators deal with the transfer of energy. So, in the presence of faults in the actuator, redundancy is essential to achieve fault tolerance. To keep the actuation system in control and transport it to the desired position actuator force is always required [29]. Nothing can avoid this requirement.

Some of the major fault modes with information regarding possible reasons, effects, and the variables to detect the faults of an electromechanical actuator are provided in table 2.1.

Table 2.1. Fault modes, reasons, effects, and the variables to detect the faults of an electromechanical actuator

Component	Failure Mode	% Failure Mode	Possible reason	Effect on the system	Effect on EMA	Variables to detect Faults
Electric motor	Winding shorted or open	35%	Overheating, over current, Insulation degradation.	Inability to provide torque. Loss of EMA. Passive Mode Fail safe activation.	The motor does not respond to the command.	Measure current, temperature, intermittent current due to insulation deterioration or wire cut.
	Rotor blocked	25%	Lack of lubrication, Excessive friction, overstressed.	Inability to provide torque.	Actuator blocked in its position.	Torque measure, current consumption.
	Maximum current		rotor blocked, jamming on ball screw	Rotor motor blocked.	Actuator blocked in its position.	Measure current, temperature.
Ball screw	Jamming	30%	Lack of lubrication, Excessive friction, overstress	EMA seized. Passive Mode Antijamming activation	Actuator blocked in its position	Torque, current consumption
Bearings	Seized	50%	Lack of lubrication, Excessive friction, overstress	Rotor motor blocked. Inability to provide torque.		Actuator blocked in its position
LVDT	Windings open or shorted	50%	Thermal stress /Vibration	Loss of EMA ball screw position. Loss of LVDT position indication.	Erroneous signal and isolation of LVDT bobbin failed	

2.4 Fault Tolerance

This is the characteristic of a system that allows it to continue operations if one or more of its components experience a fault [30]. The main aim is to avoid system failure by preventing component faults [31]. The decrease in the performance of the system is proportional to the severity of the fault. If the severity of the fault increases the chances of a sudden breakdown of the system will be more. So, in all the safety-critical applications, like nuclear reactors, aircraft, heavy passenger trains, and chemical plants the fault tolerance has become a highly desirable feature. The fault tolerance capability can be achieved by providing the system with extra resources (redundant), which include software redundancy, hardware redundancy, information redundancy, and time redundancy [32, 33].

This thesis emphasis on hardware redundancy which was achieved by integrating extra hardware elements into the system to override the effects of failed components [34]. To increase the force and travel capability of the actuation system, the HRA is integrated with extra actuation elements above the capability of an individual element. The faults of one or more individual actuation elements in the HRA will make the system performance to degrade but not an entire failure. So, this HRA can provide inherent fault tolerance and avoid the sudden failure of the system [35].

2.5 Overview of Redundancy

The word redundancy in general practice is frequently related to a negative inference of something unnecessary or over-abundance, or in some cases, it might be treated as meaningless and useless. However, redundancy can be an influential tool to overpower system errors [36]. For example, “introducing a simple repetition (redundancy) in a conversation might reduce the possibility of misunderstanding (error). In engineering, the term redundancy refers to the duplication or replication of critical components of a system (usually a safety-critical system) with the intention to increase the reliability of the system” [37]. Redundancy is very much associated with the safety and integrity of the modern engineering systems. The principle of redundancy is simple: “an element is redundant if another element exists (a backup) to do the required task if the first fails. By extension, a redundant system is a system that contains redundant elements” [38]. Therefore, a system is said to be a redundant system, if it could be integrated with several

elements that work simultaneously but also capable of performing the task individually if required (such as the engine of civil aircraft) [39]. This can also be referred to as a system with elements that are in idle condition until the system needs them, similar to the backup power supply in a computer [40]. For achieving a high-reliability system, redundancy has become essential for over decades. Especially the civil aircraft designs are heavily dependent on redundancy for their safety. Redundancy can be applied to the sensor, actuator, control computer, and any other components in a system. Parallel redundancy is also known as direct redundancy which denotes multiple independent elements that operate in parallel to form a system [42]. This has been extensively used in the aircraft industry but due to some limitations researchers and engineers are looking for an alternative to the conventional parallel redundancy especially for actuators and this generated a concept called high redundancy actuators.

2.4.1 Parallel Actuation Redundancy

Actuators are the most significant components in many of the mechatronics systems, especially in aircraft, nuclear power plants, and railways where the failure of the system may cause disasters. So, for safety-critical systems, fault tolerance is very essential. In general, fault tolerance actuation in safety-critical systems is achieved through parallel redundancy. In this arrangement, the actuation elements are connected in the triplex or quadruplex configuration. If a fault occurred in any of the actuation elements then the remaining healthy elements will be capable of achieving the requirement to avoid the failure of the system. The redundancy in common increases the reliability of the system but the cost of initial procurement, [43] weight, [44], and maintenance cost are some of the disadvantages in certain applications. For example, weight and volume are strict constraints in aerospace applications [45]. If any one of the actuation element of a parallel redundancy system affected by the lock-up fault will make the whole system fail [44, 35]. This is because the travel of the actuation system will become zero but the actuation elements that are in healthy condition will be applying the force continuously.

2.4.2 High Redundancy Actuator

To overcome the issues encountered by the traditional parallel redundancy, the concept of HRA is introduced for fault tolerance. The concept of HRA for fault tolerance

was inspired by human musculature [46, 47]. The resemblances between human muscles and an actuator in the sense that both converts energy into motion. Human muscles convert energy from food consumed into complex motion such as running and walking while EMA converts electrical energy into mechanical motion. Human musculature works ingeniously because each muscle cell provides the only minute contribution to the travel and force of the overall muscle system [48]. By adopting the same principle, the HRA was developed.

Currently, research on designing HRAs is focused on the use of a small number of electromechanical actuators (EMAs). Previously, a mathematical model for a HRA with 4 electromechanical actuation elements connected in 2 × 2 series-in-parallel configurations under closed-loop conditions was investigated [49] Results showed that this HRA could tolerate the faults and in spite of some performance degradation, it was able to complete the required task [50] Another design that was investigated had 16 electromagnetic actuation elements connected in 4 × 4 series-in-parallel configurations under an active fault-tolerance controller and a condition monitoring system that indicates the critical capability level [51, 52] Numerical and experimental work with 12 electromechanical actuation elements connected in 3 × 4 series-in-parallel configurations was also investigated under both open and closed-loop conditions [18] The present research work aims at developing a 3 × 3 (series and parallel configuration) HRA with 9 direct-driven linear EMAs tested under both healthy and faulty conditions in the simulation environment using MATLAB/Simulink/simscape multibody software tool-box. The main faults considered during the simulation are open and short circuit faults of the motor and jamming and loose faults of the lead-screw.

2.4.3 HRA as Ailerons Actuation System

Ailerons are one of the control surfaces of the aircraft which are used to roll or tilt the aircraft from one side to another during the flight. Figure 2.4 describes the operation of an aileron. The two ailerons of the aircraft will work in the opposite direction to each other. When the right aileron is moving in the upward direction then the left aileron is moving in the downwards direction and vice versa [53]. In general, to avoid the failure of the actuation system of the aileron two or three identical actuators are provided to have redundancy. Apart from the weight of the aircraft, the complexity of the system will be increased by

this approach. To overcome this, the traditional triple redundancy actuation system can be replaced by a HRA system. When the EMA rod applies the force on the flight control surface (Aileron) then the aileron will make an angular displacement along the axis of the Hing joint. If the HRA is used as the actuation source for the aileron actuation then the HRA rod is to be connected to the aileron. The HRA translation rod will be making the control surface (Aileron) to rotate like a lever arm effect. When the EMA rod applies the force on the flight control surface (Aileron) then the aileron will make an angular displacement along the axis of the Hing joint. If the HRA is used as the actuation source for the aileron actuation then the HRA rod is to be connected to the aileron. So, if there is any reduction in the performance of the HRA due to faults in the individual actuators then eventually and the performance of the aileron will be affected.

So, if there is any reduction in the performance of the HRA due to faults in the individual actuators then eventually and the performance of the aileron will be affected.

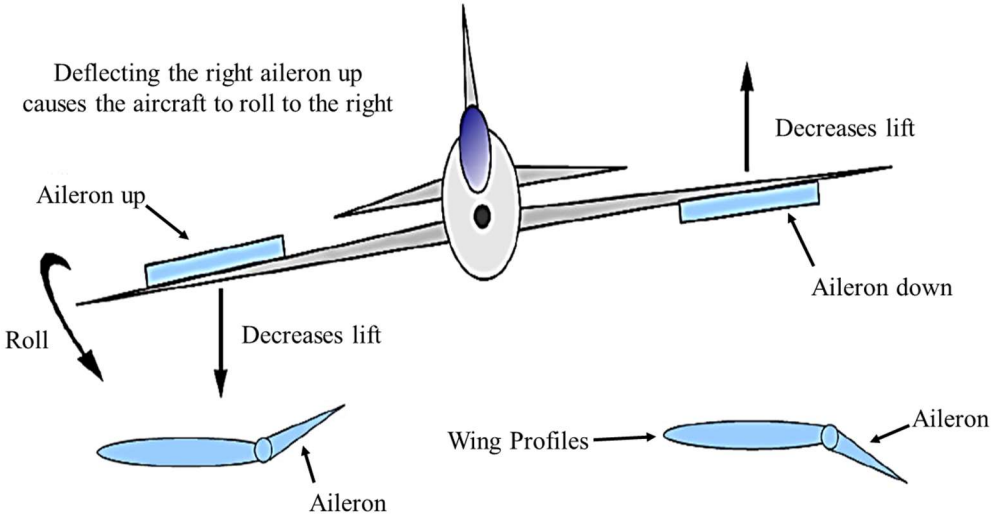

Figure 2.4 Schematic showing the operation of the aileron.

2.5 Reliability of HRA configuration

In a high redundancy actuator, the actuation elements are connected in both series and parallel (see Figure 1.5) arrangement which is also known as grid configuration [54-56]. This will increase the force and travel capability and availability over an individual actuation element [57, 58]. And also makes the actuation system robust to faults when an

actuation element was subjected to lock-up or loose fault. These faults in the system may reduce the overall capability of it but the system will remain in function [59-61]. So far, the focus of the research was on the modelling and control of the simple configurations. The reliability studies so far on electromechanical systems are rare, previously electromechanical steering was discussed [54], and electrical machines and power electronics were analyzed [55].

Finding the best suitable arrangement of actuation elements for a particular application to improve the availability and reliability of the actuation system was very much important to design a HRA [62, 63]. Just adding the actuation elements will not improve the reliability of the system [16]. The series arrangement improves the travel capability and the parallel arrangement improves the force capability of the actuation system. Depending upon the priority of the system, the number of actuation elements and the configuration of the HRA needs to be identified. This work presents an approach to find the reliabilities of series-in-parallel and parallel-in-series configurations which were discussed in chapter-3.

2.6 Controller design

There is a possibility to design different controllers for the HRA due to its robust mechanical structure. The concept of HRA was mainly proposed for flight control system and some of the popular techniques used to design flight control systems are; classical (P, PD, PI, PID) controller [80-83], robust (H1, LQ, LQG, LTR) controller [84-87], dynamic inversion [88-91], quantitative feedback theory [92, 93], linear parameter varying (LPV) control, [94, 95], model predictive control [80], adaptive control [96], model following [97], sliding mode control [98], and fuzzy logic [99], and Eigen structure assignment [100-101].

2.6.1 Classical Control

After considering the mechanical structure, it also necessary to explore some features of control structures. Some of the classical controls that are widely used in industries are: Proportional Integral Derivative (PID) controller, Lead and Lag compensations. Based on the level of feedback information, two kinds of controllers are

defined as “Local Controller” and “Global Controller”. The Local Controller is based on information feedback from each and every actuation element and the Global Controller is based on feedback information of the overall HRA. The two control structures which are based upon these two kinds of controllers are as shown in the figure 2.5 and figure 2.6.

The control structure shown in figure 2.5 is only a global controller for the full actuator assembly. A position feedback global controller is necessary for a position tracking purpose. This is possible by giving a controlled voltage signal to all the actuation elements from the global controller. Due to this reason this structure is called as a voltage-driven control structure.

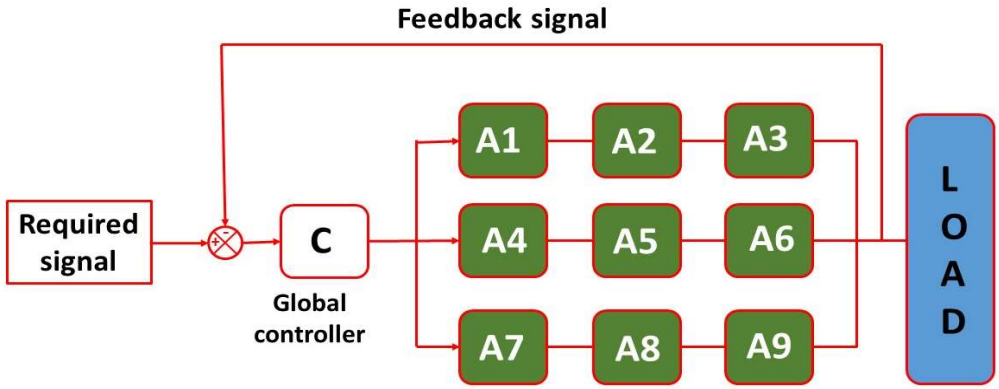

Figure 2.5 Voltage driven control structure

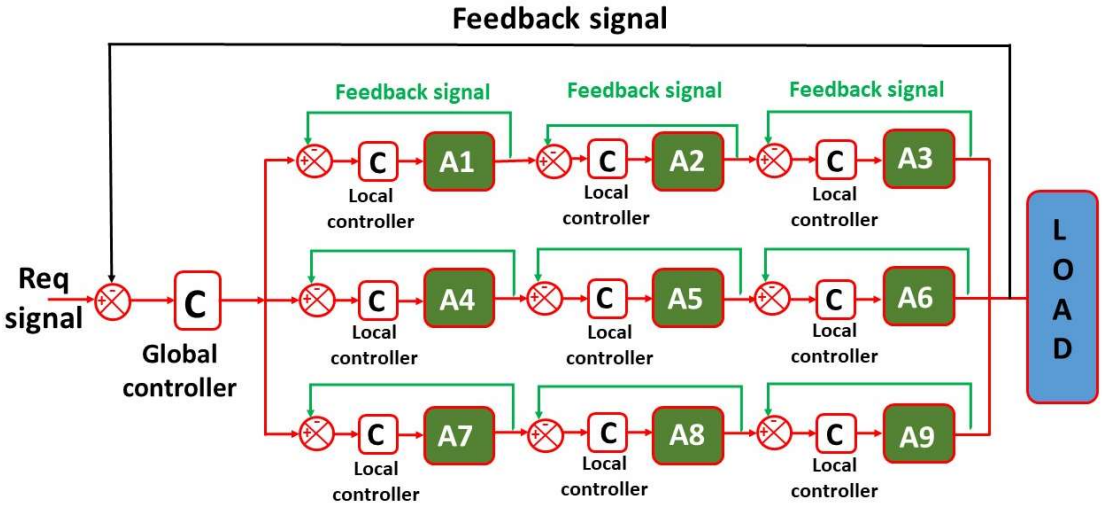

Figure 2.6 Current driven control structure

The control structure shown in figure 2.6 is a global controller for the full actuator assembly with local controllers at each actuation elements. The current feedback is used for the local controllers by adding a current inner loop along with the global controller for a better control performance. So, this is called current driven control structure because the global controller gives a current control signal to all local controllers.

In this present work, a classical global controller has been chosen to be tested with the HRA and it was chosen due to simplicity in the design process. The HRA, all the multiple actuation elements are assumed to be identical during the modelling process. But, in reality, there will be minor variances in the parameters of every individual element, and these introduce parameter uncertainties to the system. Moreover, when faults are injected into the elements of the model, the dynamics of the system will change which causes time varying uncertainties. Though classical control methods can provide good tracking performance.

2.7 Conclusions

A literature review relating to actuator faults, fault tolerance, and high redundancy actuation was presented in this section. From the literature data, the importance of the reliability of the HRA configuration was realized. So, based on the reliability results of series-in-parallel and parallel-in-series configurations, a HRA with nine actuation elements based on direct driven electromechanical actuators (DDEMAs) has opted for the present research work. The mathematical/3D modelling of the HRA based on DDEMA was derived and the experimental setup was fabricated based on the geared electromechanical actuators that are arranged in the series-in-parallel configuration. In the initial stage, a four-element HRA based on EMA was studied considering a gear-box (between the motor and the lead-screw) and a motor stiffness parameter for the EMA [14]. After that, a mathematical modelling work considering the gear ratio as one and neglecting the motor stiffness was derived [13]. And in the present work, the mathematical and a 3D model based on DDEMA was modeled. Based on the 3D model, a case study using the HRA as an aileron actuation system was analyzed in chapter-4.

2.7.1 Literature Gaps

Based on the literature so far covered in the previous sections, the gaps of the literature are identified and provided below.

- The reliability of different configurations of HRA with limited actuation elements needs to be studied to find the best suitable configuration for a particular application.
- Electromechanical actuators are widely in use for achieving fault-tolerant actuation but, the usage of compact size direct driven linear electromechanical actuators was very less. So, there is a need to work on direct driven linear EMAs.
- It is necessary to study the behavior of the HRA under various faults even more.
- There were only a few studies carried out on the experimental validation of the HRA system.

2.7.2 The Work plan

The present work was carried out based on the flow chart as shown in figure 2.7. In the first step, the identification of the suitable configuration of the HRA has to be made. So, the reliability analysis for the configurations of the HRA was described (in chapter-3). Based on the reliability results, a 3×3 series-in-parallel arrangement was considered for further analysis. For obtaining the HRA, the type of actuation element needs to be selected. So, based on the literature gaps a DDEMA was selected for the modeling. The mathematical modelling of the single DDEMA and the 3D model of the single DDEMA was derived and it was extended to the 3×3 HRA later. Two common mechanical and electrical faults of the actuators are modeled and introduced into the healthy 3×3 HRA model and the results under the fault conditions were analyzed. Finally, an experimental setup of 3×3 HRA to validate the simulation results was fabricated.

The most common mechanical faults considered are lock-up fault and the loose fault. Similarly, most common electrical motor faults that are considered include open-circuit (OC) and short-circuit (SC) faults. OC fault in the motor can occur due to the breakage of one or more turns in the winding phase. When this happens, the flow of current becomes zero in the fault phase and there is no torque generation by the motor. So, the rotation of the actuator's lead-screw (which will be connected to the motor shaft) will

become zero. SC fault occurs when turns inside the windings are shorted together. Depending on the number of short turns, a significant change in the resistance, mutual and self-inductance and also the back E.M.F changes occur. However, no positive torque is generated. Lock-up or jamming fault occurs when lead-screw or ball-screw nut gets jammed. This happens because of fragmentation or deformation of the balls or because of the locking of the gears in the gear-box. This results in the failure of the transmission of the actuator. Loose fault results from loss in applied force between the mechanical elements or the free movement of the lead-screw without any restriction/force.

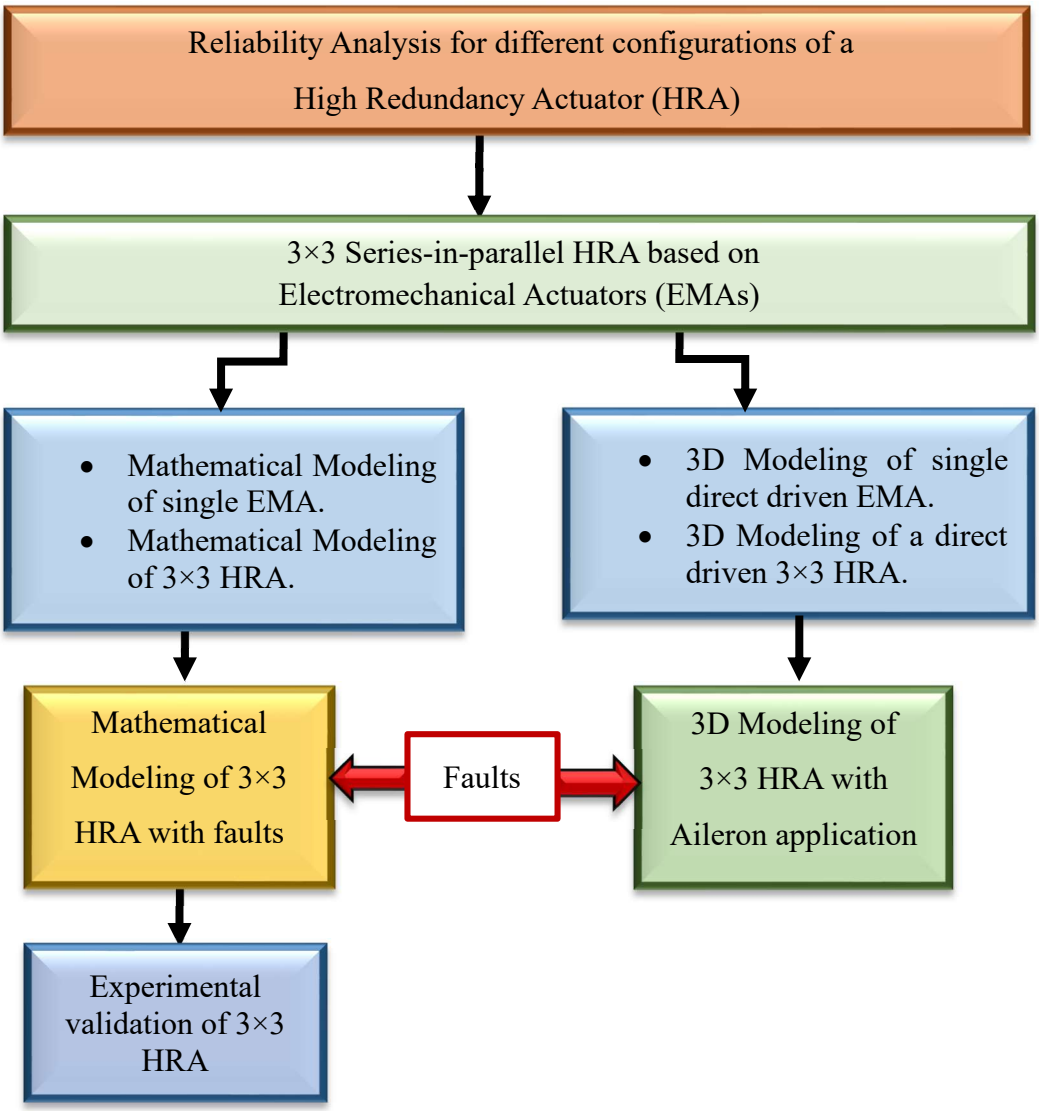

Figure 2.7 Flow chart of the work plan

CHAPTER - 3

RELIABILITY ANALYSIS OF HIGH REDUNDANCY ACTUATOR CONFIGURATIONS

3.1 Introduction

In the present development in technical systems, the industries must be fully aware of the necessity for reliability in the design and manufacturing of products. Even though "Reliability Engineering" has introduced at first during the Second World War with a huge contribution with the aid of defense people, nowadays it has become essential in all levels of the product cycle starting from design to the final product. Reliability of the system can be defined as "the probability that a system will perform its intended function adequately for a specified period, or will operate in a defined environment without failure" [56]. The increase in the system complexity will decrease the reliability of it and the reliability increases the preliminary cost of each device of the system. The manufacturing of high-quality systems with low-quality components is not possible, but improving the reliability of systems using less reliable components is possible just by changing the configuration of the system [57]. The reliability of the system can be increased by the addition of one or more similar components. The details regarding the addition of components in different configurations and calculation of reliability of it was discussed in this chapter.

3.2 Failure Modes and Causes

Failure can be defined as the "partial or complete damage of system components in such a way that its working is extremely affected or completely stopped" [58]. In the evaluation of the quantitative reliability of a system, the concept of failures and their details are very much necessary. In general, some elements of the system have well-defined failures but the failure of some elements of the system cannot be predicted. When the component is initially installed and if that component fails with high frequency then it is known as an initial failure or infant mortality. Manufacturing defects in the components

are the major root cause for these types of failures. In the initial stages, these type of failures are very high and progressively decreases and become stable over a period of time. If constant failures of the system occur due to accidental was observed for a longer period on a component then these type of failures are known as random failures. If the elements of the system gradually deteriorate due to wear and tear with the usage then these types of failures are called wear-out failures and the rate of failure of these types of failures is very high [59]. Therefore the whole pattern of failures could be depicted by a bathtub curve as shown in figure 3.1.

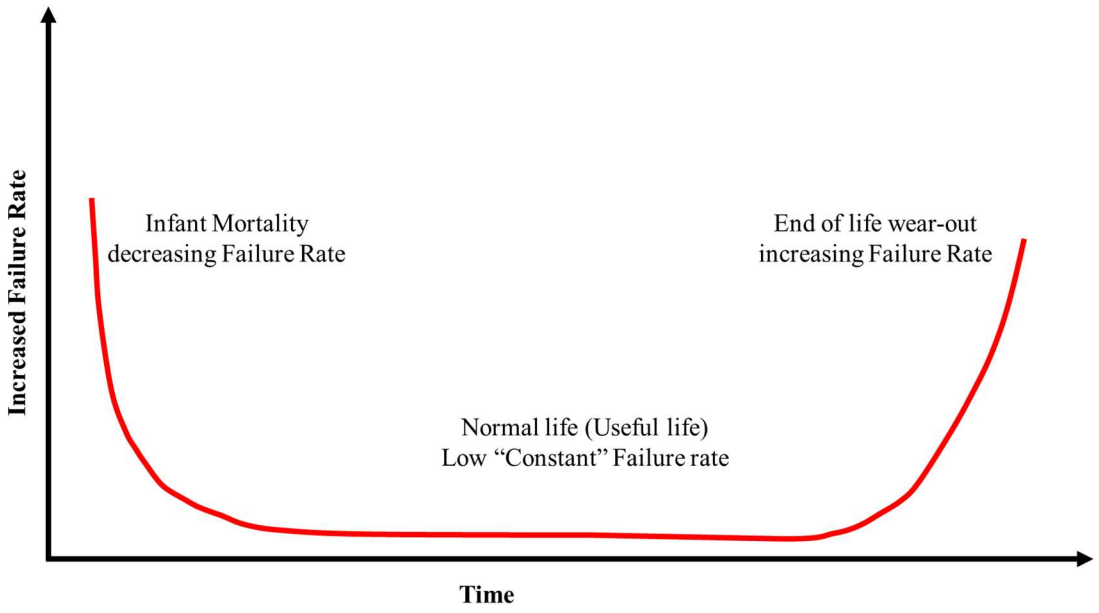

Figure 3.1. Failure rate curve (Bathtub curve)

3.3 Design for Reliability

Manufacturing of perfect components with exact tolerances is very difficult because of inherent variations and the cost of manufacturing of exact components with perfect tolerances is very high [75]. The approach becomes heavy with large and complex manufacturing systems. Proper maintenance and utilization of engineering systems and equipment were possible with the help of reliability study and it has become essential and gained much importance among the working engineers and manufacturers. The reliability analysis needs to be focused during the initial design stage of the system itself. So, before designing the system, various means of improving the reliability of the system, and the

constraints that are associated with them must be studied. The two methods to improve the reliability of a system are: one is “improving the components” and the other one is “using the redundancy technique”. Depending upon the type of the system, these two methods can be applied independently or combined manner to improve the reliability of the system. Some of the important techniques to enhance system reliability are shown in Table 3.1.

Table3.1 Techniques to enhance the reliability of the system

S.NO.	Technique	Remarks
1	Parts improvement	Leads to higher cost
2	System simplification	Leads to poor quality
3	Use of overrated components	Leads to higher cost
4	Effective and creative design	Failures cannot be completely eliminated
5	Maintenance and repair	Best for high reliability
6	Structural redundancy	An effective method for higher reliability

From the above table, the combination of structured redundancy and maintenance and repair produces maximum reliability of the system which is nearly equal to one. In general, the possibility to produce highly reliable components is very difficult due to several constraints like cost, manufacturing process, non-availability of production facilities, etc. In these types of situations, the redundancy technique is very beneficial for enhancing the reliability of the system. So, for improving the reliability of the system by introducing redundancy can be done in two methods: Element redundancy and Unit redundancy

3.3.1 Element Redundancy:

In this approach, redundant for each and every element of the system are provided individually. All the elements are added in parallel to the active components of the system which enhances the redundancy of it. The redundancy in this approach is provided at the element level only. For example, let A1 and B1 be the two elements of the system with

reliabilities $R_1(t)$ and $R_2(t)$ respectively as shown in figure 3.2. By applying the element redundancy to that system then the system will become as shown in figure 3.3, where elements A2 and B2 are the redundant elements of A1 and B1 with the same reliabilities. In this arrangement, due to the presence of redundant elements, the reliability of the system will be much better compared to the previous system. The proper condition of any one of the elements A1 or A2 and the condition of either B1 or B2 is sufficient for the successful operation of the system.

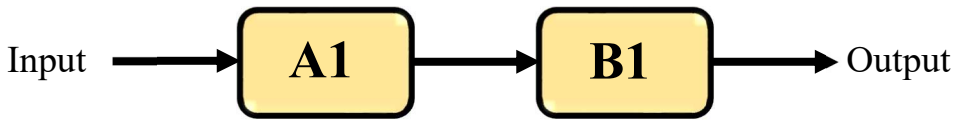

Figure 3.2. The schematic of a system with two elements A1 and B1

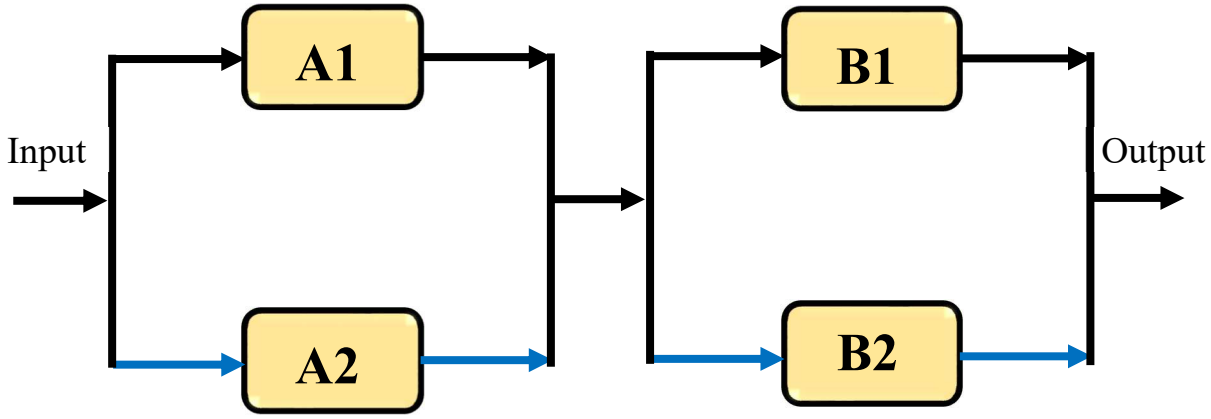

Figure 3.3. Applying element redundancy to a system of two elements A1 and B1

Reliability of the element redundancy system in terms of probability can be written as:

$$R_E = P\ [(A1 \text{ or } A2) \text{ and } (B1 \text{ or } B2)]$$

$$\Rightarrow \quad R_E = P(A1 \text{ or } A2) \times P(B1 \text{ or } B2) \qquad 3.1$$

3.3.2 Unit Redundancy:

In this approach, the redundancy for the entire system was provided. The entire elements of the system were added in parallel to an existing system which enhances the

redundancy of it. The redundancy in this approach is provided at the system level. For example, let A1 and B1 be the two elements of the system with reliabilities $R_1(t)$ and $R_2(t)$ respectively as shown in figure 3.2. By applying the unit redundancy to that system then the system will become as shown in figure 3.4, where the entire system of elements A2 and B2 are the redundant system for the existing system A1 and B1. In this arrangement, due to the redundancy of the system, the reliability will be enhanced compared to the non-redundant system. The proper working condition of any one of the systems is sufficient for the successful operation of it.

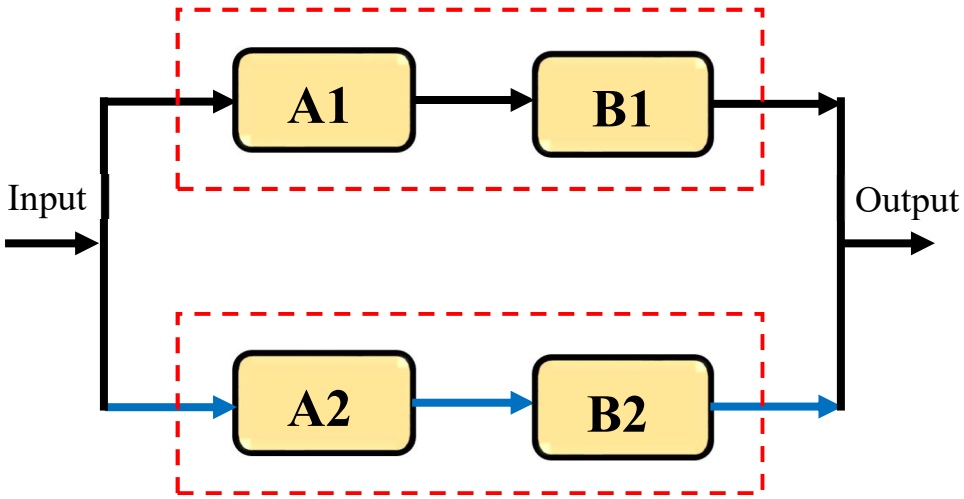

Figure 3.4. Applying unit redundancy to a system of two elements

Reliability of the element redundancy system in terms of probability can be written as:

$$R_U = P\ [(A1 \text{ and } B1) \text{ or } (A2 \text{ and } B2)] \qquad 3.2$$

The unit redundancy of the system is further classified into two types: Active redundancy and Stand by redundancy. These are the two basic types of redundancies that are used commonly.

3.3.2.1 Active Redundancy:

In active redundancy, to perform the function of decision making and switching, the system does not require any external devices or components when an element in the redundant structure fails. To share the load of the system the redundant elements of the system are always operational and picking up the load of the failed element was done

automatically. Active redundancy can also be called “Full-on redundancy or Load-sharing redundancy” [56]. The configuration of the active redundancy system with elements A1 and A2 is as shown in figure 3.5.

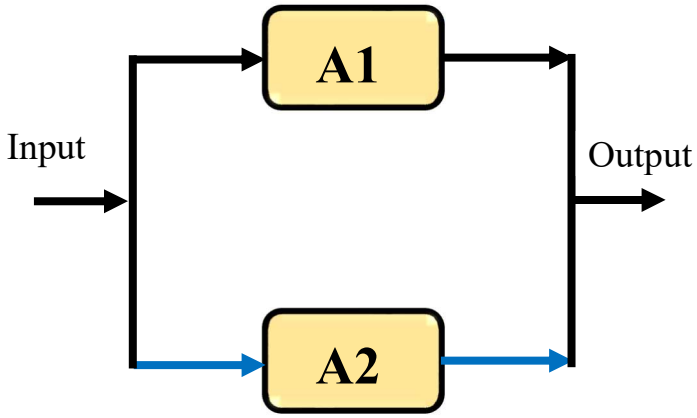

Figure 3.5. Active Redundancy

3.3.2.2 Stand by Redundancy:

Standby redundancy is defined as the “redundancy that requires the external elements or devices to detect, make a decision and switch to another element or path as a replacement for a failed element or path” [76]. This type of redundancy is more suitable for some of the mechanical devices like motors and pumps etc. The schematic diagram of the system representing the standby redundancy is shown in figure 3.6.

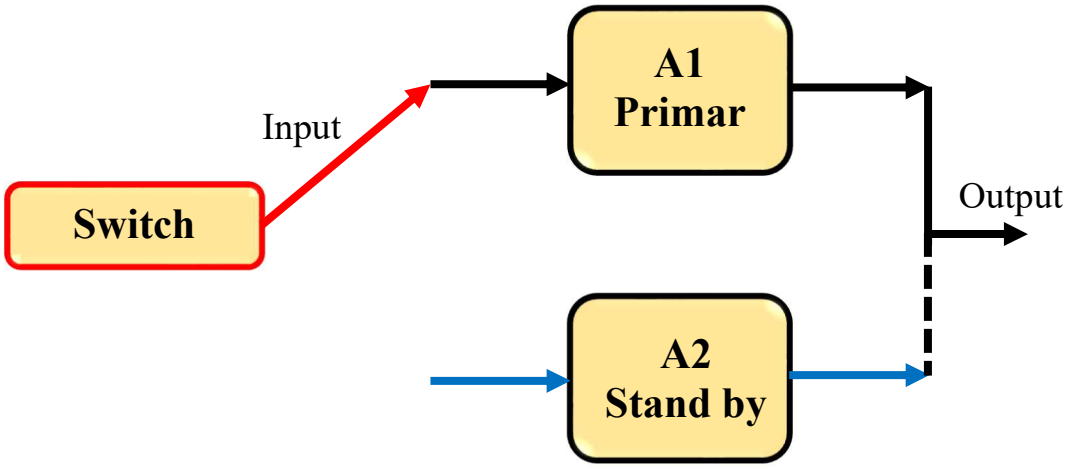

Figure 3.6. Stand by redundancy

3.4 System Reliability Models

In general, system reliability model can be described as "to determine an appropriate reliability or reliability model for each component of the system by applying the rules of the probability according to the configuration of the components within the system" [77]. The configuration of the redundant system may vary from simple to complex. In a simple system, the system may contain one or two elements whereas a complex system may involve thousands of elements. Such systems can be investigated by disintegrating them into subsystems of suitable size which represents a precise function. Then the reliability of the total system can be obtained by evaluating all the subsystems and combining them using certain probability laws. However, this method requires entire information of the system like physical structure and its functions to evaluate the system behavior when a subsystem fails. To improve the reliability of the system there exist several methods like reducing the system complexity, applying a large factor of safety, increasing the reliability of the system components, etc. Even though there are several types of configurations available but series, parallel, and combined series-parallel configurations are the main focus of the present work.

3.4.1 Reliability of Series Configuration System

In a series system, the components are connected serially as shown in figure 3.7. If a system is having a 'n' number of components connected in series then for the proper function of the system, all the components must work accurately. The failure of any one of its components leads to system failure. The information from the input end will reach the output end if and only if all the 'n' components function properly.

Fig. 3.7 Series System

Now the reliability of a series system in terms of probability can be written as,

R_{S1} = Probability that all the components are in proper condition

$$R_{S1} = P\ [(1) \text{ and } (2) \text{ and } (3) \ldots\ldots\ldots \text{ and } (n)]$$

$$R_{S1} = P\ [(1) \cap (2) \cap (3) \ldots\ldots\ldots \cap (n)]$$

$$\Rightarrow \quad R_S = P(1) \times P(2) \times P(3) \times \ldots\ldots\ldots P(n)$$

Reliability of series system, $R_S = (R_1) \times (R_2) \ldots\ldots \times (R_n)$

3.3

3.4.2 Reliability of Parallel configuration system

In the parallel system, the components in the system are connected in parallel as shown in figure 3.8. If a system is having a 'n' number of components connected in parallel then for the proper function of the system, any one of the components must work accurately. Even though (n-1) number of components failed, still the system will be in working condition. The information from the input end will reach the output end if a single component in the system is working properly. In a parallel configuration, the total reliability of the system is higher than the reliability of any single component of the system.

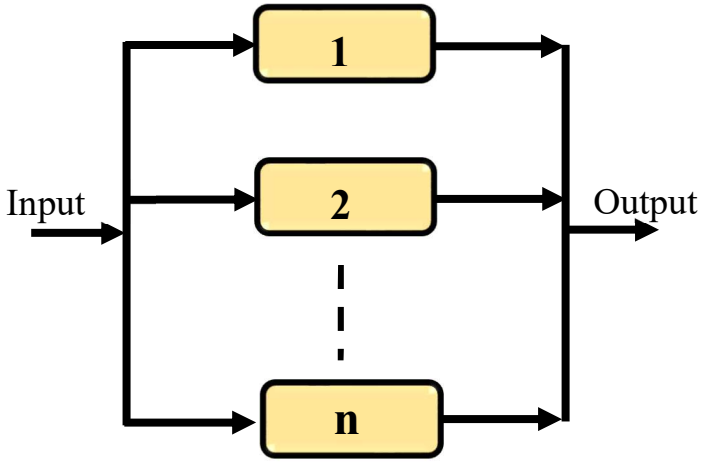

Figure 3.8. Parallel System

Now the reliability of a parallel system in terms of probability can be written as,

R_{S2} = Probability that any one component in proper condition

$$R_{S2} = P\ [(1) \text{ or } (2) \text{ or } (3) \ldots\ldots\ldots \text{ or } (n)]$$

$$= P\ [(1)^{-} \cap (2)^{-} \cap (3)^{-} \ldots\ldots\ldots \cap (n)^{-}]$$

= Product of unreliability of components.

Reliability of parallel system $R_P = 1-[(1-R_1) \times (1-R_2) \ldots\ldots \times (1-R_n)]$ 3.4

3.5 Configuration of Actuation Elements

In the previous topic, the reliabilities of two different configurations of the redundant systems were discussed. It was observed that the system having series configuration will fail if any one of the components fails and in a parallel configuration, the system will not fail unless all the components of the systems fail. The general redundant system configurations will work in this manner but in the case of a redundancy actuation system, both the series and parallel configurations have got their own benefits depending on the type of fault that the system undergoes.

3.5.1 Specification of Actuation Elements

The individual actuation elements of the actuation system are specified using several different measures but in the abstract point of view, they are divided into physical measures and reliability measures. The physical measure describes the parameters like displacement or acceleration, and force correlated to the actuation system, and the reliability measure describes the probability of a fault.

The linear actuation system performs forward and backward movement depending upon the controlled input signal. The basic functions of the actuation system are travel and force capability which are considered to be the main focus for the reliability analysis. The two capability measures lead to two main fault modes of an element they are, loss of force (loose fault) and loss of travel (lock-up fault).

For simplifying the analysis only the static case of the actuation system was considered. Both the lock-up and loose faults are assumed to be complete, this implies that a fault reduces the relevant capability to zero. It is also assumed that both faults are independent and the lock-up element is fixed in its neutral position.

3.5.2 Actuation Elements in Pure Series Configuration

In general, the most common mechanical faults considered are lock-up fault and the loose fault. Lock-up or jamming fault occurs when lead-screw or ball-screw nut gets jammed. This happens because of fragmentation or deformation of the balls or because of the locking of the gears in the gear-box. This results in the failure of the transmission of the actuator. Loose fault results from loss in applied force between the mechanical elements or the free movement of the lead-screw without any restriction/force.

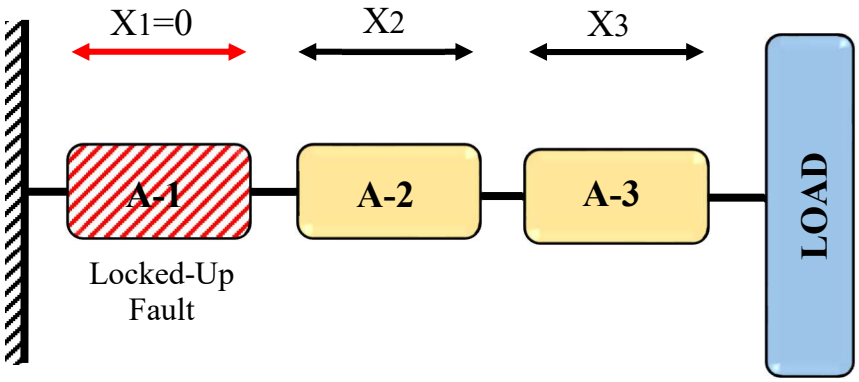

Figure 3.9 (a). Actuation elements in pure series with A-1 actuator under lock-up fault

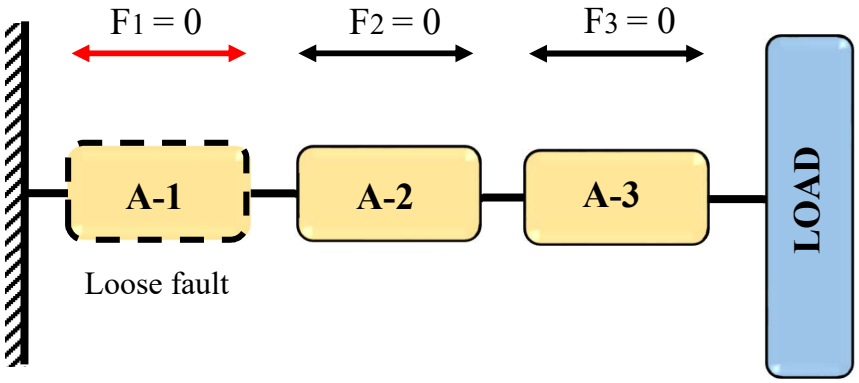

Figure 3.9 (b). Actuation elements in pure series with A-1 actuator under loose fault

The actuation elements numbering and the graphical representation of lock-up and loose faults in a pure series configuration are shown in Figures 3.9 (a) and 3.9 (b). The actuator under the lock-up fault will act as a rigid element and the actuator under the loose fault will act like there is no physical connection between the ends. The effect of lock-up

fault in any actuation element of a pure series configuration will affect the travel capability but not the force capability of the actuation system. For example, if the actuation element A-1 in the three series actuation system is subjected to a lock-up fault and it will act as a rigid link. So, the other two actuation elements which are in series are capable of providing the required force but the linear displacement of the actuation system will be affected. Because the displacement of the series actuation system is the sum of the linear displacements of the individual actuation elements. In the same way, if the actuation elements in a series actuation system are subjected to loose faults then both the force and displacement of the system will be affected. This is because of the lack of fixed support to apply the force and to make the displacement of the load. So, the series configuration of the actuation system will be completely affected due to loose faults and partially affected due to lock-up fault.

3.5.3 Actuation Elements in Pure Parallel Configuration

The graphical representation of lock-up and loose faults in a pure parallel configuration are shown in Figures 3.10 (a) and 3.10 (b). The effect of lock-up fault in any one of the actuation element of a pure parallel configuration will affect both the travel and the force capability of the actuation system because the affected actuation element will act as a rigid link between the fixed support and the load. So, even though the other two actuation elements are active and in healthy condition, the system fails. The effect of loose fault in the pure parallel configuration will affect the force capability because the force of a pure parallel actuation system is the sum of the forces of all the individual actuation elements. The travel capability of the parallel actuation system will not be affected due to the loose fault of actuation elements. So, the parallel configuration of the actuation system will be completely affected due to lock-up faults and partially affected due to loose fault.

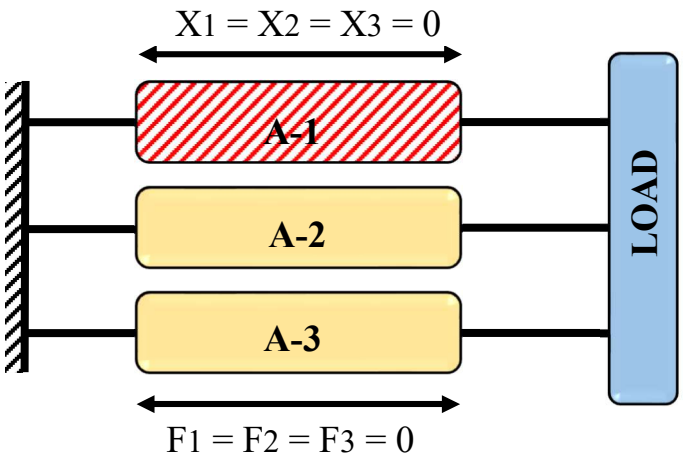

Figure 3.10 (a). Actuation elements in pure parallel with A-1 actuator under lock-up fault

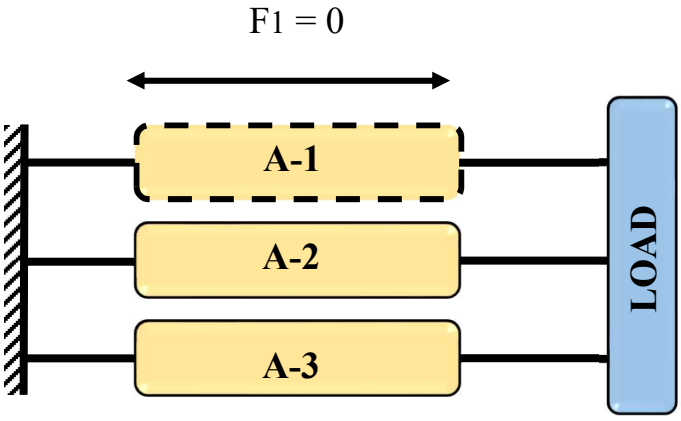

Figure 3.10 (b). Actuation elements in pure parallel with A-1 actuator under loose fault

3.5.4 Actuation Elements in Grid Configuration

The pure series configuration of the actuation system is having the capability to overcome the lock-up fault and the pure parallel configuration is having the capability to overcome the loose fault. So, for procuring both the advantages of series and parallel configurations a grid configuration with both series and parallel arrangement are graphically represented in the below figures 3.11(a) and 3.11(b).

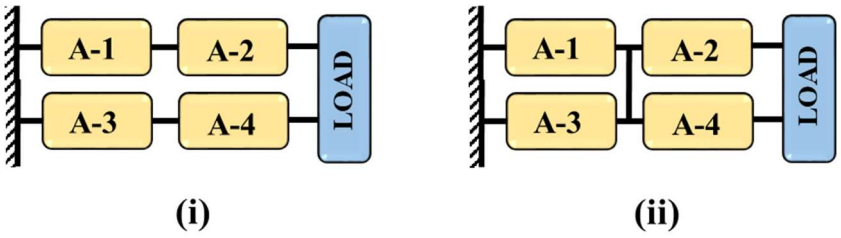

Figure 3.11(a) (i) 2×2 Series in parallel configuration (ii) 2×2 parallel in series configuration

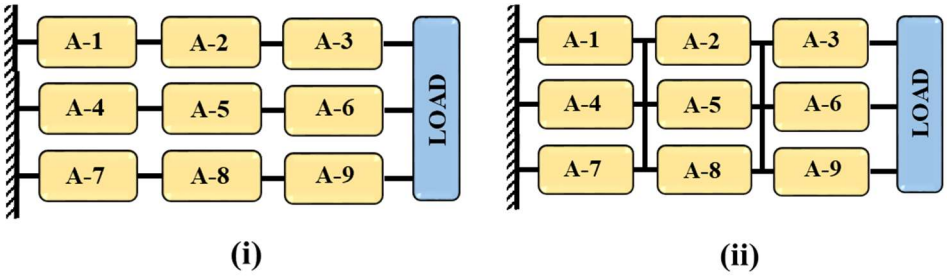

Figure 3.11(b) (i) 3×3 Series in parallel configuration (ii) 3×3 parallel in series configuration

Table 3.2 Effect of faults on force and travel capabilities

S.NO.	Type of Fault	Travel Capability	Force Capability	Probability
1	None	Normal (1)	Normal (1)	$p_t p_f$
2	Loose	Normal (1)	Affected (0)	$p_t q_f$
3	Lock-up	Affected (0)	Normal (1)	$q_t p_f$
4	Both Loose & Lock-up	Affected (0)	Affected (0)	$q_t q_f$

The two capability measures lead to two main fault modes (Lock-up and loose faults) of an element. Both faults are assumed to be total that is a fault reduces the relevant capability to zero (referee Table 3.2; Figure 3.21).

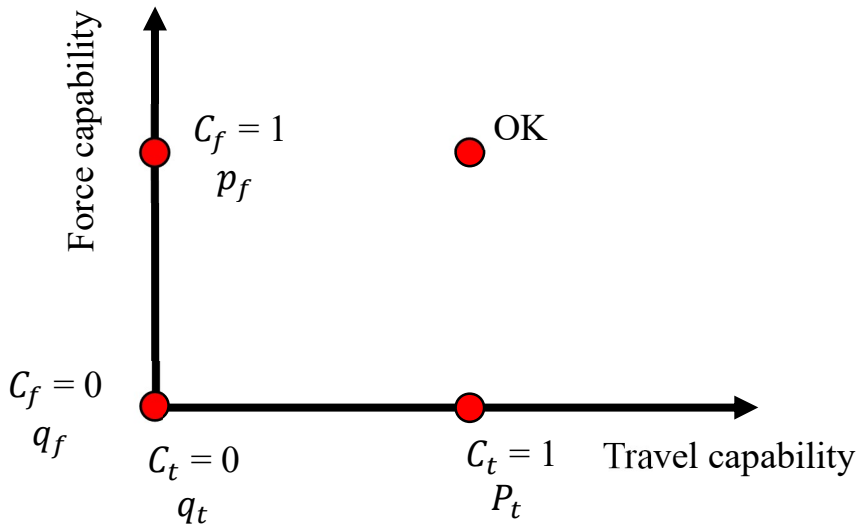

Figure 3.12 Two-dimensional capability space by fault states

3.6 Specifications of Reliability

Reliability of an element can be described in different ways, such as availability, mean time to failure (MTTF), failure probability during a particular mission, or failure probability over a given time. Depending upon the application the relevant specification was used. However, all these measures are based on probability or probability density over time. By using any of the above measures these functions over time can be interpreted. So, the present work uses fault probabilities as a generic way to measure reliability.

$$P(\text{loose}) = P(C_f = 0) = q_f$$

$$P(\text{lock-up}) = P(C_t = 0) = q_t$$

where 'P' is the probability of an event, 'q' is the failure probability (unreliability) of an element, typically close to zero. 'C_f' and 'C_t' are the force and travel capabilities.

3.7 Element Capabilities

The primary aim of using redundant elements is to increase the capabilities of the actuation system. For example, two actuation elements in series can achieve twice the travel and two actuation elements in parallel can achieve twice the force.

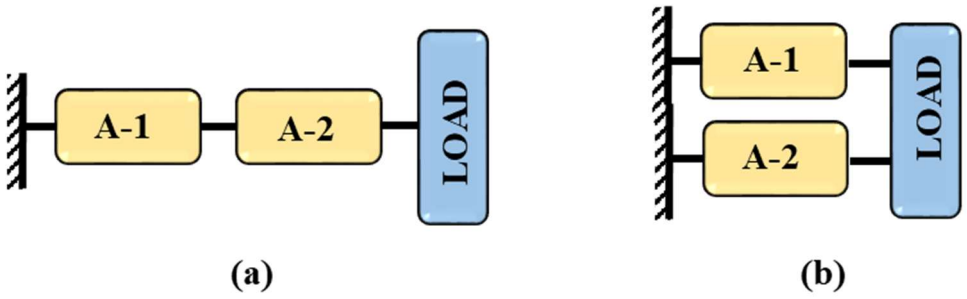

Figure 3.13 (a) Two elements in pure series (b) two elements in pure parallel configurations

3.7.1 Limiting Capabilities

The capabilities of the systems will not increase always even though 'n' number of subsystems or elements are combined. Instead, the capability of the actuation system is determined by the weakest element. For example, the force capability 'C_f' of actuation elements in series (see figure 3.13(a)) is:

$$C_{fs}(c_f) = min\{C_{f1}, C_{f2}\} \tag{3.5}$$

where c_f is a vector $(C_{f1}, C_{f2})^T$

And the travel capability of elements in parallel configuration (see figure 3.13(b)) will be the same, which is:

$$C_{tp}(c_t) = \min\{C_{t1}, C_{t2}\} \tag{3.6}$$

These equations follow directly from the physical laws and the specification. In both pure series and parallel cases, the capability of the combined system is having a minimum capability of overall elements of the system. So, the limiting capability can be written as:

$$C_{lim}(c) = \min\{C_1, C_{2,} \dots \dots, C_n\} \tag{3.7}$$

If n elements with the cumulative reliability distributions R_i(c) are connected so that the overall capability is limited by the weakest element according to Equation (3.7), the cumulative reliability distribution $R_{lim}(c_{lim})$ of the new system, it can be calculated as

$$R_{lim}(C) = R_1 * R_2 * \ \ldots\ldots \ * R_n(C) \tag{3.8}$$

$$(R_1 * R_2)(\mathrm{C}) = R_1(\mathrm{C})R_2(\mathrm{C}) \tag{3.9}$$

3.7.2 Additive capability

The capabilities of some of the actuation systems will be increased when the actuation elements are combined. This will motivate us to use several actuation elements together in the first place. For example, the force capability c_f of two elements in parallel (see figure 13.3(b)) is in contrast to the minimum operator in equation 3.5.

$$C_{fp}(c_f) = C_{f1} + C_{f2} \tag{3.10}$$

And the travel capability of two elements in series will increase the travel to twice.

$$C_{ts}(c_t) = C_{t1} + C_{t2} \tag{3.11}$$

In both pure series and parallel cases, the capability of the combined system is having an additive capability over all the elements of the system. So, the additive capability can be written as:

$$C_{add}(c) = C_1 + C_2 + \ldots\ldots + C_n \tag{3.12}$$

If n elements with cumulative reliability distributions $R_i(c_i)$ are arranged so that the capabilities add up according to Equation (3.12), the cumulative reliability distribution $R_{add}(c_{add})$ of the resulting system is defined by

$$R_{add}(C_{add}) = R_1 \fatsemi R_2 \fatsemi \ldots\ldots \fatsemi R_n(C)$$

The state-space of the system C_{add} can be larger than the state space of any element C_i. So, with this additive '$\fatsemi$' operator

$$(R_1 \fatsemi R_2)(C) = \ \sum_{i=0}^{c}(R_1(i) - R_1(i+1))R_2(C-i) \tag{3.13}$$

3.8 Capability of High Redundancy Actuation System Configurations

The High Redundancy Actuator (HRA) contains actuation elements that are connected in series and a parallel configuration. Thus, it is essential to analyze the reliability resulting from numerous levels of aggregations. In this section, the reliability distribution of the overall system, and some demonstrative examples of series-parallel configurations will be discussed. The first two systems shown in figure 3.11(a) are two-level arrangements which are called series-in-parallel and parallel-in-series arrangements. Later the analysis is extended to all 3×3 configurations.

3.8.1 Force capability of series in parallel configuration

The actuation system which consists of two series elements, duplicated in parallel as shown in figure 3.11(a) is called 2×2 series-in-parallel or SP configuration for short. This configuration consists of two serial elements on the top (upper left A1 and upper right A2), and two more corresponding serial elements on the bottom (lower left A3 and lower right A4). The force capability of the top elements is limited by the weakest element as they are connected in series but the overall force capability will be the addition of capabilities of the top and a bottom series group of elements. The reliability of the system is analyzed for the capability to generate the force of a single element.

Let the force capabilities or states of the top row be c_{f1} and c_{f2}, and the capabilities on the bottom c_{f3} and c_{f4}. By considering all elements have the same force reliability *pf*. The force capability of the system is:

$$C_{fSP}(c_f) = C_{ftop} + C_{fbottom} \tag{3.14}$$

$$C_{fSP}(c_f) = \ min\{C_{f1}, C_{f2}\} + min\{C_{f3}, C_{f4}\} \tag{3.15}$$

From the above equation, the force capability of series in a parallel system is the sum of the minimum force capability of top elements in series and minimum force capability of bottom elements in series. So, the cumulative reliability distribution $R_{fS(c)}$ for a single row of two elements in the series needs to be determined first.

$$R_{fS} = R_{f1} * \ R_{f2} \tag{3.16}$$

And the results that are obtained with the corresponding capabilities of a single actuation element then

$$R_{fS}(0) = 1$$

$$R_{fS}(1) = P_f^2 = (1 - q_f)^2 = 1 + q_f^2 - 2q_f \quad 3.17$$

If they are expressed in terms of q (failure probability or unreliability) then these reliabilities computation is easier from a numerical perspective. So, polynomials in q_f will be used to describe them here. This reliability distribution R_{fS} is used to describe the two-row subsystems that compose the whole system. As the subsystems are binary in this case, it is simple with capabilities 0 and 1.

Now the resulting force capability distribution of series in parallel configuration of subsystems with the operator '⫫' is

$$R_{fsp} = R_{fs} \fatslash R_{fs} \quad 3.18$$

The resulting capability distribution is

$$R_{fsp}(C_f) = R_{fs} \fatslash R_{fs} = \sum_{C_f=0}^{2} \binom{2}{C_f} {p_f}^{2C_f} {q_f}^{2-C_f} \quad 3.19$$

Expanding the resulting polynomials produces

$$R_{fsp}(0) = 1 \quad 3.20$$

$$R_{fsp}(1) = 1 - 4{q_f}^2 + 4{q_f}^3 - {q_f}^4 \quad 3.21$$

$$R_{fsp}(2) = 1 - 4q_f + 6{q_f}^2 - 4{q_f}^3 + {q_f}^4 \quad 3.22$$

3.8.2 Force capability of parallel in series configuration

In the parallel in series configuration, two elements are connected in parallel, and two of these blocks are arranged in series as shown in figure 3.11(a). The only difference between the previous configuration and this is the addition of the cross-connection at the middle of the actuation elements. Now this configuration of the actuation system can be divided into the left group of elements (A1 and A3) and the right group of elements (A2 and A4). The force will be added up in each group as the actuation elements are connected

in parallel, but the force capability of the overall system configuration is limited by the weakest group. This results in the capability function

$$C_{fPS} = min\{C_{fleft}, C_{frigh}\}$$

$$C_{fPS} = min\{C_{f1} + C_{f3}, C_{f2} + C_{f4}\} \quad 3.23$$

The force capability of parallel in series is the minimum of additive capabilities of the left group and the right group of elements. So, for each group of two parallel elements,

$$R_{fp}(C_f) = R_f = \sum_{i=C_f}^{2} \binom{2}{i} {p_f}^i {q_f}^{2-i} \quad 3.24$$

Expanding the resulting polynomials produces

$$R_{fp}(0) = 1 \quad 3.25$$

$$R_{fp}(1) = 1 - {q_f}^2 \quad 3.26$$

$$R_{fp}(2) = 1 - 2q_f + {q_f}^2 \quad 3.27$$

Now the second stage of the analysis is more complex because each group is now a multi-state system with three distinct capabilities. Equation 3.16 has to be applied, which uses the operator * as defined in Equation (5). This leads to

$$R_{fPS} = R_{fP} * R_{fP}$$

$$R_{fPS}(C_f) = R_{fP}^2(C_f) \quad 3.28$$

This leads to the polynomial solution

$$R_{fPS}(0) = 1 \quad 3.29$$

$$R_{fps}(1) = 1 - 2{q_f}^2 + {q_f}^4 \quad 3.30$$

$$R_{fps}(2) = 1 - 4q_f + 6{q_f}^2 - 4{q_f}^3 + {q_f}^4 \quad 3.31$$

The difference between the two configurations is found by comparing Equation (3.21) with Equation (3.30) which are plotted as shown in Figure 3.14. The reliability

values of all the remaining are identical, but $R_{fsp}(1) \neq R_{fps}(1)$ shows a clear difference. The parallel in series structure is superior by nearly a factor of two for low fault probabilities *qf*. The reason becomes obvious when multiple faults are classified into fatal ones (leading to a force capability of 0) and non-fatal ones (maintaining a force capability of 1). Multiple faults are fatal if it involves several elements that are working in parallel. Assuming that one fault has already occurred, it is interesting to analyze which further fault would be fatal. In the PS configuration, there is only the one element directly in parallel, while a further fault in either element of the other serial group does not affect the force capability. However, in the SP structure, there are always two elements in parallel to the faulty element. The second fault in either of these reduces the force capability to 0.

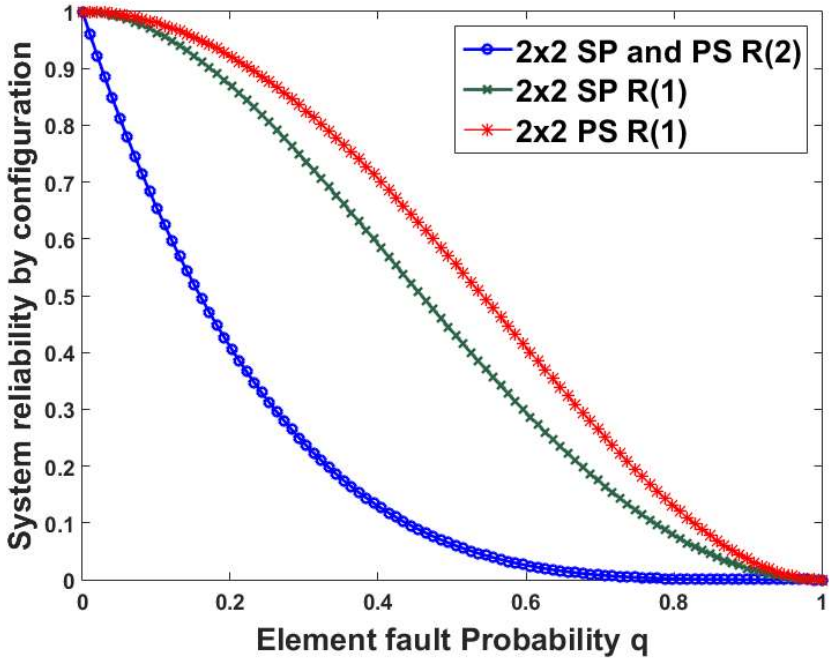

Figure 3.14 Reliability $R_{fx}(1)$ of 2×2 configurations

3.8.3 Travel capability of series in parallel configuration

The travel capability of the series in parallel configuration is similar to the force capability of parallel in series configuration. The configuration of actuation systems can be divided into the top group of elements (A1 and A2) and the bottom group of elements (A3 and A4). The travel/displacement will be added up in each group as the actuation elements

are connected in series, but the travel capability of the overall system configuration is limited by the weakest group. This results in the capability function

$$C_{tSP} = min\{C_{ttop}, C_{tbottom}\}$$

$$C_{tSP} = min\{C_{t1} + C_{t3}, C_{t2} + C_{t4}\} \quad 3.32$$

The travel capability of series in parallel is the minimum of additive capabilities of the top group and the bottom group of elements. So, for each group of two series elements,

$$R_{tS}(C_t) = R_t = \sum_{i=C_t}^{2} \binom{2}{i} {p_t}^i {q_t}^{2-i} \quad 3.33$$

Expanding the resulting polynomials produces

$$R_{ts}(0) = 1 \quad 3.34$$

$$R_{ts}(1) = 1 - {q_t}^2 \quad 3.35$$

$$R_{ts}(2) = 1 - 2q_t + {q_t}^2 \quad 3.36$$

Now the second stage of the analysis is more complex because each group is now a multi-state system with three distinct capabilities. Equation 3.16 has to be applied, which uses the operator * as defined in Equation (5). This leads to

$$R_{tSP} = R_{ts} * R_{ts}$$

$$R_{tSP}(C_t) = R_{tS}^2(C_t)$$

This leads to the polynomial solution

$$R_{tSP}(0) = 1 \quad 3.37$$

$$R_{tSP}(1) = 1 - 2{q_t}^2 + {q_t}^4 \quad 3.38$$

$$R_{tSP}(2) = 1 - 4q_t + 6{q_t}^2 - 4{q_t}^3 + {q_t}^4 \quad 3.39$$

3.8.4 Travel capability of parallel in series configuration

The travel capability of the parallel in series configuration is similar to the force capability of series in parallel configuration. This configuration consists of two parallel elements on the left (A1 and A3), and two more corresponding parallel elements on the right (A2 and A4). The travel capability of the left elements is limited by the weakest element as they are connected in parallel but the overall travel capability will be the addition of capabilities of the left and right parallel group of elements.

Let the travel capabilities or states of the left column be c_{t1} and c_{t2}, and the capabilities on the right c_{t3} and c_{t4}. By considering all elements have the same travel reliability p_t. The travel capability of the system is:

$$C_{tPS}(c_t) = C_{tleft} + C_{tright} \tag{3.40}$$

$$C_{tPS}(c_t) = \ min\{C_{t1}, C_{t3}\} + min\{C_{t2}, C_{t4}\} \tag{3.41}$$

From the above equation, the travel capability of parallel in series system is the sum of the minimum travel capability of left elements in parallel and minimum travel capability of right elements in parallel. So, the cumulative reliability distribution $R_{tP}(c)$ for a single row of two elements in parallel needs to be determined first.

$$R_{tp} = R_{t1} * \ R_{t3} \tag{3.42}$$

And the results that are obtained with the corresponding capabilities of a single actuation element then

$$R_{tp}(0) = 1$$

$$R_{tP}(1) = \ P_t^2 = (1 - q_t)^2 = 1 + \ q_t^2 - 2q_t \tag{3.43}$$

This reliability distribution R_{tp} is used to describe the two-column subsystems that compose the whole system. As the subsystems are binary in this case, it is simple with capabilities 0 and 1.

Now the resulting travel capability distribution of parallel in series configuration of subsystems with the operator '⫫' is

$$R_{tPS} = R_{tp} \Vdash R_{tp}$$

The resulting capability distribution is

$$R_{tPS}(C_t) = R_{tp} \Vdash R_{tp}$$
$$= \sum_{C_t=0}^{2} \binom{2}{C_t} {p_t}^{2C_t} {q_t}^{2-C_t} \quad 3.44$$

Expanding the resulting polynomials produces

$$R_{tPS}(0) = 1 \quad 3.45$$

$$R_{tPS}(1) = 1 - 4{q_t}^2 + 4{q_t}^3 - {q_t}^4 \quad 3.46$$

$$R_{tPS}(2) = 1 - 4q_t + 6{q_t}^2 - 4{q_t}^3 + {q_t}^4 \quad 3.47$$

For travel capability, the difference between the two configurations is found by comparing Equation (3.38) with Equation (3.46) which are plotted as shown in Figure 3.15. The reliability values of all the remaining are identical, but $R_{tsp}(1) \neq R_{tps}(1)$ shows a clear difference. The series in parallel structure is superior by nearly a factor of two for low fault probabilities *qf*. The reason becomes observable when multiple faults are classified into fatal ones (leading to a travel capability of 0) and non-fatal ones (maintaining a travel capability of 1). Multiple faults are fatal if it involves several elements that are working in parallel. Assuming that one fault has already occurred, it is interesting to analyze which further fault would be fatal. In the SP configuration, there are two elements directly connected in series, while a further fault in either element of the other parallel group does not affect the travel capability. However, in the PS structure, there is only one element in parallel to the faulty element. So, the second fault in either of the elements in the series group will reduce the travel capability to 0.

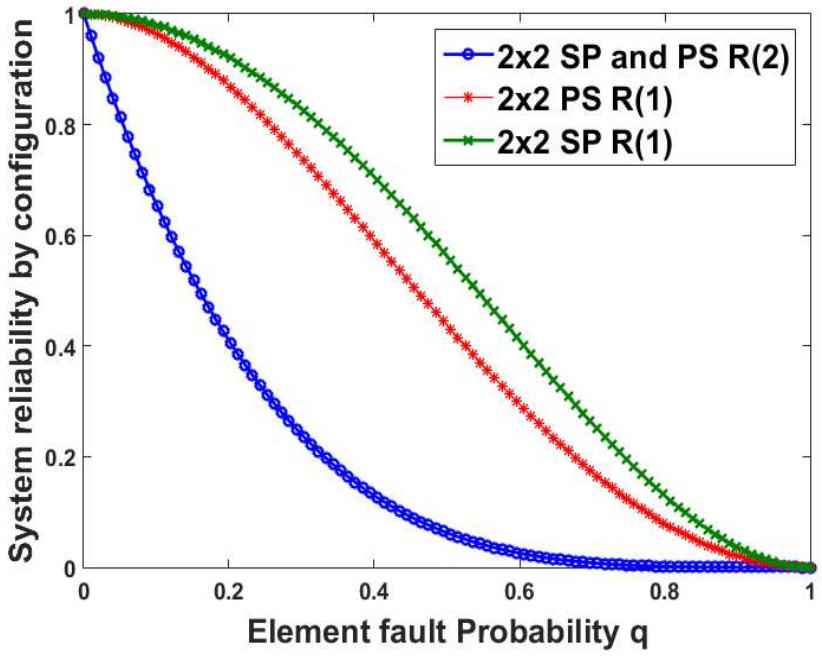

Figure 3.15 Reliability $R_{tx}(1)$ of 2×2 configurations

3.8.5 Reliability of HRA configurations

A method to calculate the reliability of SP and PS configurations was described in the above sections. Similarly, the same considerations can be applied to any assembly that follows a series in parallel or parallel in series structure. Extension of the 2×2 arrangement to a square system of 3 columns and 3 rows connected in series in parallel configuration is given below:

3.8.5.1 Force capability of 3×3 HRA series in parallel configuration

$$R_{fsp}(0) = 1 \tag{3.48}$$

$$R_{fsp}(1) = 1 - 27{q_f}^3 + 81{q_f}^4 - 108{q_f}^5 + 81{q_f}^6 - 36{q_f}^7 + 9{q_f}^8 - {q_f}^9 \tag{3.49}$$

$$R_{fsp}(2) = 1 - 27{q_f}^2 + 108{q_f}^3 - 207{q_f}^4 + 234{q_f}^5 - 165{q_f}^6 + 7{q_f}^7 - 18{q_f}^8 + 2{q_f}^9 \tag{3.50}$$

$$R_{fsp}(3) = 1 - 9q_f + 36{q_f}^2 - 84{q_f}^3 + 126{q_f}^4 - 126{q_f}^5 + 84{q_f}^6 - 36{q_f}^7 + 9{q_f}^8 - {q_f}^9 \tag{3.51}$$

3.8.5.2 Travel capability of 3×3 HRA series in parallel configuration

$$R_{tsp}(0) = 1 \quad 3.52$$

$$R_{tsp}(1) = 1 - 3{q_t}^3 + 3{q_t}^6 - {q_t}^9 \quad 3.53$$

$$R_{tsp}(2) = 1 - 9{q_t}^2 + 6{q_t}^3 + 27{q_t}^4 - 36{q_t}^5 - 15{q_t}^6 + 54{q_t}^7 - 36{q_t}^8 + 8{q_t}^9 \quad 3.54$$

$$R_{tsp}(3) = 1 - 9q_t + 36{q_t}^2 - 84{q_t}^3 + 126{q_t}^4 - 126{q_t}^5 + 84{q_t}^6 - 36{q_t}^7 + 9{q_t}^8 - {q_t}^9 \quad 3.55$$

3.8.5.3 Force capability of 3×3 HRA parallel in series configuration

$$R_{fps}(0) = 1 \quad 3.56$$

$$R_{fps}(1) = 1 - 3{q_f}^3 + 3{q_f}^6 - {q_f}^9 \quad 3.57$$

$$R_{fps}(2) = 1 - 9{q_f}^2 + 6{q_f}^3 + 27{q_f}^4 - 36{q_f}^5 - 15{q_f}^6 + 54{q_f}^7 - 36{q_f}^8 + 8{q_f}^9 \quad 3.58$$

$$R_{fps}(3) = 1 - 9q_f + 36{q_f}^2 - 84{q_f}^3 + 126{q_f}^4 - 126{q_f}^5 + 84{q_f}^6 - 36{q_f}^7 + 9{q_f}^8 - {q_f}^9 \quad 3.59$$

3.8.5.3 Travel capability of 3×3 HRA parallel in series configuration

$$R_{tps}(0) = 1 \quad 3.60$$

$$R_{tps}(1) = 1 - 27{q_t}^3 + 81{q_t}^4 - 108{q_t}^5 + 81{q_t}^6 - 36{q_t}^7 + 9{q_t}^8 - {q_t}^9 \quad 3.61$$

$$R_{tps}(2) = 1 - 27{q_t}^2 + 108{q_t}^3 - 207{q_t}^4 + 234{q_t}^5 - 165{q_t}^6 + 7{q_t}^7 - 18{q_t}^8 + 2{q_t}^9 \quad 3.62$$

$$R_{tps}(3) = 1 - 9q_t + 36{q_t}^2 - 84{q_t}^3 + 126{q_t}^4 - 126{q_t}^5 + 84{q_t}^6 - 36{q_t}^7 + 9{q_t}^8 - {q_t}^9 \quad 3.63$$

3.9 Results and Discussion

The reliability of 2×2 SP and PS configurations with respect to the force requirement and travel requirements are plotted with the help of MATLAB software. So, from the results, it was observed that parallel in series configuration is generally superior for providing the required amount of force. The series in parallel configuration is superior for providing a required amount of travel or velocity. If the requirements are reduced or if

the number of elements are increased then the difference between both configurations increases significantly. Depending on the travel or force requirements, the roles are interchanged between the SP and the PS configurations.

The reliability of 3×3 SP and PS configurations with element fault probability for force requirements are as shown in figure 3.16 and 3.17 and also the comparison of the reliabilities with different level of the requirement are plotted in figures 3.18 and 3.19. The reliabilities of the particular configuration will vary depending on the required capabilities. The reliabilities of 3×3 configurations of the HRA will be decreased if the required capability of force or travel increased from 1 to 3. This is because the maximum number of actuation elements involvement is required as the required capability was increased and the chances of failure of the elements will become more.

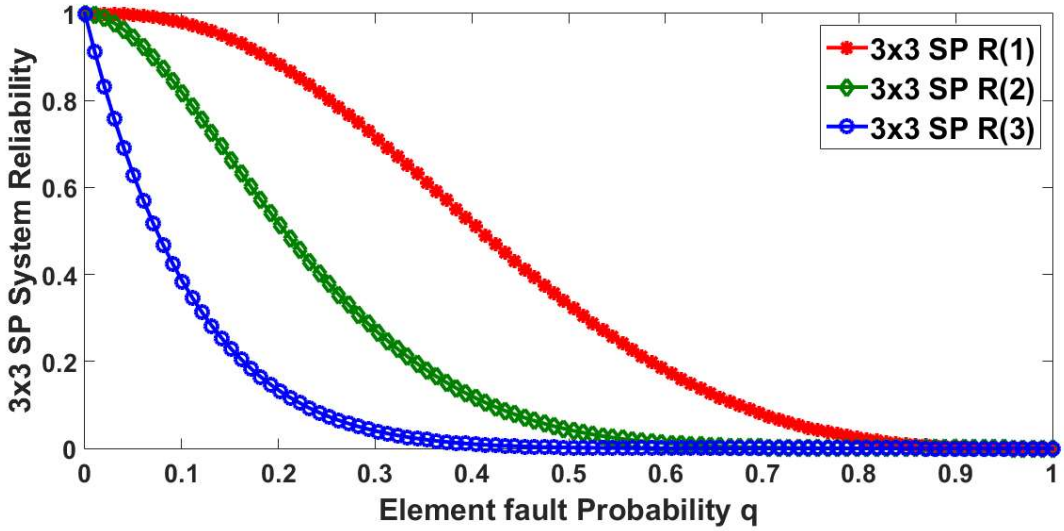

Figure 3.16 Reliability of 3×3 SP configuration concerning force requirements

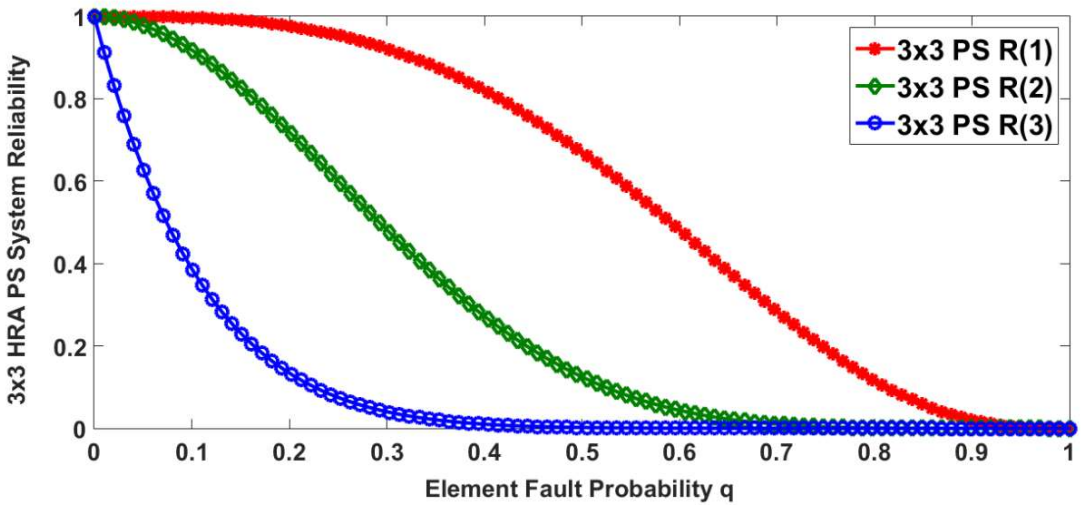

Figure 3.17 Reliability of 3×3 PS configuration concerning force requirements

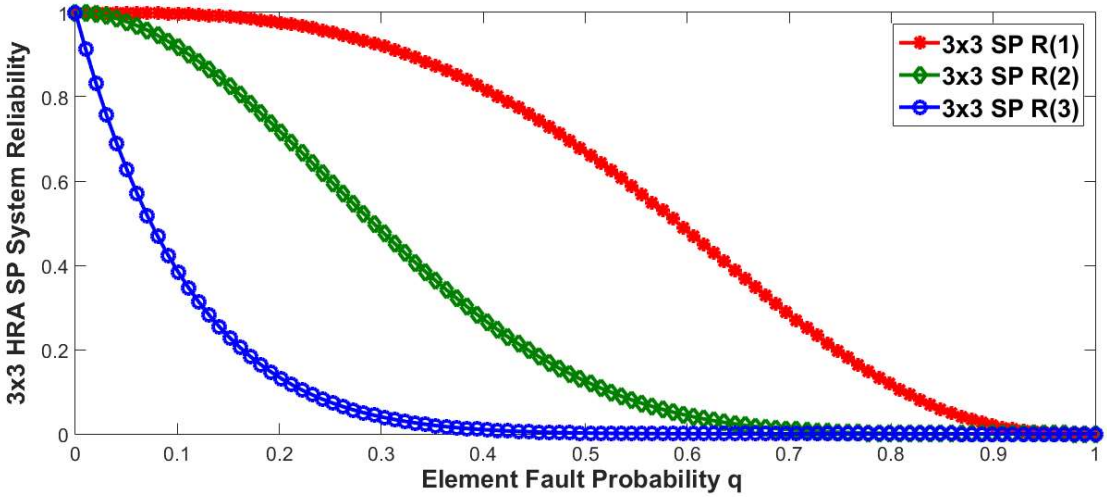

Figure 3.18 Reliability of 3×3 SP configuration concerning travel requirements

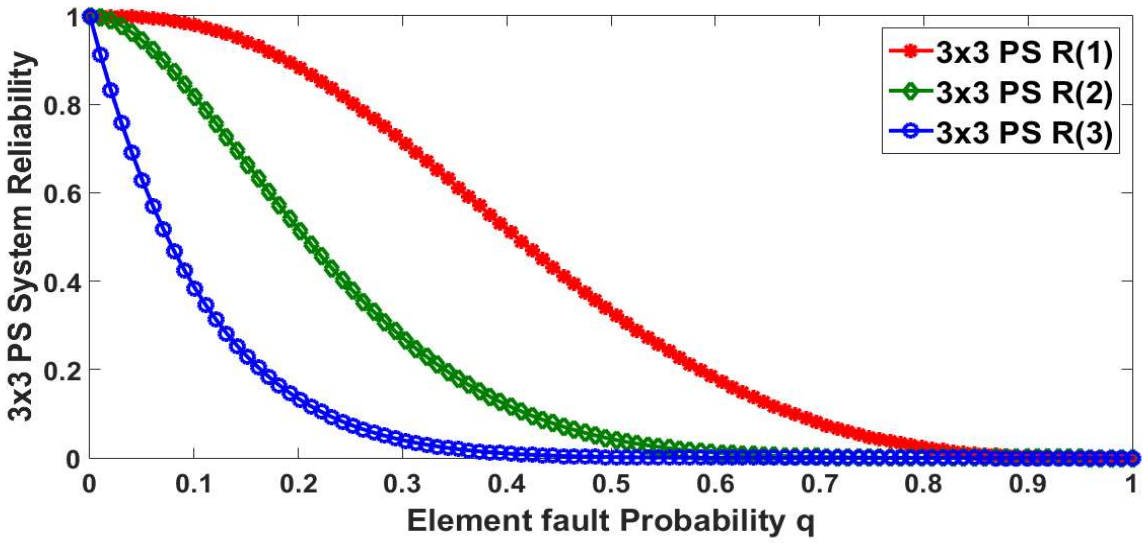

Figure 3.19 Reliability of 3×3 PS configuration concerning travel requirements

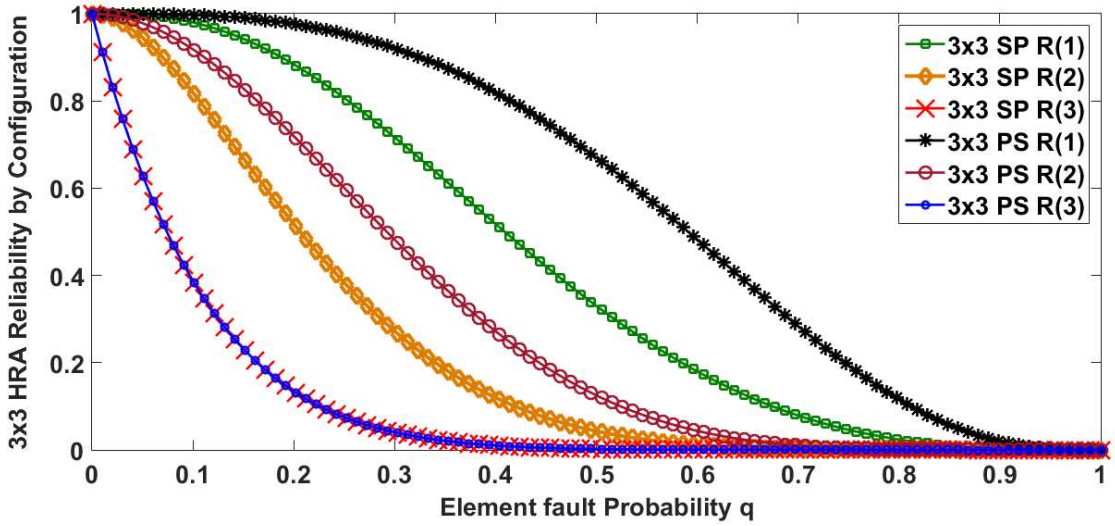

Figure 3.20 Reliability of 3×3 SP and PS configuration concerning different force requirements

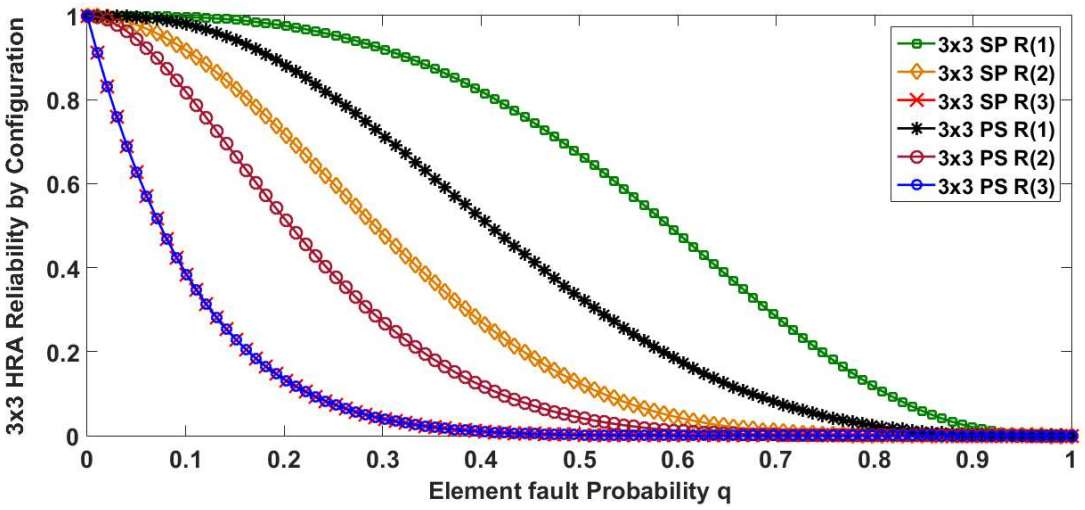

Figure 3.21 Reliability of 3×3 SP and PS configuration concerning different travel requirements

3.10 CONCLUSIONS: RELIABILITY ANALYSIS OF HRA CONFIGURATIONS

Based on the above discussions the following conclusions are drawn:

- The selection of the best suitable configuration has a significant influence on the reliability of HRA, even with the same number of elements in the same two-dimensional arrangement.
- The reliability of HRA will be decreased if the required capability of force or travel increases.
- The force capability of parallel in series structure is superior by nearly a factor of two for low fault probabilities. So, for a particular application, if force is the major required consideration then the best HRA configuration was parallel-in-series configuration.
- The travel capability of series in parallel structure is superior by nearly a factor of two for low fault probabilities. So, for a particular application, if travel is the major required consideration then the best HRA configuration was series-in-parallel configuration.

CHAPTER - 4

MODELING OF THE ACTUATOR

In the previous chapters, a HRA comprises several actuation elements to provide the fault tolerance capability was discussed. But before building up a real physical model of the HRA, a few investigations must be replied. What kind of structure can be employed to interface the actuation elements, and whether the HRA can accommodate component deficiencies without reconfiguration? Every one of these inquiries is needed to be studied in a computer associated environment based on a series of simulation models. Hence, a suitable mathematical or a 3D modeling study is necessary to investigate some key features and behaviors of an HRA system. Based on mathematical expressions of physical laws, all the mathematical and 3D models were designed. Here all the models are built and solved with the aid of the MATLAB/Simulink software.

This chapter discusses the mathematical and 3D modeling of the EMA. The first half of the chapter will give the mathematical modeling of a single EMA then based on this, by combining the actuation elements until the 3×3 High Redundancy Actuator (HRA) is obtained. The second half of the chapter will give the 3D iconic model of the single EMA as well as the 3×3 HRA.

4.1 Electromechanical Actuator

The electromechanical actuators (EMAs) are a combination of an electric motor (electrical system) and a mechanical gear-box (mechanical system). EMAs are classified into rotary and linear actuators. The linear actuators are further classified into geared and direct-driven linear EMAs. In general, the geared linear electromechanical actuator consists of a DC motor with a lead-screw (or ball-screw or roller-screw) and a nut assembly. The motor shaft is seen connected to the lead-screw with the aid of a shaft-coupling or a gear-box as shown in figure 4.1. The DC motor converts the electrical energy into the rotational motion of the shaft and the lead-screw will then convert this rotary

motion into linear motion. The motor shaft will rotate either in the clockwise or anti-clockwise direction depending upon the input polarity. Once the rotations of the shaft are transferred to the lead-screw, the nut makes a translational motion (X_N) either in the forward or backward direction depending on the rotational direction of the shaft.

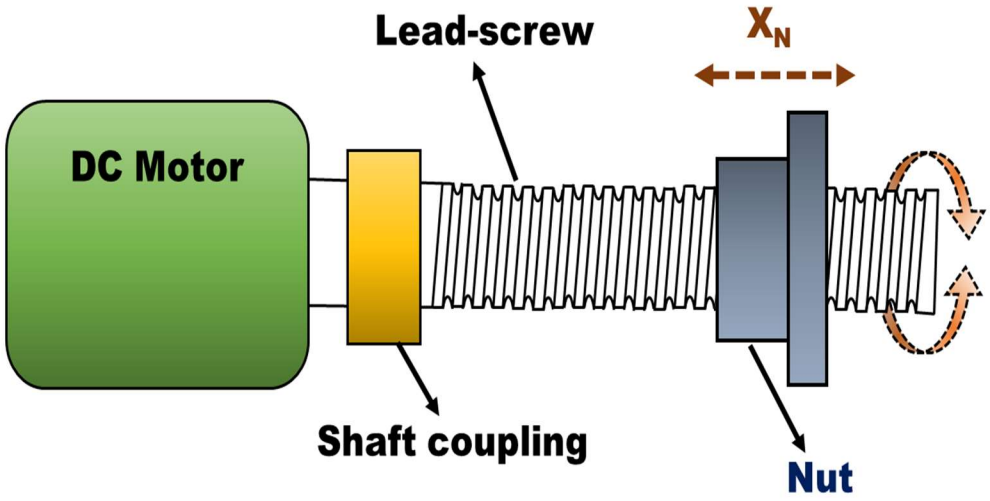

Figure 4.1 Geared Linear EMA

In the direct-driven linear electromechanical actuator, the nut serves as the rotational element and lead-screw acts as the translational element. As shown in figure 4.2, the lead-screw arrangement has been accommodated inside the motor itself. The internally threaded nut is fixed inside the hollow portion of the rotor. When the motor is supplied with electrical energy, both the rotor and the nut rotate and this rotational motion of the nut will help the lead-screw travel linearly. The shaft that is attached to the end of the lead-screw has slotted grooves that restrict the rotational motion of the lead-screw along with the nut. In terms of their function, these two actuators are not very different. However, the direct-driven EMA has a compact size compared to the geared EMA. This is what makes the direct-driven EMA most suitable and appropriate for aerospace industries, robotics, and other industrial machinery.

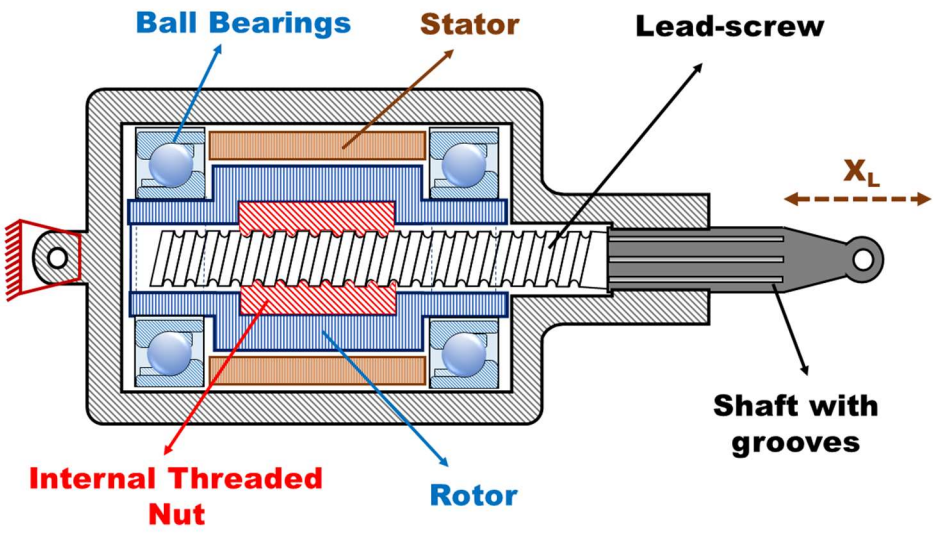

Figure 4.2 The cross-sectional view of a direct-driven linear EMA

Table 4.1 Actuator parameters used in the simulation

S.No.	Parameter	Value
1	Resistance of the armature (R_a)	0.4Ω
2	Inductance of the armature (La)	0.8 mH
3	Motor back e.m.f constant (K_e)	0.036867 V/rads^{-1}
4	Motor torque constant (K_t)	0.030892 Nm/A
5	Motor and ball screw inertia (J)	4.4574e^{-5} kgm^2
6	Motor and ball screw viscous friction (D)	8.2985e^{-4} Nm/rads^{-1}
7	Screw damping coefficient (C_s)	25610 N/ms^{-1}
8	Screw stiffness (K_s)	201060000 N/m
9	Ball screw lead (l)	0.002 m/rev
10	Gear ratio (N)	1
11	Motor mass	1kg
12	External Load mass	5kg

Table 4.2 Material and Geometrical Parameters of Actuator Components

S.No.	Component	Material	Geometry
1	Lead screw	Stainless Steel screw, copper nut	Pitch= 1mm Lead of thread = 6mm Screw Diameter = 6mm Screw Length = 100mm Nut Size =10x13x25mm
2	Shaft Coupling	Aluminum alloy	Outer Diameter = 12mm Inner diameters = 3mm & 6mm Length = 25mm
3	Ball bearing	Stainless Steel	Inner diameter = 3mm Outer diameter = 10mm
4	Linear Bearing	Steel balls with aluminum housing	Length = 30mm Width = 30mm Inner diameter = 8mm

4.2 Mathematical Modeling of Single EMA

Before constructing a multi-element actuator like HRA, modeling of a single EMA system is very essential to understand the behavior of it. The schematic diagram of the single EMA as shown in the figure 4.3 was drawn to obtain the mathematical equations. The motor armature equations were obtained by applying Kirchhoff's Voltage Law (KVL) which states that "*for a closed loop series path the algebraic sum of all the voltages around any closed loop in a circuit is equal to zero*". The torque equations were obtained to get the mechanical loads and also the Free Body Diagram (FBD) of the external load were drawn and based on all the equations the mathematical modeling of the single EMA was obtained.

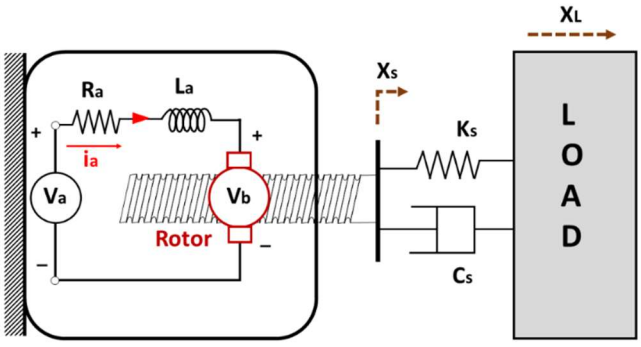

Figure 4.3 The Schematic Diagram of a Direct-Driven linear EMA

4.2.1 Motor armature current

The modeling of the EMA starts with developing the equations related to the DC motor. The schematic diagram with an electrical motor circuit, lead-screw, dampers, and the load of a direct-driven EMA with all the notations is shown in figure 4.3. The electric circuit in the schematic diagram indicates that the applied electrical power with a voltage (V_a) is opposed by the conducting path resistance (R_a), inductance (L_a) and a back e.m.f (V_b) which is equal to $K_e(d\,\theta_m/dt)$ then the voltage expressed by applying the KVL to motor armature circuit is:

$$V_a = K_e(d\,\theta_m/dt) + R_a i_a + L_a(di_a/dt) \tag{4.1}$$

$$\frac{di_a}{dt} = \frac{1}{L_a}[V_a - K_e(d\,\theta_m/dt) - R_a i_a\,] \tag{4.2}$$

Where K_e is the back e.m.f constant and θ_m is the angular displacement of the motor. In the mechanical system, damping, inertia, and frictional properties are concentrated quantities. When the electromagnetic torque generated by the electric circuit is applied to the mechanical system's (lead-screw and nut) rotary element, it rotates at a speed of $(d\,\theta_m/dt)$ which has a moment of inertia (J_m). The rotational speed of both the rotor and the nut is the same because both are attached. X_s and X_L are the linear displacements of the lead-screw and the load respectively. K_s represents the equivalent stiffness that exists between lead-screw and nut and the damping that exists between bearing and rotor is represented by C_s.

4.2.2 Motor mechanical load

The generated torque (τ_m) is opposed by damping torque (τ_d), load torque (τ_l) and an inertial torque (τ_i). Hence, the generated electromagnetic torque is balanced by the other three torques and it is expressed in the equation 4.3.

$$\tau_m = \tau_d + \tau_l + \tau_i \tag{4.3}$$

$$\tau_m = K_t i_a \tag{4.4}$$

$$\tau_d = D(d\,\theta_m/dt) \tag{4.5}$$

$$\tau_i = J_m(d^2\,\theta_m/dt^2) \quad 4.6$$

where D is the equivalent viscous damping coefficient at the armature

The torque (τ_m) generated by the current (i_a) which is passing through the armature is given by the equation (3), where K_t is the motor torque constant. Similarly, the damping, inertial and load torques are given in the subsequent equations (4.5, 4.6, and 4.8) respectively. In the equation (4.8), the term $(l/2\pi N)$ is used for converting the angular displacement of the nut into linear displacement of the lead-screw, where l is the screw lead, N is the gear ratio, β is the helix angle, $\theta_m(t)$ represents the angular advancement generated by the motor as shown in figure 4.4.

$$X_s(t) = \frac{l}{2\pi}\theta_m(t) \quad 4.7$$

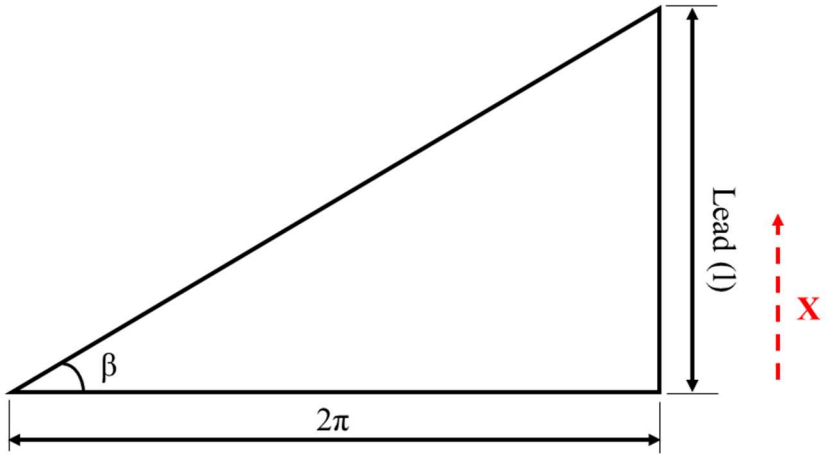

Figure 4.4 One unwind thread of a lead screw

$$\tau_l = (C_s l/2\pi\, N)\left(\dot{X}_s - \dot{X}_L\right) + (K_s l/2\pi N)(X_s - X_L) \quad 4.8$$

Where X_s *= Screw linear displacement*

X_L *= Load linear displacement*

C_s *= Screw damping coefficient*

K_s *= Screw stiffness*

l *= Lead of the screw*

N *= Gear ratio*

Therefore the motor torque

$$\tau_m = \tau_d + \tau_i + \tau_l$$

$$K_t i_a = D(d\,\theta_m/dt) + J_m(d^2\,\theta_m/dt^2) + (C_s l/2\pi\, N)\left(\dot{X}_s - \dot{X}_L\right) + (K_s l/2\pi N)(X_s - X_L) \qquad 4.9$$

By rewriting the above equation

$$\ddot{\theta}_m = \frac{1}{J_m}[K_t i_a - D\dot{\theta}_m - \left[(C_s l/2\pi\, N)\left(\dot{X}_s - \dot{X}_L\right)\right] - [(K_s l/2\pi N)(X_s - X_L)] \qquad 4.10$$

Let us consider N = 1 and replace $(l/2\pi N)$ by 'P' and $X_s(t) = \frac{l}{2\pi}\theta_m(t)$

=> $X_s(t) = P\theta_m(t)$ then equation 4.10 becomes

$$\ddot{\theta}_m = \frac{1}{J_m}[K_t i_a - D\dot{\theta}_m - \left[C_s P\left(P\dot{\theta}_m - \dot{X}_L\right)\right] - [K_s P(P\theta_m - X_L)]$$

$$\rightarrow \ddot{\theta}_m = \frac{1}{J_m}[K_t i_a - \dot{\theta}_m(D + C_s P^2) - \theta_m K_s P^2 + C_s P\dot{X}_L + K_s P X_L] \qquad 4.11$$

4.2.3 External Load

The free body diagram (FBD) of the single EMA's external load was drawn as shown in figure 4.5 and based on that, the following mathematical equations were obtained.

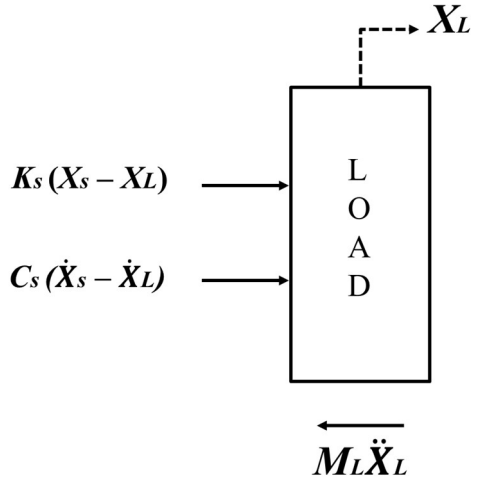

Figure 4.5 The free body diagram of external load of a single EMA

$$M_L\ddot{X}_L = K_s(X_s - X_L) + C_s(\dot{X}_s - \dot{X}_L) \quad 4.12$$

By substituting $X_s = P\theta_m$ and rewriting the equations, then

$$\ddot{X}_L = \frac{1}{M_L}[K_sP\theta_m\ - K_sX_L + C_sP\dot{\theta}_m - C_s\dot{X}_L] \quad 4.13$$

For solving the derived equations from 4.2 to 4.13 a Simulink model was built and the parameter values given in were substituted. In the Simulink model, a square wave signal builder block was used as input signal and an integrator block that is used to integrate actuator velocity to linear position. The value of the square wave was set to 6V and -6V to make the actuator to move forward and backward directions. The Simulink model block diagram of single EMA was shown in Figure 4.6.

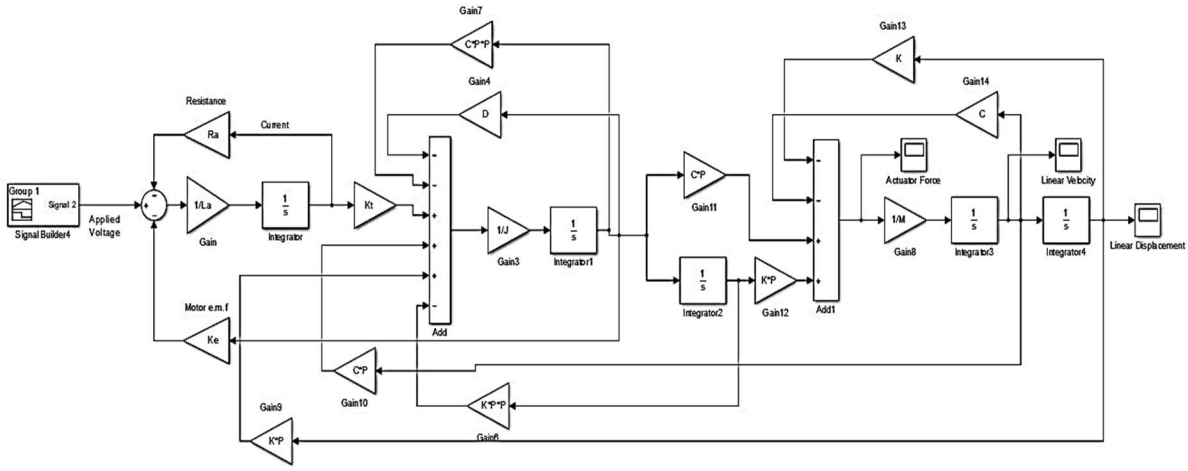

Figure 4.6 Simulink Block diagram of a single actuator

4.3 Mathematical Modeling of Actuators in Series

4.3.1 Two actuators connected in series

Figure 4.7 shows a schematic diagram of two actuators connected in series with a load attached to the second actuator. The first actuator A1 has its base connected to a fixed support and treated as nonmoving while the second actuator A2 has its base connected to the actuation end of actuator A1 which means that the base of actuator A2 will move due to the force exerted by actuator A1. The linear displacement of actuator A1 is X_{S1} and the

linear displacement of actuator A2 is the sum of $X_{b2} + X_{s2}$, where X_{b2} is the displacement of the actuator A2 base, and X_{s2} is the displacement of A2 actuator. So an additional equation for the base of actuator A2 was considered. Figure 4.8 shows the Free Body Diagram (FDB) of the actuators A2 connected in series, and from the FBD, all the mathematical expressions were derived. Based on these schematic diagrams and FBD, any number of series actuators can be modeled.

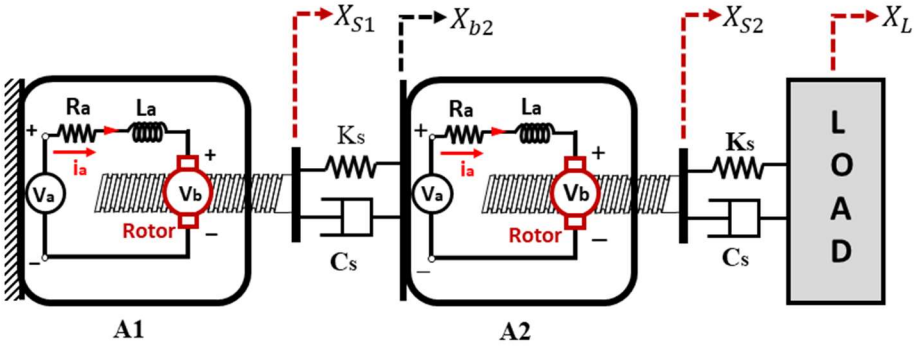

Figure 4.7 Schematic diagram of two actuators A1 and A2 connected in series

4.3.1.1 Mathematical Model of Actuator A1

i. Armature Current

All the actuators are identical to each other, so the equation for the armature current is the same as equation 4.2 which is:

$$\frac{di_{a1}}{dt} = \frac{1}{L_{a1}}[V_{a1} - K_{e1}(d\,\theta_{m1}/dt) - R_{a1}i_{a1}\,]$$

Where i_{a1} *refers to the armature current,* L_{a1} *refers to the armature inductance* R_{a1} *refers to armature resistance,* K_{e1} *refers to motor back e.m.f constant* θ_{m1} *refers to the angular displacement of the A1 armature.*

ii. Mechanical Loading

Actuator A2 is connected to actuator A1, so the external load for actuator A1 is the mass of the actuator A2. The mechanical equations can be obtained by the FBD of the actuator A2 and the external load connected to the actuator A2. The torque equation of actuator A1 by considering A2 as external load is:

$$\ddot{\theta}_{m1} = \frac{1}{J_{m1}}[K_t i_{a1} - \dot{\theta}_{m1}(D + C_s P^2) - \theta_{m1} K_s P^2 + C_s P\dot{X}_{b2} - K_s P X_{b2}] \quad 4.14$$

Where X_{b2} and $\dot{X}_{b2}$ are the linear displacement and velocity of the actuator A2.

4.3.1.2 Mathematical Modeling of Actuator A2

i. Armature Current

All the actuation elements are identical to each other, so the equation for the armature current is the same as equation 4.2 which is,

$$\frac{di_{a2}}{dt} = \frac{1}{L_{a2}}[V_{a2} - K_{e2}(d\,\theta_{m2}/dt) - R_{a2} i_{a2}\,]$$

where i_{a2} refers to the armature current, R_{a2} refers to armature resistance, L_{a2} refers to the armature inductance, K_{e2} refers to motor back e.m.f constant, θ_{m2} refers to the angular displacement of the A2 actuator.

ii. Mechanical loading

Similar to equation 4.11, the equations for the mechanical loading can be obtained by replacing the external load with actuation element A2.

$$\ddot{\theta}_{m2} = \frac{1}{J_{m2}}[K_t i_{a2} - \dot{\theta}_{m2}(D + C_s P^2) - K_s P^2 \theta_{m2} - K_s P X_{b2} + K_s P X_L - C_s P\dot{X}_{b2} + C_s P\dot{X}_L] \quad 4.15$$

iii. Equations of the base

The equation of the base was obtained by considering actuator A2 as the external load. The FBD of actuator A2 was shown in the figure 4.8.

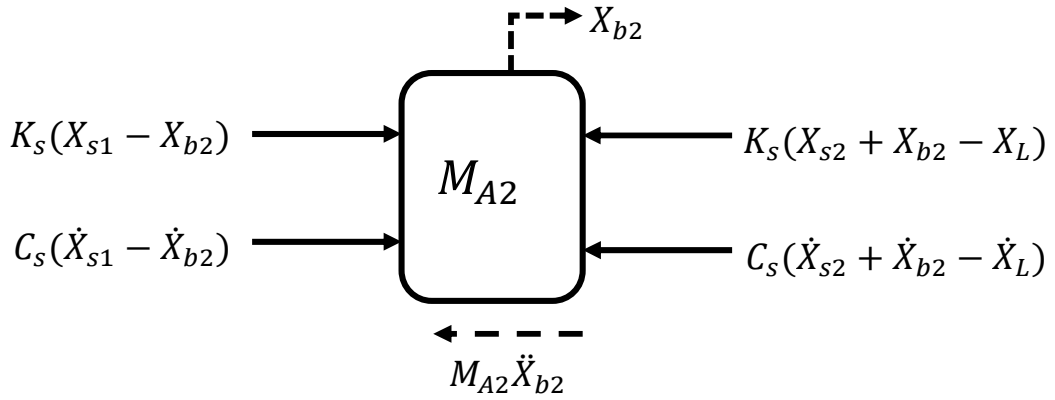

Figure 4.8 FBD of A2 actuator's motor

$$M_{A2}\ddot{X}_{b2} = K_s(X_{s1} - X_{b2}) + C_s\left(\dot{X}_{s1} - \dot{X}_{b2}\right) - K_s(X_{s2} + X_{b2} - X_L) - C_s\left(\dot{X}_{s2} + \dot{X}_{b2} - \dot{X}_L\right)$$

$$\Rightarrow \ \ddot{X}_{b2} = \frac{1}{M_{A2}}[K_sP\theta_{m1} - 2K_sX_{b2} + C_sP\dot{\theta}_{m1} - 2C_s\dot{X}_{b2} - K_sP\theta_{m2} + K_sX_L - C_sP\dot{\theta}_{m2} + C_s\dot{X}_L] \qquad 4.16$$

iv. External Load

The FBD of the external load connected to the actuator A2, and the linear acceleration was provided in the equation 4.17.

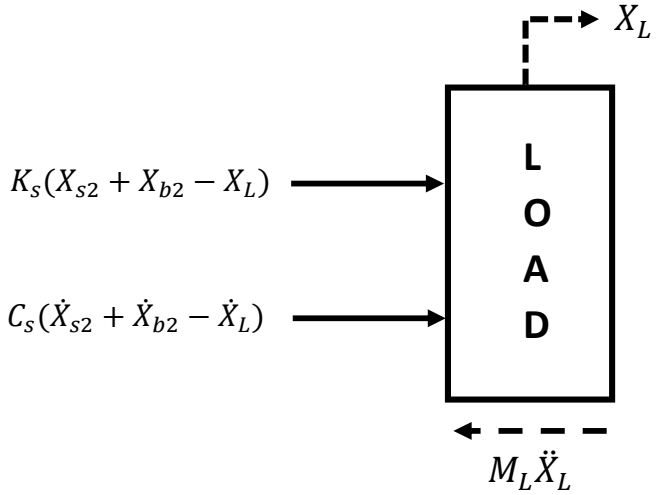

Figure 4.9 FBD of external load connected to actuator A2

$$\Rightarrow M_L\ddot{X}_L = K_s(X_{s2} + X_{b2} - X_L) + C_s(\dot{X}_{s2} + \dot{X}_{b2} - \dot{X}_L)$$

$$\Rightarrow \ddot{X}_L = \frac{1}{M_L}[K_s(P\theta_{m2} + X_{b2} - X_L) + C_s(P\dot{\theta}_m + \dot{X}_{b2} - \dot{X}_L)]$$

$$\ddot{X}_L = \frac{1}{M_L}[K_sP\theta_{m2} + C_sP\dot{\theta}_m + K_sX_{b2} + C_s\dot{X}_{b2} - K_sX_L - C_s\dot{X}_L] \quad 4.17$$

4.3.2 Three Actuators connected in Series

Similarly, when three actuators are connected in series and the schematic and free body diagram are shown in figure 4.10 and 4.11. Equations 4.18 to 4.23 are the equations of angular accelerations and linear accelerations of the actuators A1, A2, A3 and the linear acceleration of the load which are drawn from the free body diagram. Here, mass of actuator A2 will act as the external load for actuator A1 and mass of actuator A3 will act as the external load for actuator A2.

The equations are solved with the help of MATLAB/Simulink and the results of the actuator parameters such as displacement, force and linear accelerations of single actuator, two actuators in series and three actuators in series are plotted in the figure 4.12 and the values of the same are provided in the table 4.3.

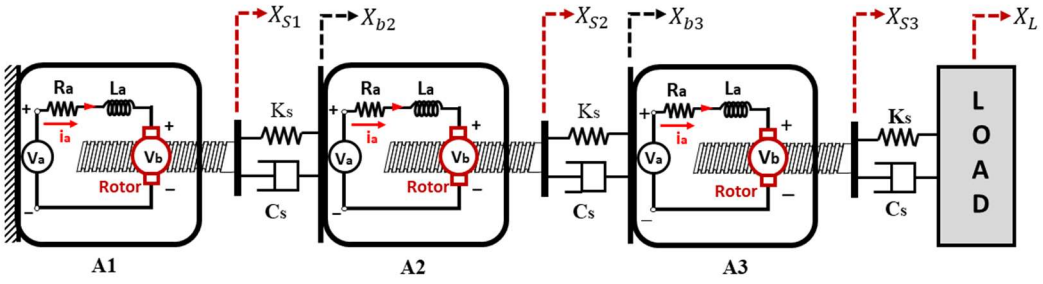

Figure 4.10 Schematic diagram of three actuators A1, A2 and A2 connected in series

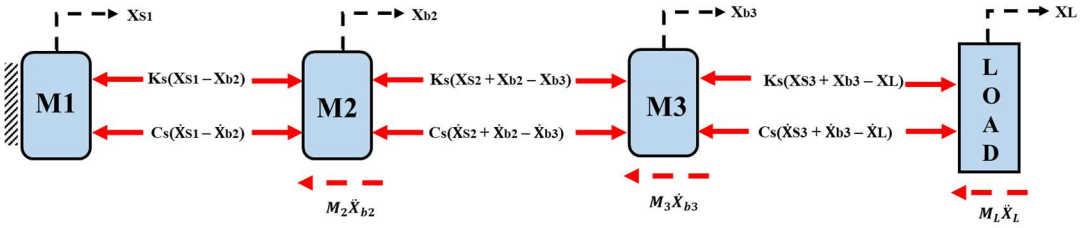

Figure 4.11 FBD of three actuators which are connected in series

$$\ddot{\theta}_1 = \frac{1}{J}[K_t I_1 - D\dot{\theta}_1 - K(P^2\theta_1 - hX_{b2}) - C(P^2\dot{\theta}_1 - h\dot{X}_{b2})] \quad 4.18$$

$$\ddot{X}_{b2} = \frac{1}{M_2}[K(P\theta_1 - 2X_{b2} - P\theta_2 + X_{b3}) + C(P\dot{\theta}_1 - 2\dot{X}_{b2} - P\dot{\theta}_2 + \dot{X}_{b3})] \quad 4.19$$

$$\ddot{\theta}_2 = \frac{1}{J}[K_t I_2 - D\dot{\theta}_2 - K(P^2\theta_2 + PX_{b2} - hX_{b3}) - C(P^2\dot{\theta}_2 + P\dot{X}_{b2} - P\dot{X}_{b3})] \quad 4.20$$

$$\ddot{X}_{b3} = \frac{1}{M_3}[K(P\theta_2 - 2X_{b3} - P\theta_3 + X_L) + C(P\dot{\theta}_2 - 2\dot{X}_{b3} - P\dot{\theta}_3 + \dot{X}_L)] \quad 4.21$$

$$\ddot{\theta}_3 = \frac{1}{J}[K_t I_3 - D\dot{\theta}_3 - K(P^2\theta_3 + PX_{b2} + PX_{b3} - PX_L) - C(P^2\dot{\theta}_3 + P\dot{X}_{b2} + P\dot{X}_{b3} - P\dot{X}_L)] \quad 4.22$$

$$\ddot{X}_L = \frac{1}{L}[K(P\theta_3 + X_{b2} + X_{b3} - X_L) + C(P\dot{\theta}_3 + \dot{X}_{b2} + \dot{X}_{b3} - \dot{X}_L)] \quad 4.23$$

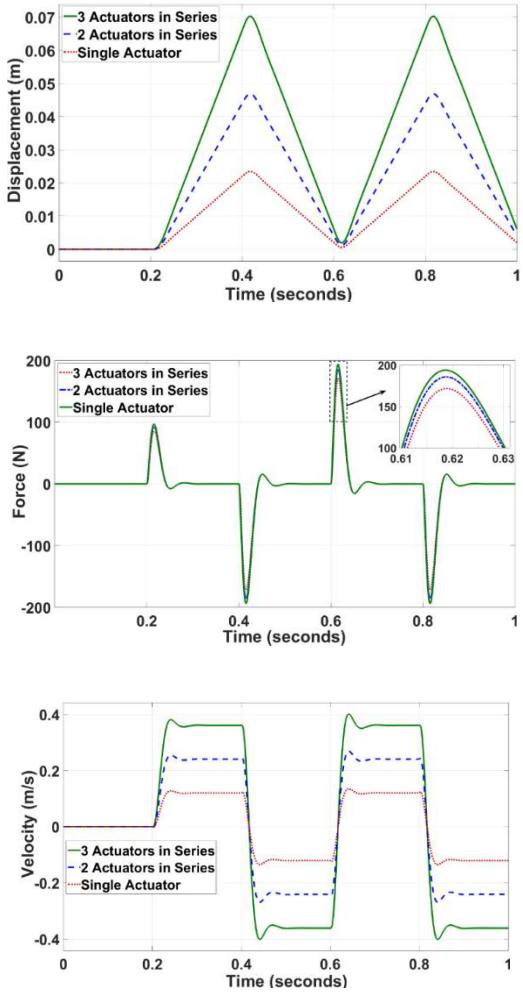

Figure 4.12 The displacement, force, and velocities of first, second and third actuators which are connected in a pure series configuration.

Table 4.3 Performance value of actuation elements connected in series

Actuation Element	Displacement (cm)	Force (N)	Velocity (cm/s)
First	2.346	193.9	12.03
Second	4.687	185.7	24.04
Third	7.027	171.6	36.09

4.4 Mathematical Modeling of Actuators in Parallel

4.4.1 Two actuators connected in parallel

Figure 4.13 shows the schematic diagram of two actuators A1 and A2 connected in parallel. In this particular configuration, both actuators are connected to the same load, and both elements have a fixed base. Therefore the equation for the load needs to be modified. Equation for the armature current of both actuation elements will be similar to Equation 4.2 and equation for the mechanical loading of both actuation elements will be similar to Equation 4.11.

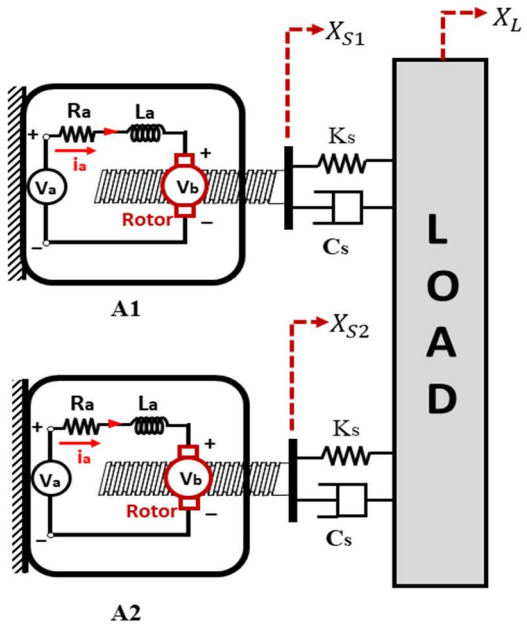

Figure 4.13 Schematic diagram of two actuators A1 and A2 connected in parallel

i. Armature Current

All the actuation elements are identical to each other, so the equation for the armature current and mechanical loading are the same as equation 4.2 and 4.11 which are:

$$\frac{di_{a1}}{dt} = \frac{1}{L_{a1}}[V_{a1} - K_{e1}(d\,\theta_{m1}/dt) - R_{a1}i_{a1}\,]$$

ii. Mechanical loading

$$\ddot{\theta}_m = \frac{1}{J_m}[K_t i_a - \dot{\theta}_m(D + C_s P^2) - \theta_m K_s P^2 + C_s P\dot{X}_L + K_s P X_L]$$

iii. External Load

The two actuators are connected to the same load as they are connected in parallel. So, the FBD of the load will be as shown in the figure 4.14.

$$M_L\ddot{X}_L = K_s(X_{s1} - X_L) + C_s\left(\dot{X}_{s1} - \dot{X}_L\right) + K_s(X_{s2} - X_L) + C_s(\dot{X}_{s2} - \dot{X}_L)$$

$$\ddot{X}_L = \frac{1}{M_L}[K_s P\theta_{m1} + C_s P\dot{\theta}_{m1} - 2K_s X_L - 2C_s\dot{X}_L + K_s P\theta_{m2} + C_s P\dot{\theta}_{m2}] \qquad 4.24$$

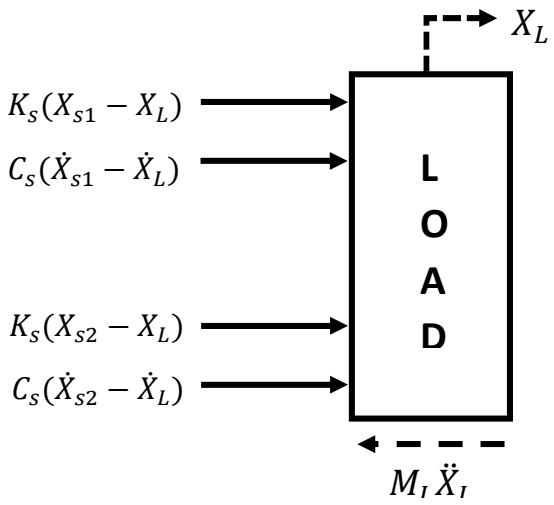

Figure 4.14 FBD of external load when actuators connected in parallel

4.4.2 Three actuators connected in parallel

Similarly, when three actuators are connected in parallel then the schematic and free body diagram are shown in figure 4.15 and 4.16. Equation 4.25 is the equation of linear acceleration of the load which was drawn from the free body diagram.

The equations are solved with the help of MATLAB/Simulink and the results of the actuator performance such as displacement, force and linear accelerations of single actuator, two actuators in parallel and three actuators in parallel are plotted in the figure 4.17 and the values of the same are provided in the table 4.4.

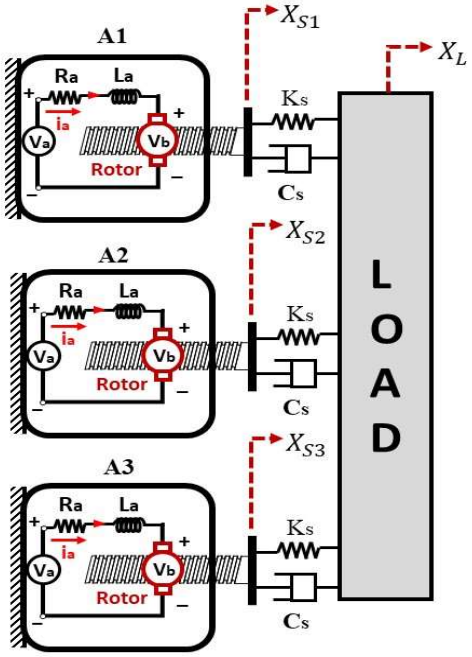

Figure 4.15 Schematic diagram of three actuators A1, A2, A3 Connected in parallel

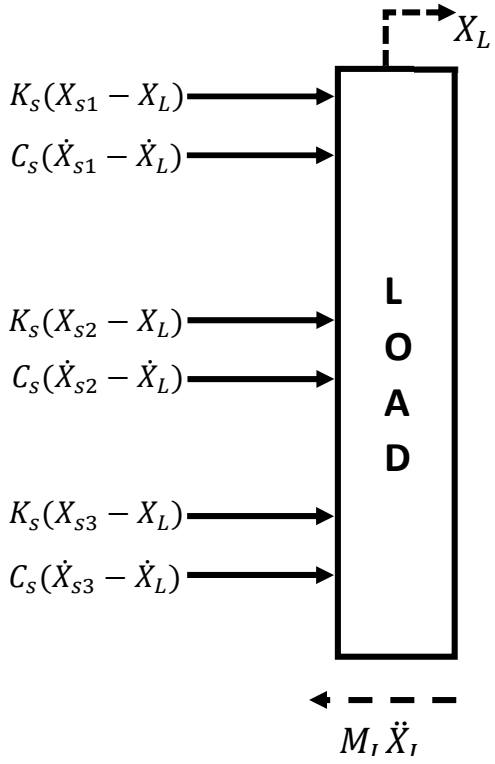

Figure 4.16 FBD of external load of three actuators A1, A2 and A3 connected in parallel

$$\ddot{X}_L = \frac{1}{M_L}[K_s P\theta_{m1} + C_s P\dot{\theta}_{m1} - 2K_s X_L - 2C_s \dot{X}_L + K_s P\theta_{m2} + C_s P\dot{\theta}_{m2}] \qquad 4.25$$

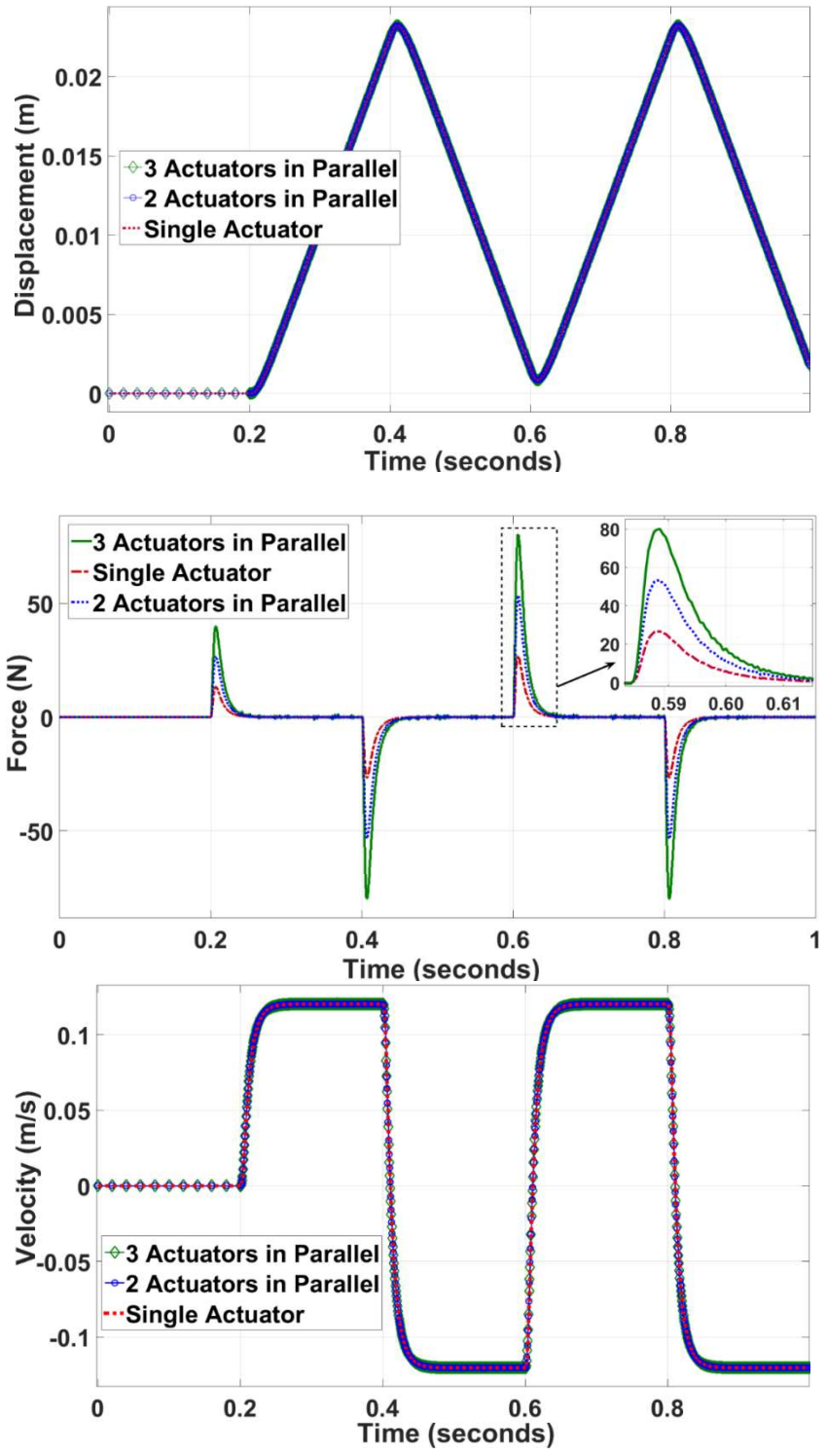

Figure 4.17 The displacement, force, and velocities of first, second and third actuators which are connected in a pure parallel configuration.

Table 4.4 Performance values of three actuation elements in parallel

Actuation Element	Displacement (cm)	Force (N)	Velocity (cm/s)
First	2.323	26.8	12.04
Second	2.323	53.59	12.04
Third	2.323	80.39	12.04

The performance values of actuators which are connected in pure series and pure parallel configurations are given in the below table 4.5.

Table 4.5 Performance of three actuation elements in pure parallel and pure series configuration.

S.No.	Output	Actuators in Parallel		Actuators in Series	
		Single Actuator (A1)	Three Actuators	Single Actuator (A1)	Three Actuators
1	Displacement (cm)	2.323	2.323	2.346	7.027
2	Force (N)	26.8	80.39	193.9	171.6
3	Velocity (cm/s)	12.04	12.04	12.03	36.09

4.5 Mathematical Modeling of 3×3 HRA in Series-in-Parallel Configuration

The schematic diagram of nine actuators in 3×3 configuration of series-in-parallel with an external load was given in the figure 4.18. It can be considered as three sets of three actuators in series are connected to the external load. The equations of a single row of three actuation elements in series are provided in the equations 4.18 to 4.23. From these equations the linear displacement capability of the HRA can be obtained and by adding the

forces of all the three sets of series elements which are connected to the external load will provide the force capability of the HRA. So, by solving all the equations, the displacement, force and linear velocity values of the 3×3 HRA compared with the single EMA were provided in the table 4.6.

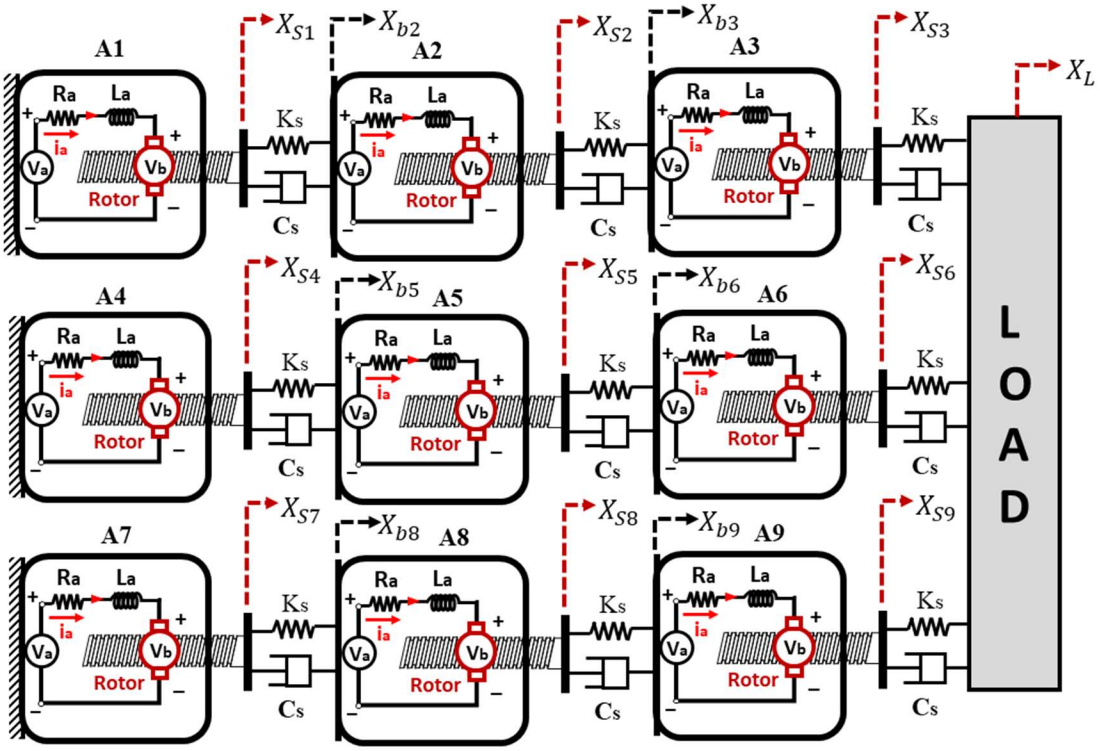

Figure 4.18 Schematic diagram of nine actuators in 3×3 series-in-parallel configuration with an external load

Table 4.6 Comparison of performance of single actuator with 3×3 HRA

S.No.	Output	Single Actuator	3x3 HRA
1	Displacement (cm)	2.346	7.007
2	Force (N)	26.8	204.4
3	Velocity (cm/s)	12.03	36.1

4.6 EMA Faults and the Implementation of faults in the Simulation

As EMA is a combination of electrical and mechanical elements, there is an equal chance of occurrence of a fault in either of these elements. Although there are many faults that can occur in both the elements [15]. Researchers mainly focused on the common faults which cause the individual actuators to fail. The most common mechanical faults considered are lock-up fault and the loose fault. Similarly, most common electrical motor faults that are considered include open-circuit (OC) and short-circuit (SC) faults.

OC fault in the motor can occur due to the breakage of one or more turns in the winding phase. When this happens, the flow of current becomes zero in the fault phase and there is no torque generation by the motor. This fault can be simulated in the simulation model by keeping the current passing through the winding and the torque of the motor as zero for a particular actuator.

SC fault occurs when turns inside the windings are shorted together. Depending on the number of short turns, a significant change in the resistance, mutual and self-inductance and also the back E.M.F changes occur. However, no positive torque is generated. This fault can be simulated by setting the supply voltage of a particular actuator to zero.

Lock-up or jamming fault occurs when lead-screw or ball-screw nut gets jammed. This happens because of fragmentation or deformation of the balls or because of the locking of the gears in the gear-box. This results in the failure of the transmission of the actuator. To analyze the consequences of this fault in the HRA, the fault was introduced into the simulation model manually by making the displacement of a particular actuator as zero.

Loose fault results from loss in applied force between the mechanical elements or the free movement of the lead-screw without any restriction/force. This fault can be modeled by making the output force of the element, zero, which is equivalent to making the input voltage, zero. Hence, there is not much variation in the effect due to SC fault and loose fault in the simulation point of view. So, for this particular simulation, both faults under consideration were treated as equal. Table 4.7 provides the information regarding the implementation of faults in the model.

Table 4.7 Implementation of faults in the mathematical model

S.NO.	Fault	Reason	Effect	Influenced	Implementing in the simulation
1	Open circuit	One or more turns break	No current or torque	Torque and speed	Making current as zero
2	Short circuit	One or more turns get shorted	Resistance, self-inductance, and back EMF changes	No positive torque	Making the voltage as zero
3	Lockup	Ball screw may be jammed by fragments, Ball deformation or deformation of the gear train	Failure of transmission	Travel or actuator position	Making the displacement of the actuator to zero
4	Loose	Loss in applied force between the mechanical elements or free movement of the lead-screw without any restriction/force	No applied force	Force of the actuator	Making the voltage as zero

4.6.1 Faults in the Pure Series and in the Pure Parallel Configuration

Figure 4.19(a) and (b) shows the pure parallel and pure series configuration with three actuation elements A1, A2 and A3 out of which actuator A1 was subjected to fault. In the initial stage, the performance of three actuators connected in a pure parallel configuration and three actuators connected in the pure series configuration were analyzed under both healthy and faulty conditions. When the actuators were moving in the forward and backward direction, the linear displacement, force and the linear velocities of the actuators with respect to time were plotted. Figure 4.20 and figure 4.21 shows the

performance of actuators connected in pure parallel and in a pure series configuration under actuator A1 subjected to different faults individually and table 4.8 provides the performance values of it.

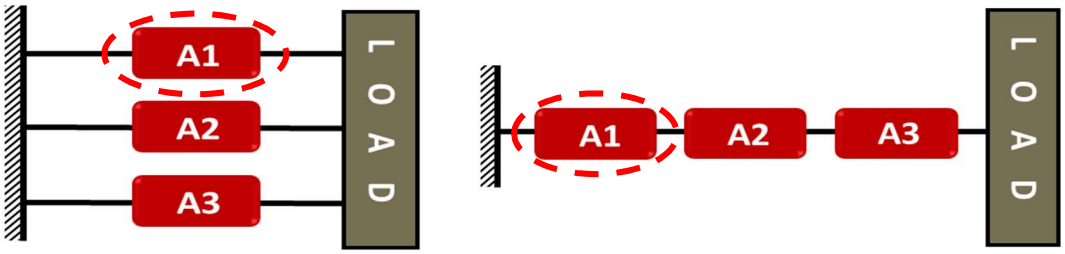

(a) **(b)**

Figure 4.19 (a) A pure parallel configuration (b) A pure series configuration.

Table 4.8 Performance of the pure parallel and pure series configurations of three actuators under A1 actuator subjected to fault.

S.No.	Fault	Three Actuators in Parallel			Three Actuators in Series		
		Displacement (cm)	Force (N)	Velocity (cm/s)	Displacement (cm)	Force (N)	Velocity (cm/s)
1	Healthy	2.323	80.39	12.04	7.027	164.6	36.17
2	Lock-up	0	970.4	0	4.679	127.3	24.07
3	Open circuit	0.52	52.58	6.06	4.712	114.5	24.0
4	Loose/ short-circuit	1.548	53.33	8.022	4.678	108.0	24.05

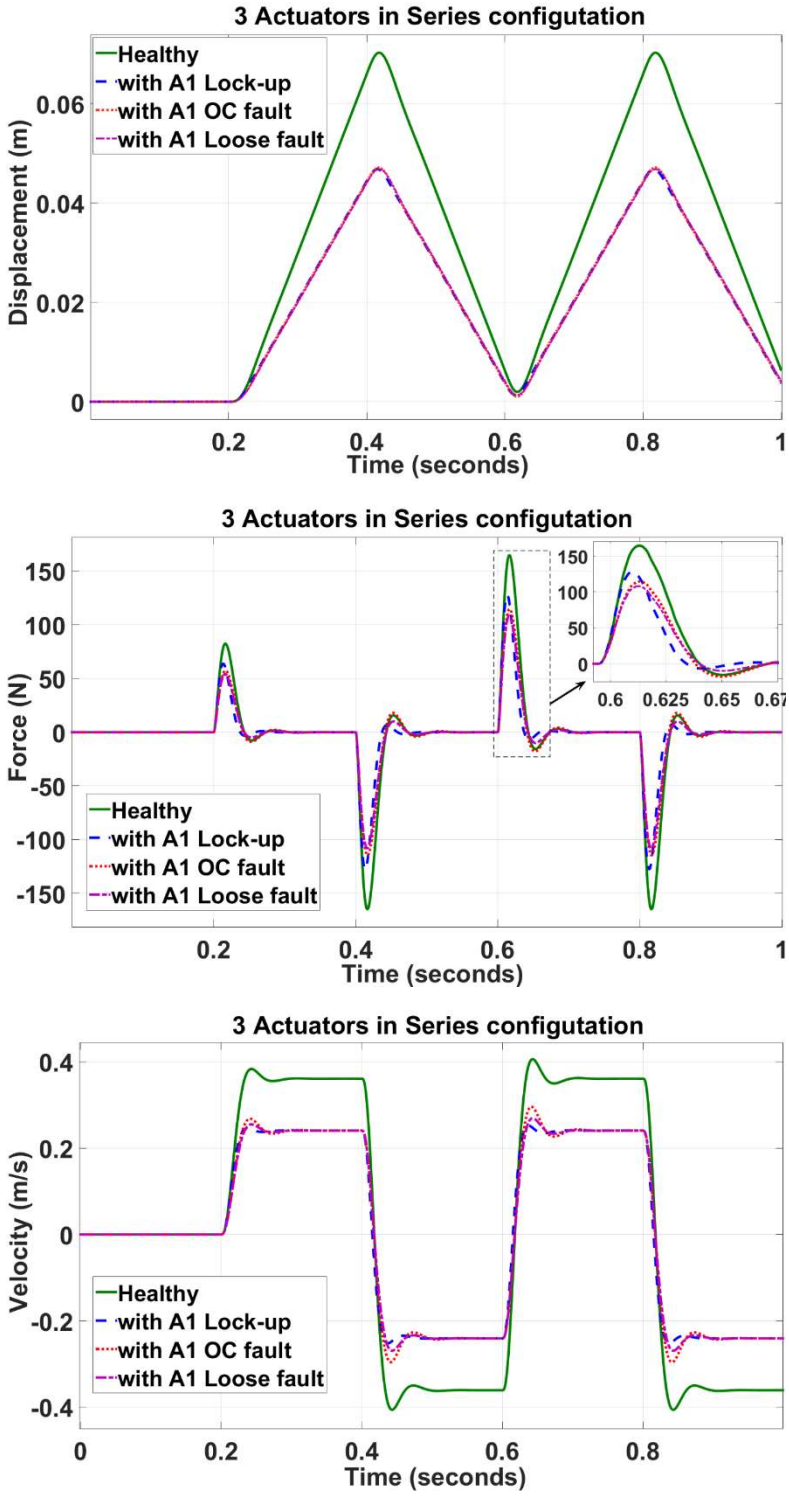

Figure 4.20 The comparison of displacement, force, and velocities of pure series configuration of three actuators, when actuator A1 subjected to lock-up, open-circuit and short circuit/loose faults individually.

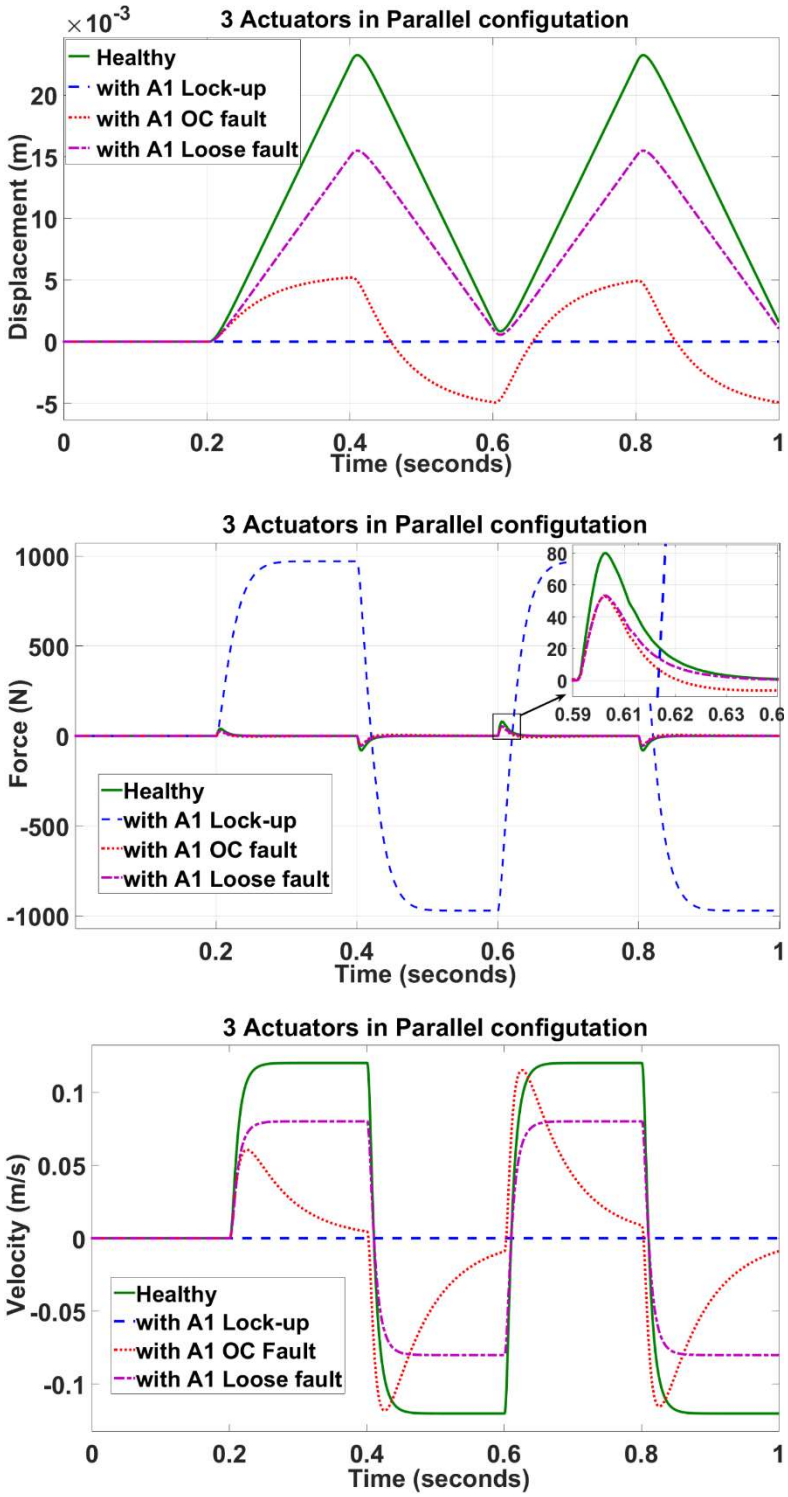

Figure 4.21 The comparison of displacement, force, and velocities of a pure parallel configuration of three actuators, when actuator A1 subjected to lock-up, open-circuit and short-circuit/loose faults individually.

4.6.2 Lock-up Faults in the 3×3 HRA

The 3×3 HRA actuation elements numbering and the representation of lock-up faults was shown in figure 4.22(a) and (b). The actuator A1 under the lock-up fault will act as a rigid element and there was no movement in that particular actuator. The lock-up fault in the HRA are introduced by increasing the number of faults in the column wise starting from A1 to A9. To avoid the confusion by plotting all the nine faulty actuation element results in a single plot it was divided into three results per plot. Figure 4.23(a), Figure 4.23(b) and Figure 4.23(c) show the resultant linear displacement, force and velocities of 3×3 HRA under lock-up fault. The values of the performance of the 3×3 HRA under lock-up faults are provided in the table 4.9.

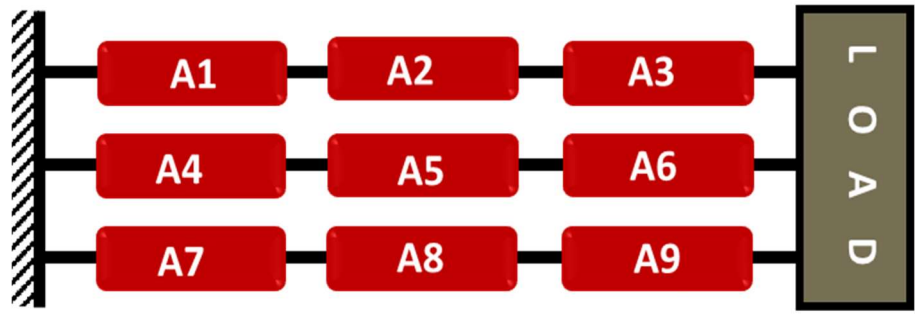

(a)

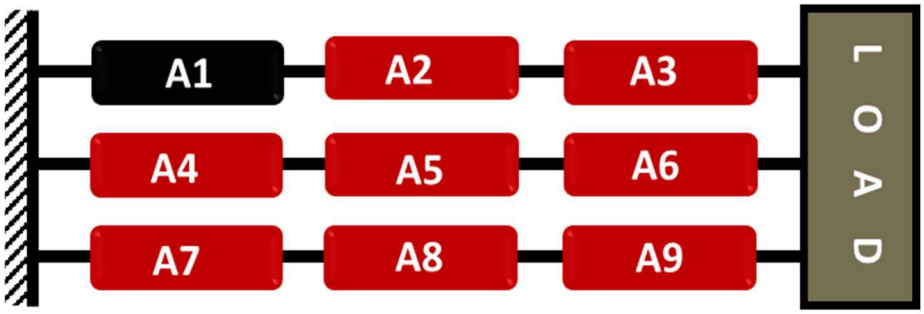

(b)

Figure 4.22 Block diagram representation of a 3× 3 HRA (a) Healthy condition (b) with A1 actuator under lock-up fault

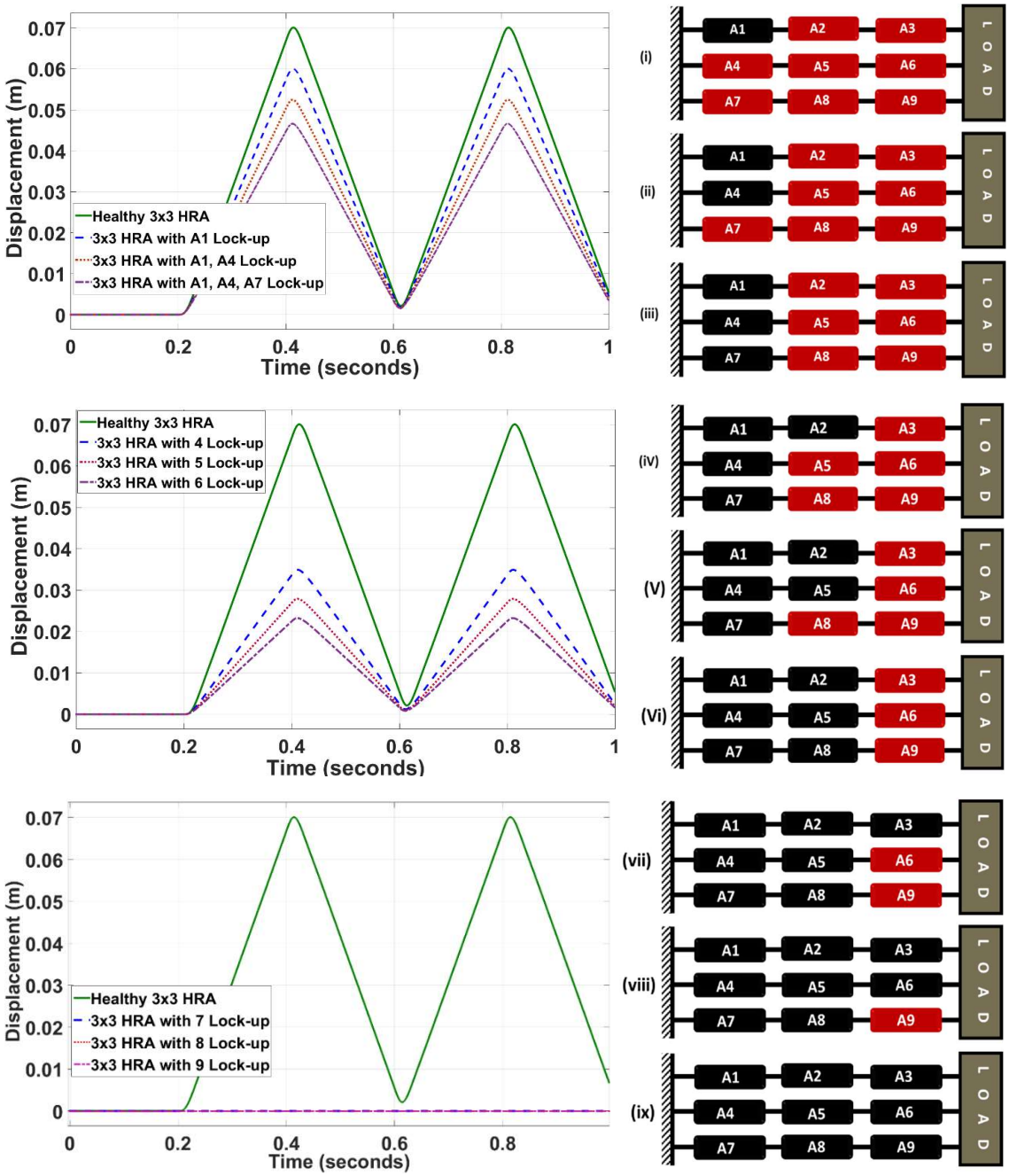

Figure 4.23(a) Displacements of a 3×3 HRA under increasing the number of lock-up faults in the actuator from A1 to A9 (column-wise).

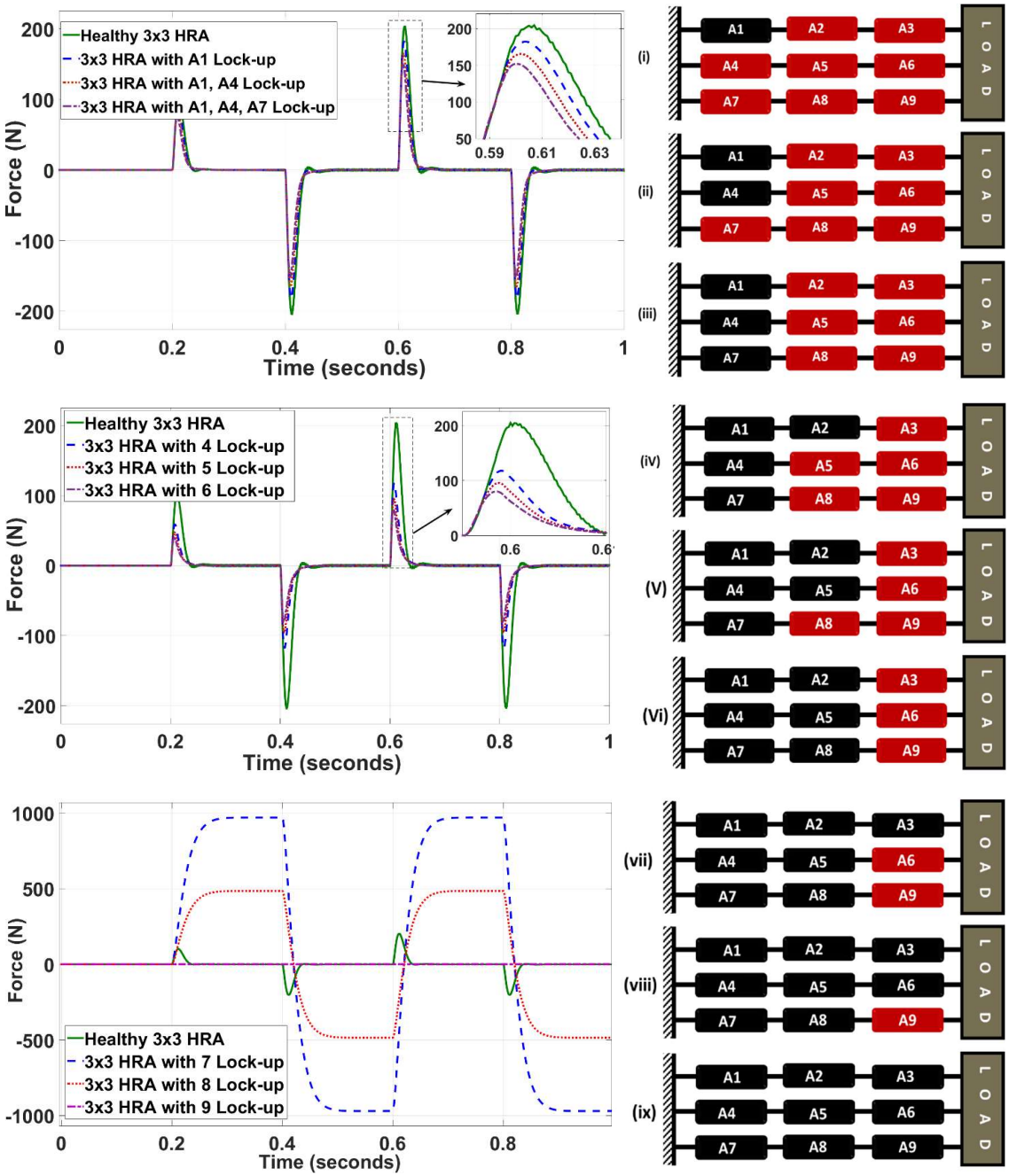

Figure 4.23(b) Force of a 3×3 HRA under increasing the number of lock-up faults in the actuator from A1 to A9 (column-wise).

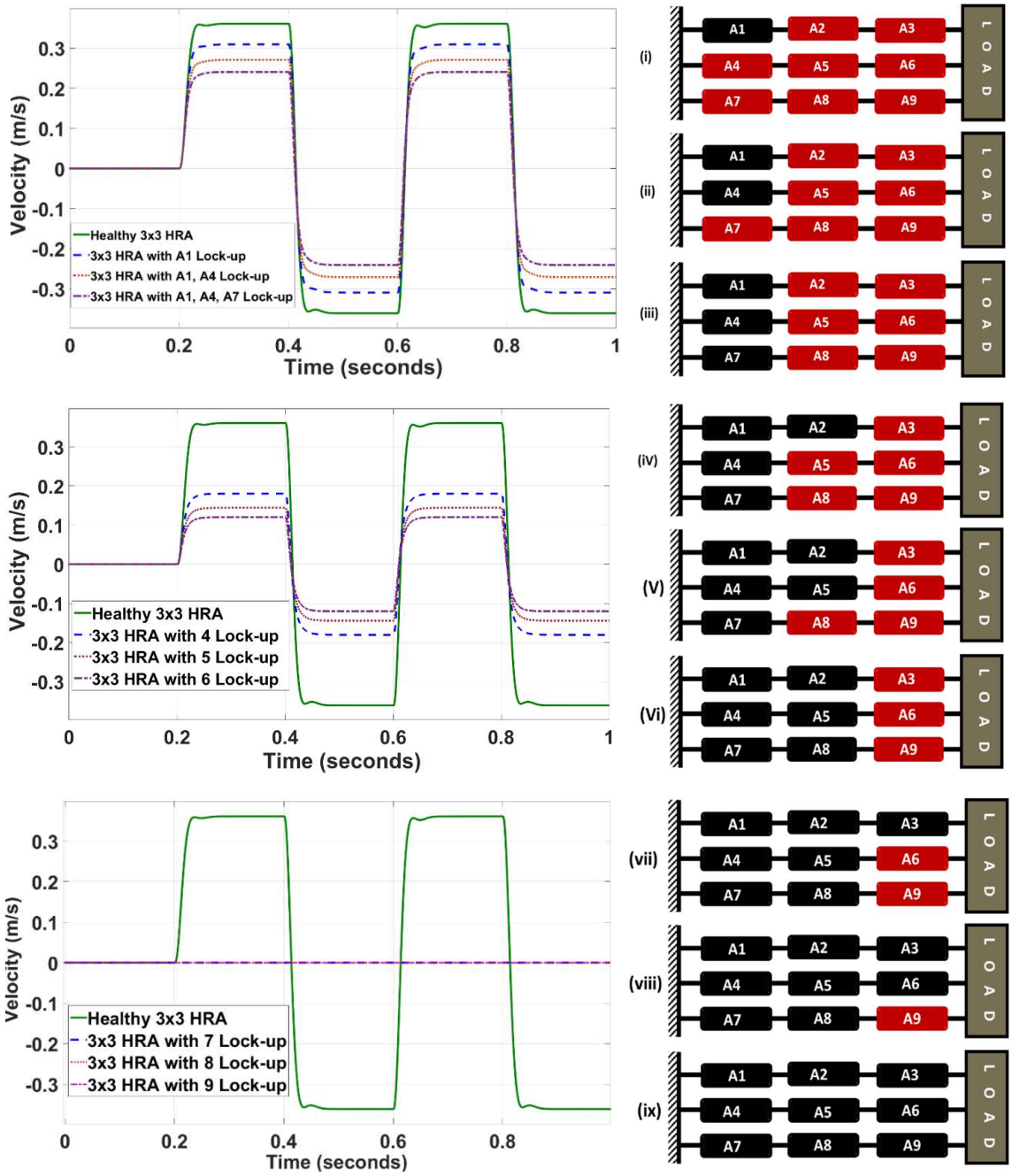

Figure 4.23(c) Linear velocity of a 3×3 HRA under increasing the number of lock-up faults in the actuator from A1 to A9 (column-wise).

Table 4.9 Performance values of 3×3 HRA under the lock-up faults.

S.No.	Max output	Healthy	Fault introduced in Column-1			Fault introduced in Column-1 and 2			Fault introduced in Column-1, 2 and 3		
		0-fault	1-fault (A1)	2-faults (A1,A4)	3-faults (A1,A4,A7)	4-faults (A1,A4,A7, A2)	5-faults (A1,A4, A7,A2, A5)	6-faults (A1,A4,A 7,A2,A5, A8)	7-faults (A1,A4,A 7,A2,A5, A8,A3)	8-faults (A1 to A8)	9-faults (A1 to A9)
1	Displacement (cm)	7.007	6.002	5.245	4.661	3.491	2.789	2.323	0	0	0
2	Force (N)	204.4	182.0	165.4	151.8	117.7	95.62	79.96	970	485.2	0
3	Velocity (cm/s)	36.1	30.94	27.07	24.06	18.05	14.44	12.03	0	0	0

4.6.2 Loose fault/Short circuit Faults in the 3×3 HRA

The 3×3 HRA actuation elements numbering and the representation of loose/short-circuit faults was shown in figure 4.24(a) and (b). The actuator under the loose fault will act like there is no physical connection between the ends. The loose fault/short circuit fault in the HRA are introduced by increasing the number of faults in the column wise starting from A1 to A9. To avoid the confusion by plotting all the nine faulty actuation element results in a single plot it was divided into three results per plot. Figure 4.25(a), Figure 4.25(b) and Figure 4.25(c) show the resultant linear displacement, force and velocities of 3×3 HRA under loose fault/short circuit faults. The values of the performance of the 3×3 HRA under lock-up faults are provided in the table 4.10.

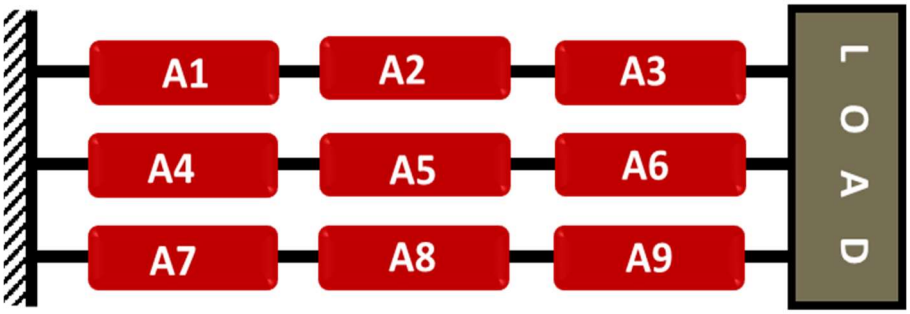

(a)

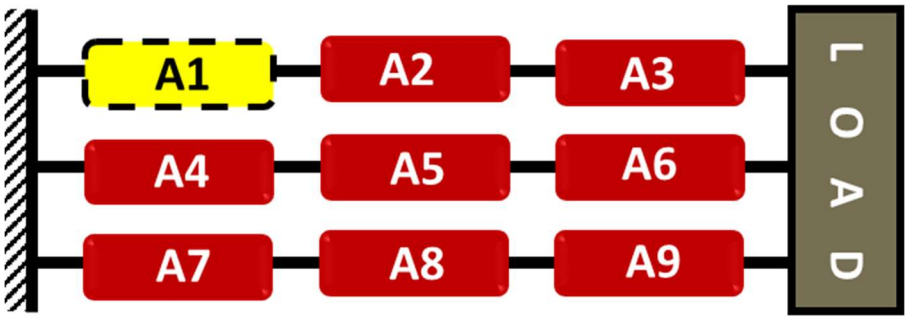

(b)

Figure 4.24 Block diagram representation of a 3× 3 HRA (a) Healthy condition (b) with A1 actuator under loose fault

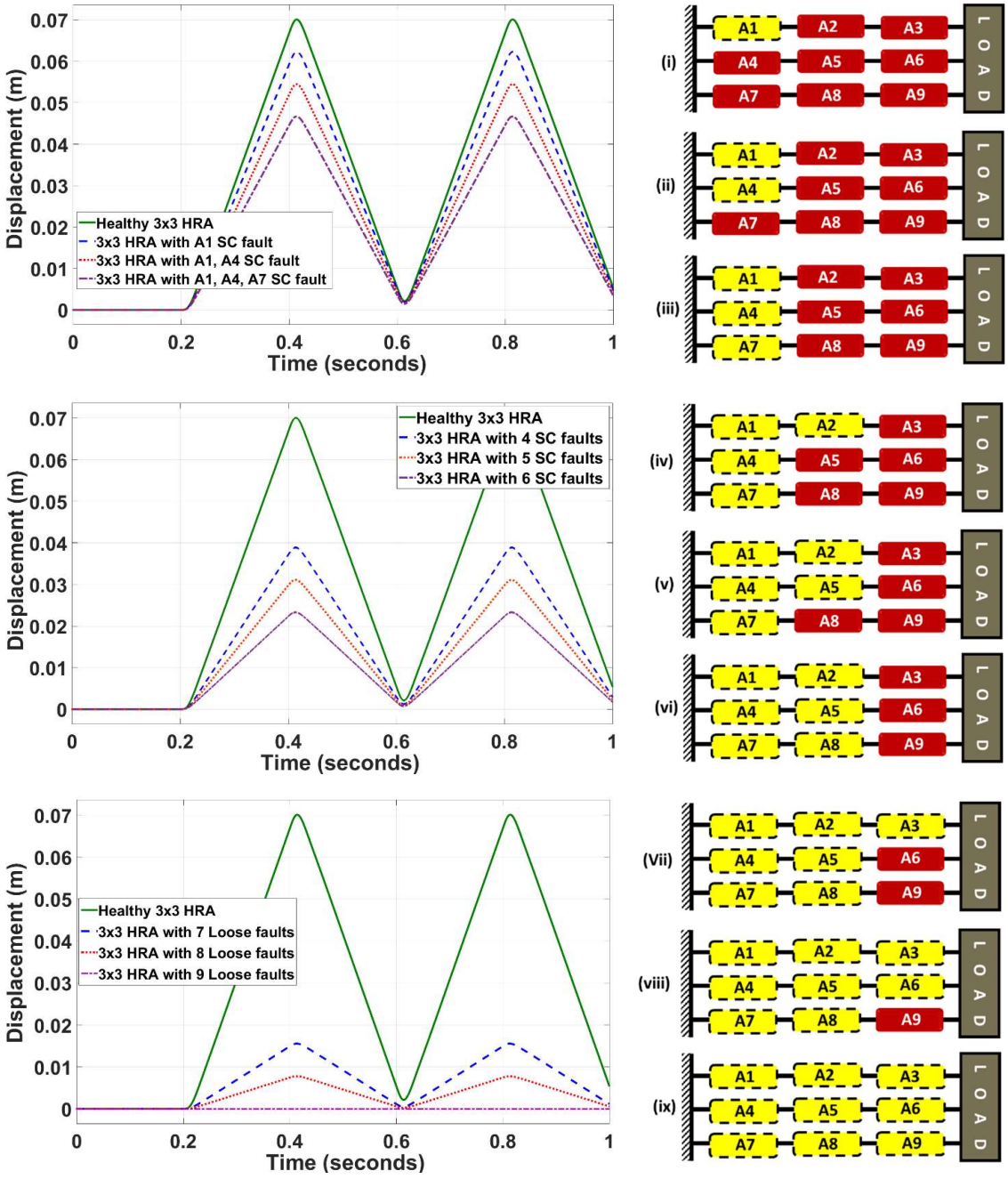

Figure 4.25(a) Displacements of a 3×3 HRA under increasing the number of short circuit/loose faults in the actuator from A1 to A9 (column-wise)

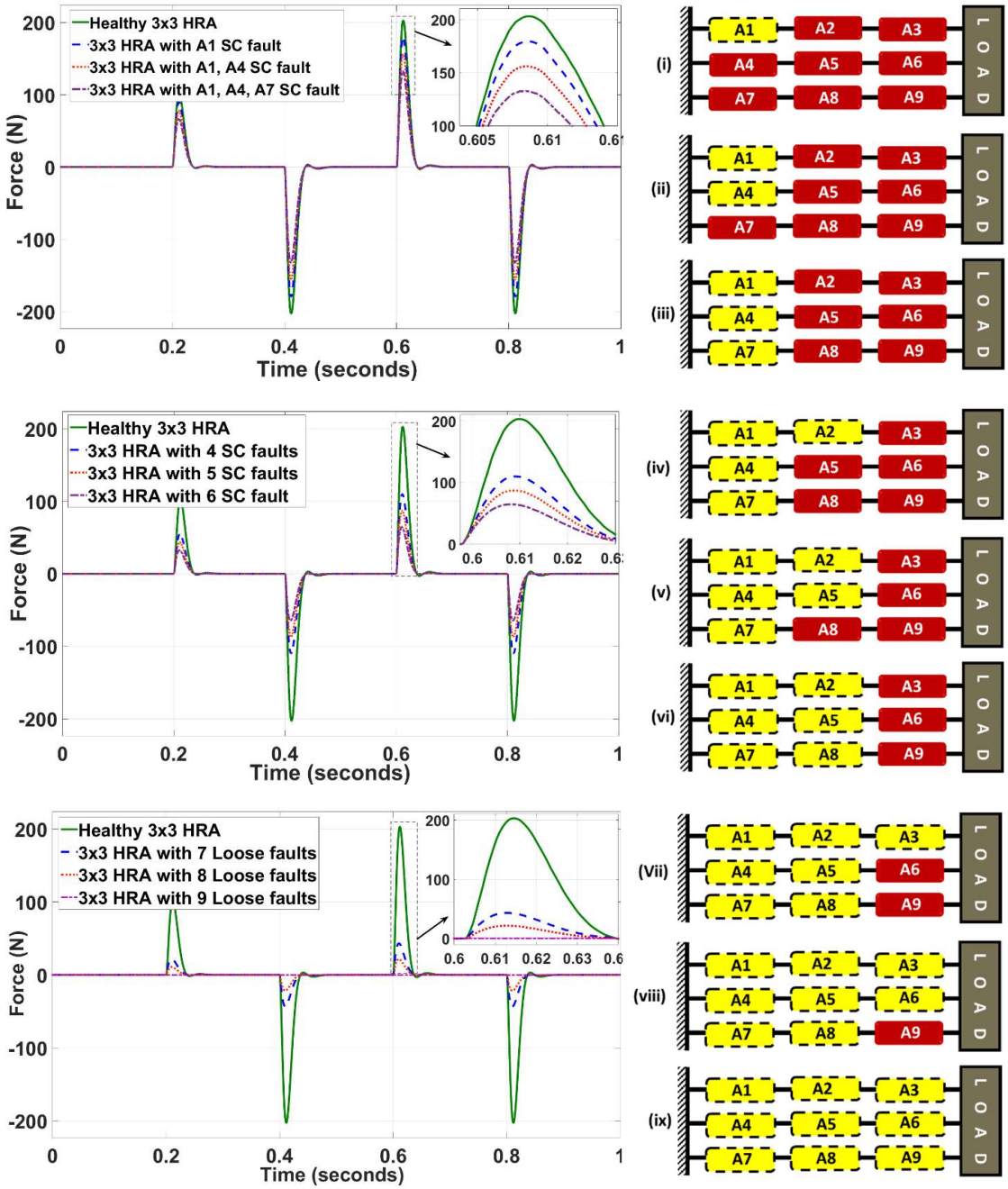

Figure 4.25(b) Force of a 3×3 HRA under increasing the number of short circuit/loose faults in the actuator from A1 to A9 (column-wise)

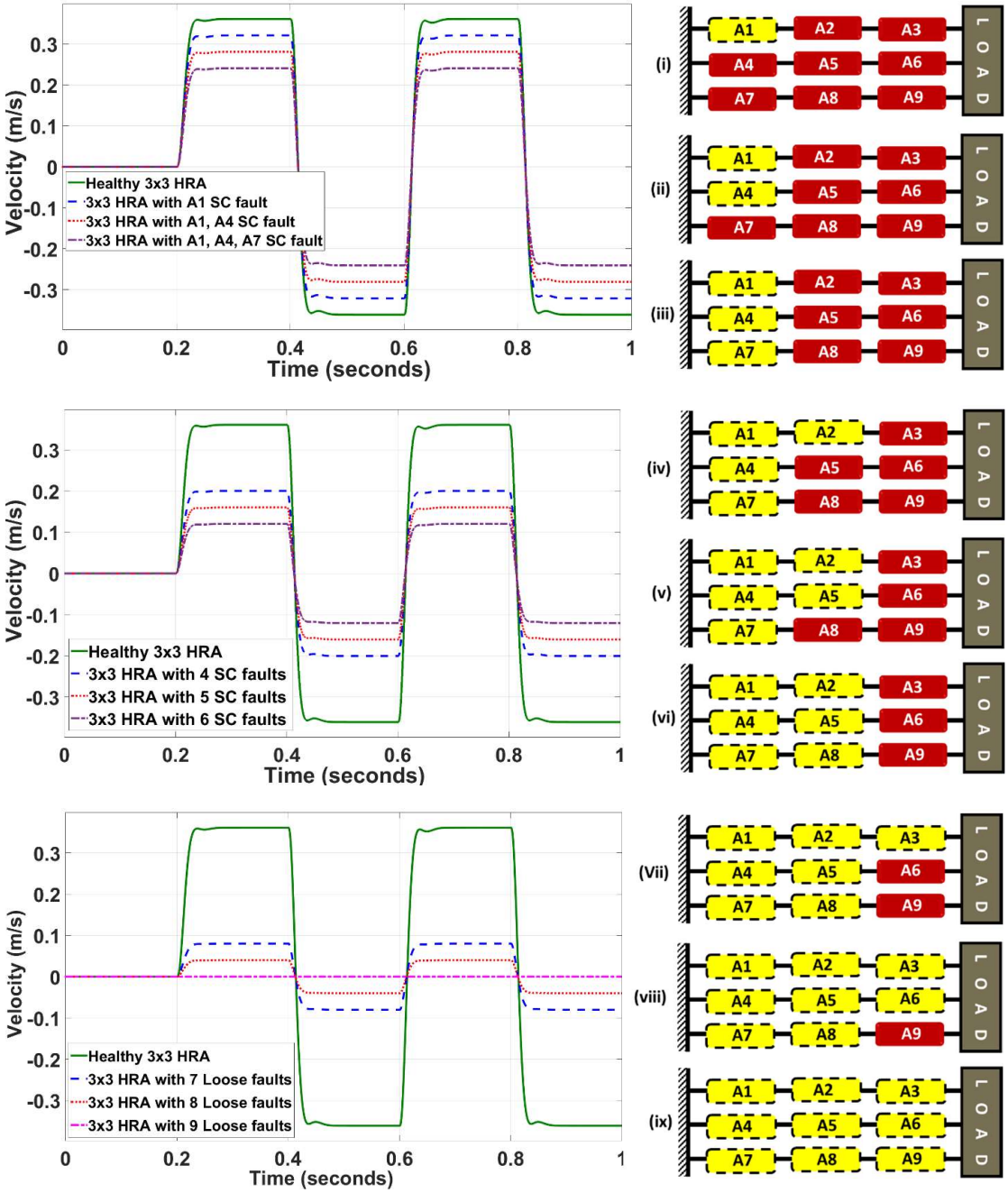

Figure 4.25(c) Linear velocity of a 3×3 HRA under increasing the number of short circuit/loose faults in the actuator from A1 to A9 (column-wise)

Table 4.10 Performance values of 3×3 HRA under the loose/short circuit faults.

S.No.	Max output	Healthy	Fault introduced in Column-1			Fault introduced in Column-1 and 2			Fault introduced in Column-1, 2 and 3		
		0-fault	1-fault (A1)	2-faults (A1,A4)	3-faults (A1,A4,A7)	4-faults (A1,A4, A7,A2)	5-faults (A1,A4, A7,A2,A5)	6-faults (A1,A4,A7, A2,A5,A8)	7-faults (A1,A4, A7,A2, A5,A8, A3)	8-faults (A1 to A8)	9-faults (A1 to A9)
1	Displacement (cm)	7.007	6.227	5.447	4.668	3.888	3.109	2.33	1.6	0.8	0
2	Force (N)	204.4	179.5	156	132.6	109.9	87.14	64.66	43	21.6	0
3	Velocity (cm/s)	36.1	32.08	28.07	24.06	20.05	16.04	12.03	8.0	4.0	0

4.6.3 Open circuit Faults in the 3×3 HRA

The 3×3 HRA actuation elements numbering and the representation of open circuit faults was shown in figure 4.26(a) and (b). This fault can be simulated in the simulation model by keeping the current passing through the winding and the torque of the motor as zero for a particular actuator. The open circuit fault in the HRA are introduced by increasing the number of faults in the column wise starting from A1 to A9. To avoid the confusion by plotting all the nine faulty actuation element results in a single plot it was divided into three results per plot. Figure 4.27(a), Figure 4.27(b) and Figure 4.27(c) show the resultant linear displacement, force and velocities of 3×3 HRA under open circuit faults. The values of the performance of the 3×3 HRA under open circuit fault are provided in the table 4.11.

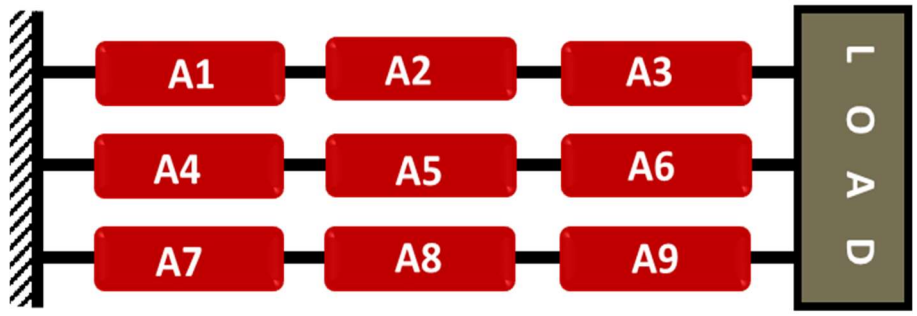

(a)

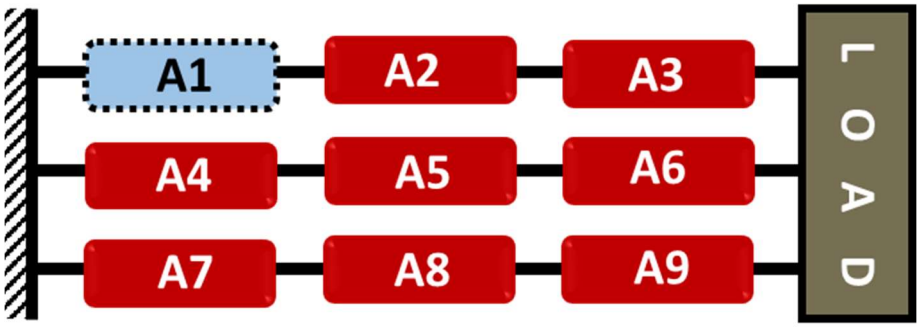

(b)

Figure 4.26 Block diagram representation of a 3× 3 HRA (a) Healthy condition (b) with A1 actuator under open circuit fault

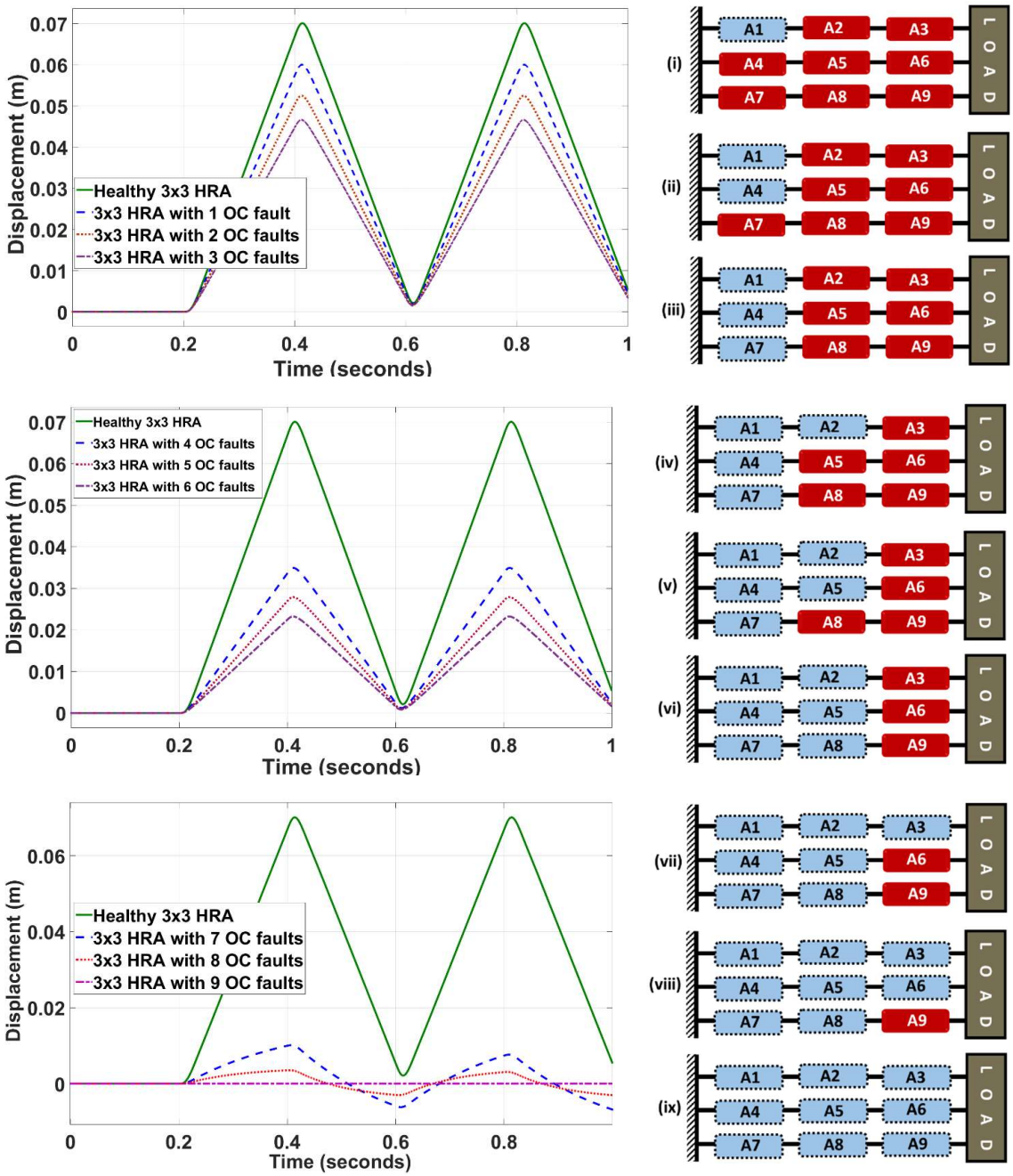

Figure 4.27(a) Displacements of a 3×3 HRA under increasing the number of open-circuit faults in the actuator from A1 to A9 (column-wise)

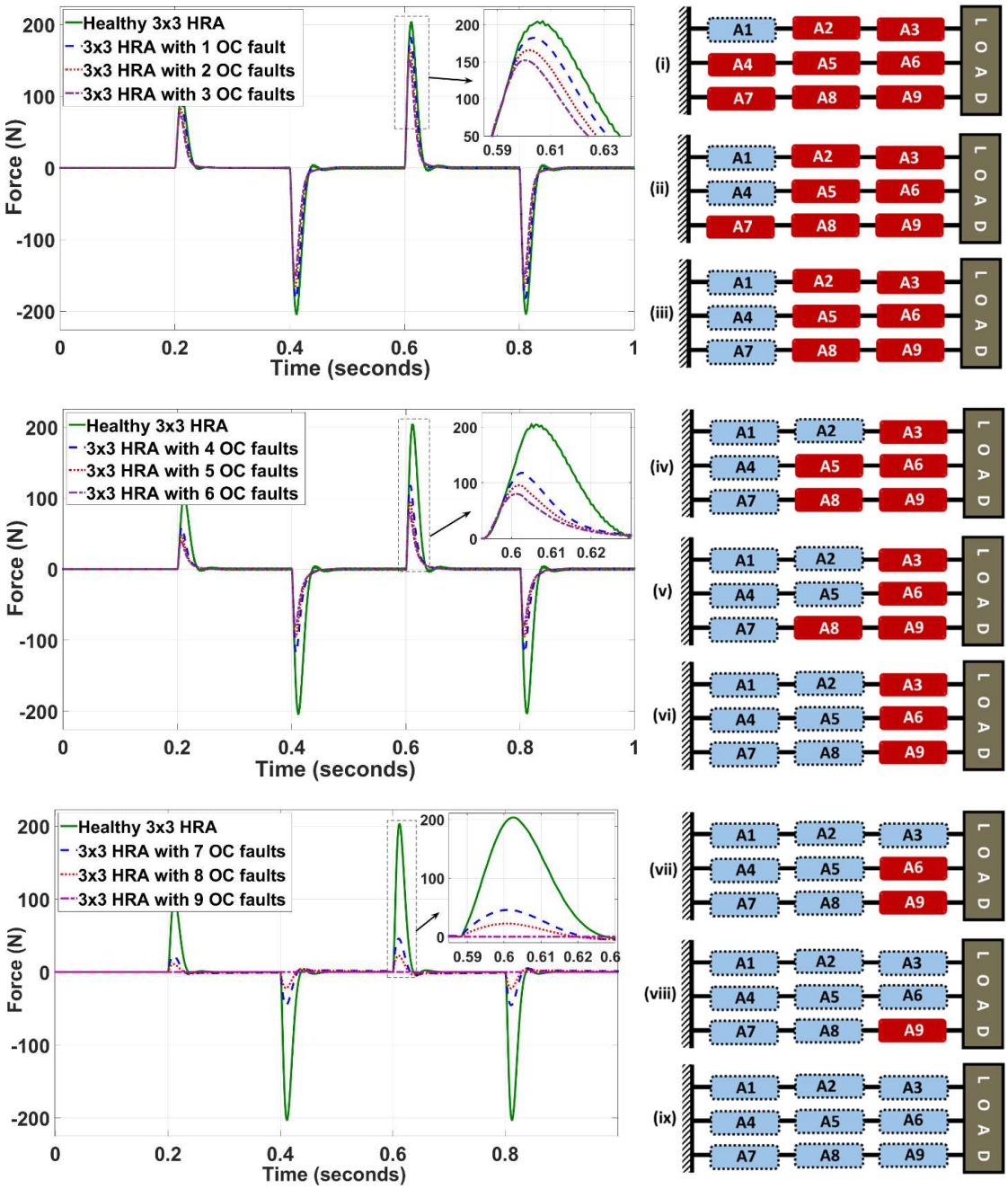

Figure 4.27(b) Forces induced due to 3×3 HRA under increasing the number of open-circuit faults in the actuator from A1 to A9 (column-wise)

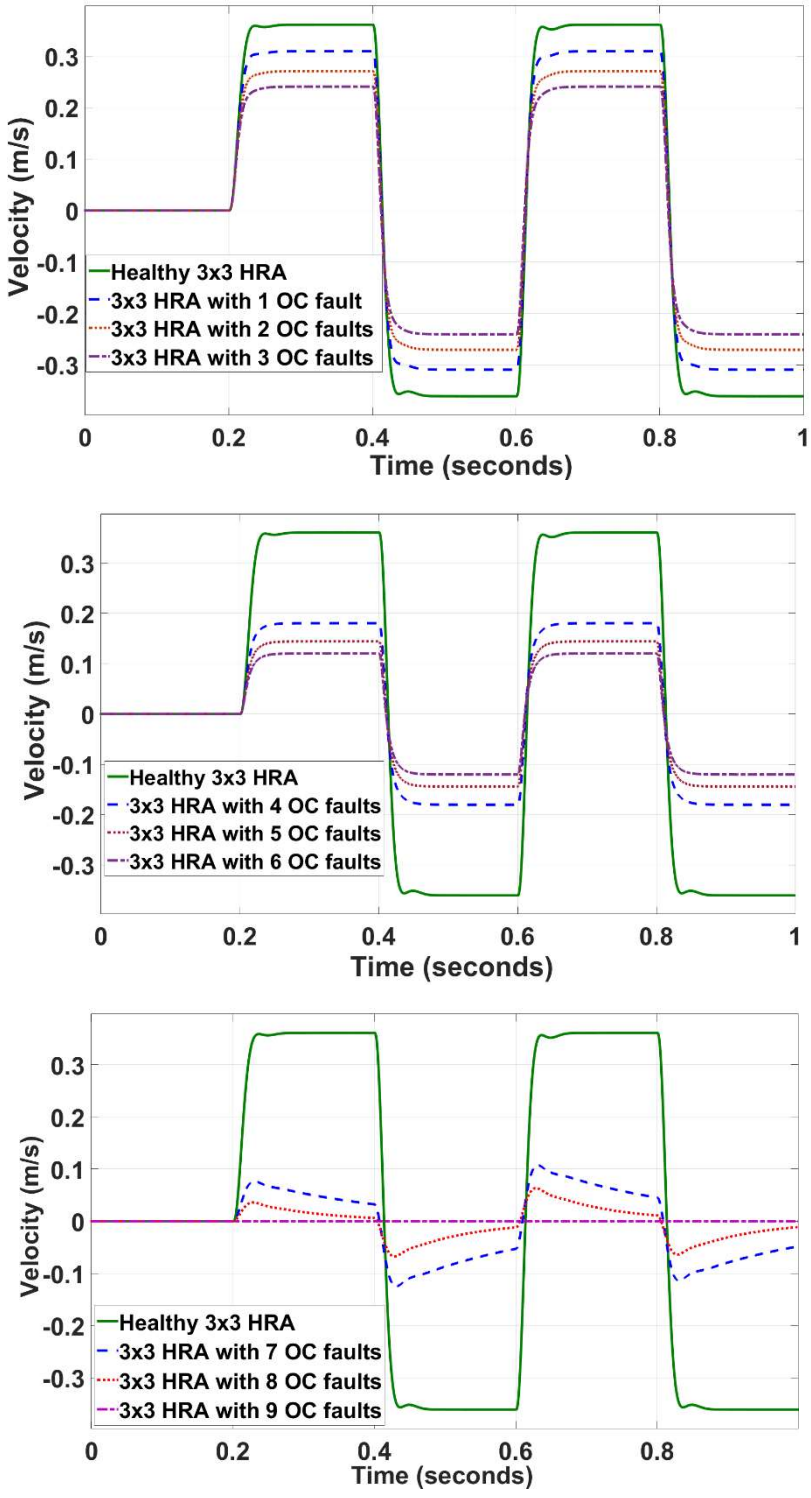

Figure 4.27(c) Linear Velocities of 3×3 HRA under increasing the number of open-circuit faults in the actuator from A1 to A9 (column-wise)

Table 4.11 Performance value of 3×3 HRA under the open-circuit faults.

		Healthy	Fault introduced in Column-1			Fault introduced in Column-1 and 2			Fault introduced in Column-1, 2 and 3		
S.No.	Max output	0-fault	1-fault (A1)	2-faults (A1,A4)	3-faults (A1,A4 ,A7)	4-faults (A1,A4, A7,A2)	5-faults (A1,A4, A7,A2, A5)	6-faults (A1,A4, A7,A2, A5,A8)	7-faults (A1,A4,A7 ,A2,A5,A8 ,A3)	8-faults (A1 to A8)	9-faults (A1 to A9)
1	Displacement (cm)	7.007	6.03	5.3	4.7	3.6	2.9	2.3	1.0	0.4	0
2	Force (N)	204.4	181	159	137.2	113.6	90.2	67.2	45.7	22.4	0
3	Velocity (cm/s)	36.1	31.0	27.0	24.0	18.0	15.0	12.0	5.0	2.0	0

4.7 3D Model of a Direct-Driven Linear EMA

To visualize the shape and motion of the actuator in action a 3D model of a HRA based on direct driven liner EMA was designed using MATLAB/Simulink/simscape. Simscape is one of the toolboxes available for 3D mechanical system modelling and simulation in the MATLAB's Simulink library. Using the blocks like bodies, joints, sensor elements that were available in the simscape tool box, a 3D model of a direct-driven linear EMA was designed. In the following section, the assembling of individual parts of a single DDEMA modeled in simscape is described in detail.

Initially, the individual bodies of required size and shape (according to figure 4.2) were created using simscape. An assembled DDEMA as shown in figure 4.28 was obtained by connecting the individual simscape bodies shown in figure 4.29. The outer hollow casing of the EMA has been sealed on both ends with a bottom and top disc. The bottom disc is nothing but a plane sheet which is fixed at the bottom end of the outer casing with a permanent joint. The two bearings are assembled at the two ends of the rotor with revolute joints between them. This assembled rotor was then placed inside the inner casing which remains to be stationary inside the outer casing. One end of the shaft/lead-screw was inserted into the nut which was inside the rotor and the other end of the shaft with the grooves was extruded out of the top disc. A lead-screw joint present between the lead-screw and the nut along with the prismatic joint between the shaft and the top disc will ensure the conversion of rotatory motion to translational motion.

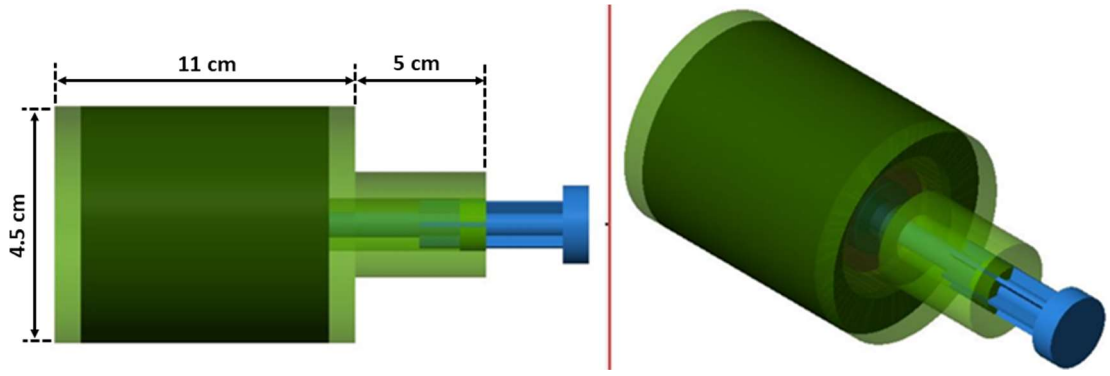

Figure 4.28 The simscape model of a direct-driven linear EMA.

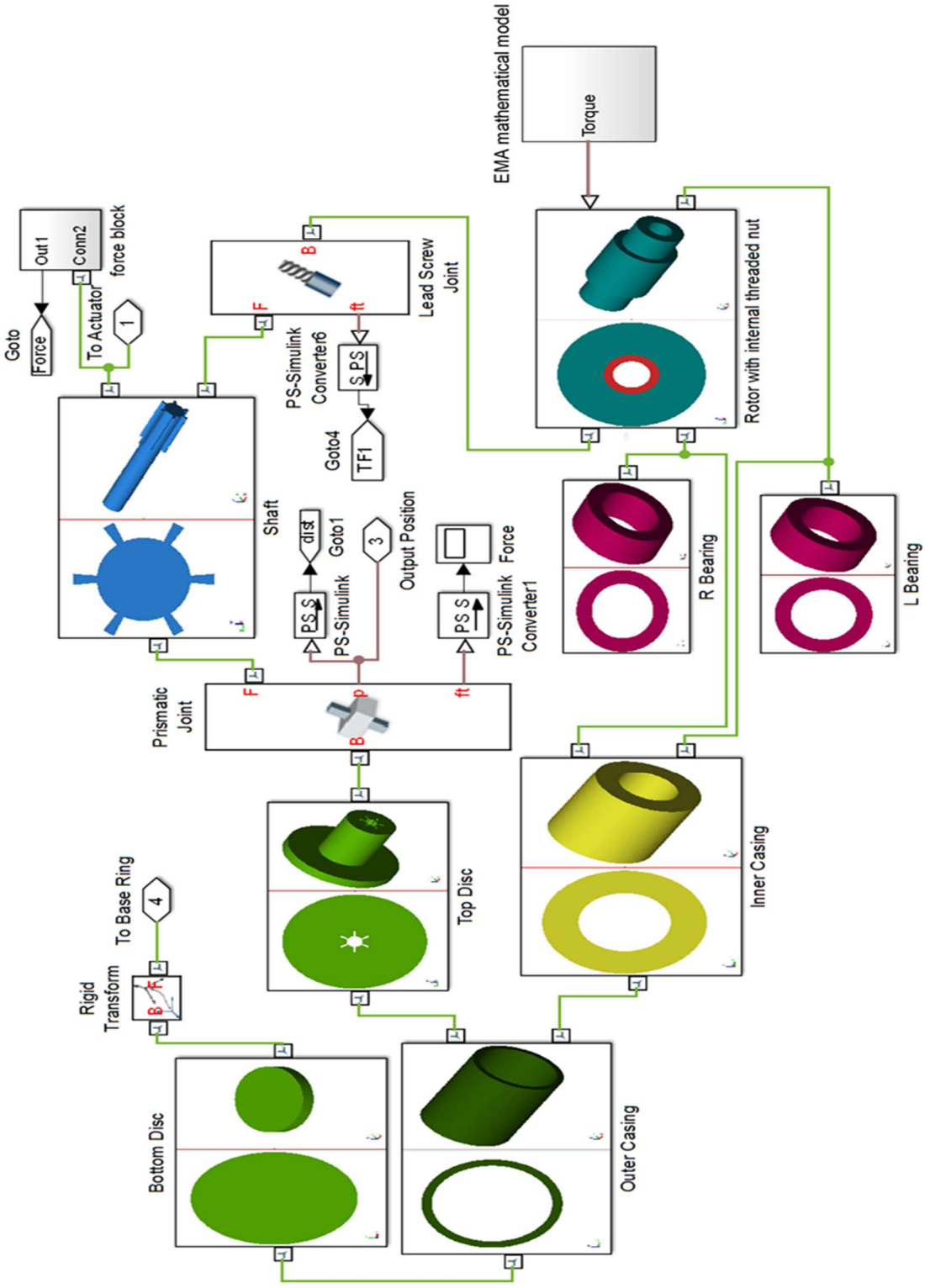

Figure 4.29 The block diagram showing the arrangement of direct-driven linear electromechanical actuator bodies in simscape module.

For developing the 3×3 HRA, Three single EMAs (shown in figure 4.28.) were connected back to back to form a pure series configuration and two more similar series configurations were arranged in parallel. Thus, all the series, as well as the parallel actuation elements will collectively act as a single unit. The simscape model of the HRA developed with 3×3 series in the parallel configuration is shown in figure 4.30. The three actuators which are towards the fixed end of the HRA have a fixed base while the other six actuators have a moveable base. The torque which was obtained from the mathematical model of EMA was provided as the input for the simscape EMA model.

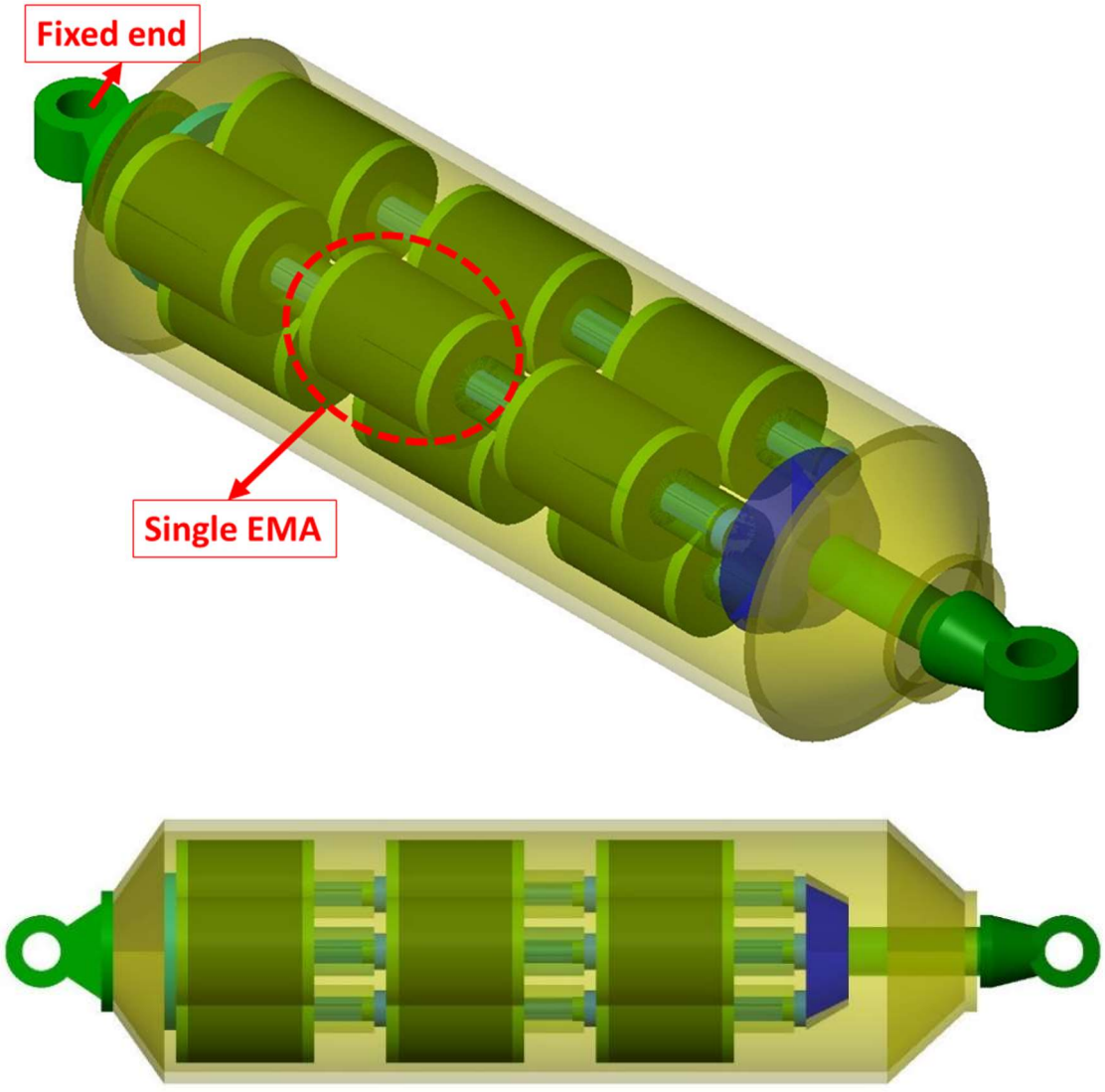

Figure 4.30 The simscape model of a 3×3 HRA with direct-driven linear EMA.

4.7.1 Case study: HRA as an Aileron Actuation System

The operation of the aileron was already described in the literature review (Chapter-2). Controlling the roll of the aircraft is the main function of the aileron. In order to do that, the aileron has to make some angular displacement according to the control signal. So, the actuation end of the HRA was attached eccentrically from the hinge support of the aileron. Therefore, the linear displacement of the actuator will make the aileron to have an angular movement. The 3D model of the HRA connected with aileron was shown in the below figure 4.31 and the response of the angular position of the aileron was shown in the figures 4.32. The comparison of desired angular position of the aileron under healthy and faulty conditions of the HRA actuation elements were plotted and the result shows that up to three actuation element faults the aileron was following the desired path of angular motion.

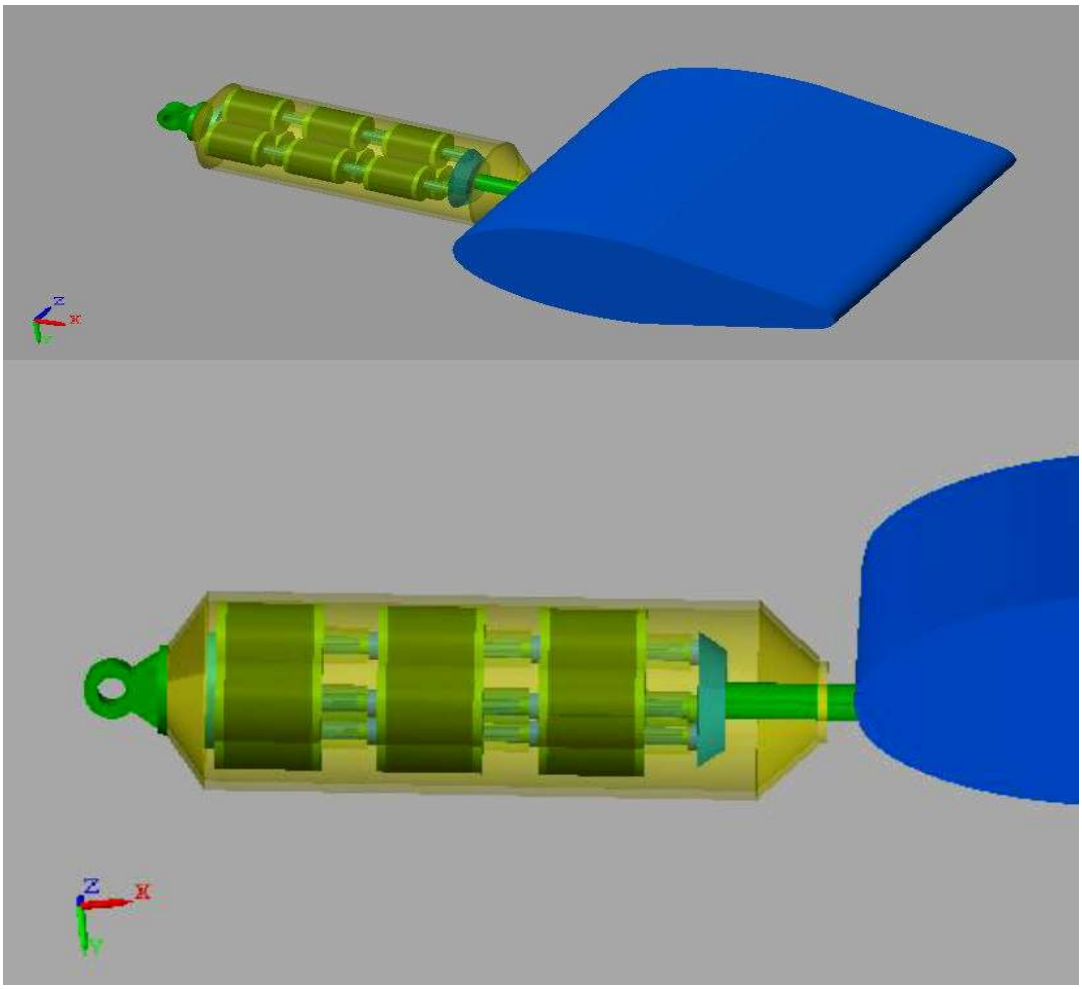

Figure 4.31 The 3D simscape model of a 3×3 HRA with an Aileron attached at the end

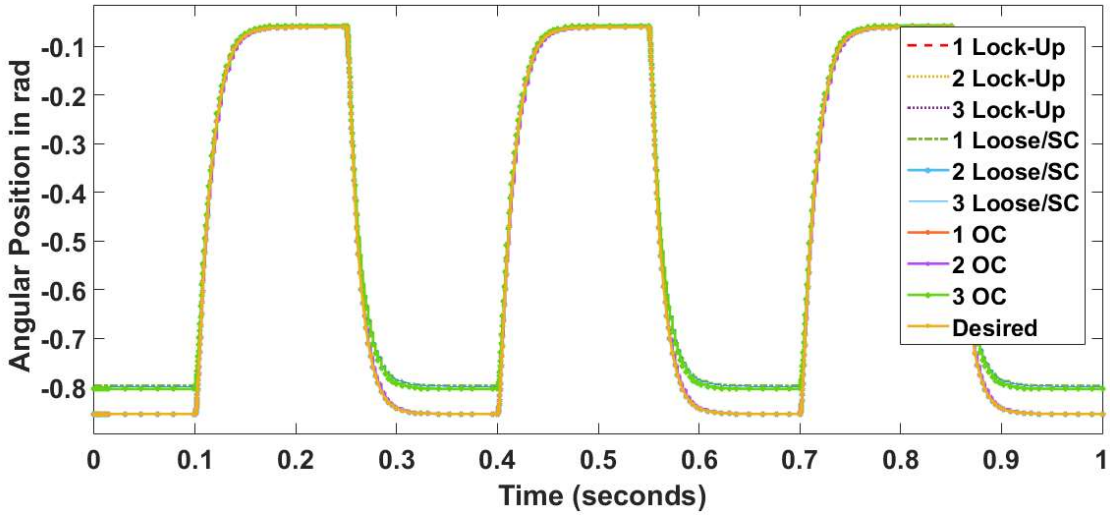

Figure 4.32 Angular position of the Aileron actuation system

4.8 Results and Discussion

In the initial stage, the performance of 3 actuators connected in a pure parallel configuration and 3 actuators connected in the pure series configuration were analyzed under both healthy and faulty conditions. When the actuators were moving in the forward and backward direction, the linear displacement, force and the linear velocities of the actuators with respect to time were plotted. Figure 4.12 and figure 4.16 shows the performance of actuators connected in pure series and in a pure parallel configuration.

In the pure parallel configuration, there is no variation in the linear displacement and velocity of the actuator compared to the single actuator's linear displacement and velocity which is equal to 2.323 cm and 12.04 cm/s respectively. However, the force increased by three times (from 26.8 N to 80.39 N) that of a single actuator's force.

In the Pure series configuration, the linear displacement and linear velocities increased by three times i.e. 2.346 cm to 7.027 cm and 12.03 cm/s to 36.09 cm/s respectively. The forces of all the 3 actuators in the series is expected to be the same. However, the first/single (A1) actuator experiences more impact due to the mass of the second (A2) and third (A3) actuators. Similarly, the actuator A2 also experiences some impact due to the mass of the third (A3) actuator. Because of this reason, the force exerted by the first/single (193.9 N) actuator is more than the overall force (171.6 N) of the series actuators as shown in the force plot in figure 4.12. The values showing the performance of

the pure parallel and pure series configurations without introducing faults are provided in table 4.4.

The figures 4.20 and figure 4.21 are the plots obtained by introducing the lock-up, loose/SC and OC faults in pure parallel and in a pure series configuration with 3 actuation elements. The pure parallel configuration was able to overcome loose/SC fault but not completely. As evident from the plot, the displacement value reduced from 2.323 cm to 1.548 cm and the force reduced from 80.39 N to 53.33 N. In case there is a lock-up fault in any of the actuators connected in the parallel configuration, the displacement becomes zero because the locked-up element acts as a rigid link. However, the other two actuation elements which are in parallel will continue to exert the force on the load. Because of this reason, the force increased drastically (80.39 N to 970.4 N) as evident from force plot of figure 4.21. In such a situation, the entire system fails. Similarly, in the presence of OC fault, the displacement of the actuator was completely distorted but the force exerted showed only minor variation (52.58 N). All the values showing the performance of the pure parallel and pure series configurations with the introduced faults are provided in table 4.7. The pure series configuration was able to tolerate all types of faults and showed a graceful degradation with each of them. However, the force under loose/SC fault is a bit less compared to other force values.

The performance of a 3x3 HRA was analyzed by introducing lock-up, SC/loose and OC faults independently. The faults were introduced one by one into the HRA starting from A1 to A9 and following the sequence of A1, A4, A7, A2, A5, A8, A3, A6 and A9 (refer figure 4.22(a)). To avoid the confusion by plotting all the 9 faulty actuation element results in a single plot it was divided into 3 results per plot. Figures 4.23(a), 4.23(b) and 4.23(c) show the resultant linear displacement, force and linear velocity of the 3x3 HRA under lock-up fault respectively. The results show that the HRA can tolerate up to 6 lock-up faults by degrading the performance from 7.007 cm to 2.323 cm of displacement and force from 204.4 N to 79.96 N provided that at least one actuation element in each series is in healthy condition. However, it fails immediately if the faults are increased beyond 6. Table 4.8 gives the values of displacement, force, and velocity of 3x3 HRA under lock-up faults.

The performance values of the HRA under SC/loose faults are provided in table 4.9 and the resultant displacement, force, and velocity are shown in figures 4.25(a), 4.25(b)

and 4.25(c) respectively. The HRA under the SC/loose fault can operate up to a failure of 8 actuation elements with a graceful degradation from 7.007 cm to 0.8 cm of displacement and 204.4 N to 21.6 N of force. However, the force exerted by the actuator under the SC/loose fault was the minimum value compared to the force exerted due to other fault types. The figures 4.27(a), 4.27(b) and 4.27(c) show the linear displacement, force and linear velocities of the 3×3 HRA under OC fault. The HRA can tolerate up to 6 OC faults with a graceful degradation of displacement from 7.007 cm to 2.33 cm and force from 204.4 N to 64.66 N. Introducing faults further will make the system to behave unusually. The values of all the OC faults are given in table 4.10.

4.9 Conclusions

The High Redundancy Actuator (HRA) design proved to have many advantages compared to the pure parallel configurations that are in existence. Some of the advantages include; improved reliability, size reduction, reduced weight, and reduced cost of the actuation system. As a part of the current work, we mainly focused on the behavior of the 3×3 HRA under a number of fault conditions in the simulation environment as discussed above. Our results showed an increase in the number of faulty elements in a HRA will reduce the performance of actuation gradually. However, the chances of sudden failure of the system are unlikely.

The pure series configuration of 3 actuation elements that we studied showed that the travel capability improved by three times (i.e. from 2.323 cm to 7.027 cm) and the velocity also enhanced by three times (i.e. from 12.03 cm/s to 36.09 cm/s). The results also showed that a system with 3 actuators in a series configuration can tolerate the lock-up fault, open-circuit fault, and short-circuit/loose fault. As long as the failure is limited to 2 actuation elements, the system remains to perform with graceful degradation. However, the tolerance to the force capability of series actuators under loose/short-circuit fault is nearly 18% less than the other types of faults.

On the other hand, The pure parallel configuration of 3 actuation elements that we studied showed an increased force capability by almost three times (i.e. from 26.8 N to 80.39 N). Although this system was able to tolerate the loose/short-circuit fault with graceful degradation of 33.4%, it failed to perform with the other two faults.

The 3×3 HRA that was designed for this work had a combination of series and parallel elements with the capability to tolerate all types of faults. Figures 4.33, 4.34 and 4.35 show the performance of 3×3 HRA displacement, force and velocity aspects in the presence of 4 different faults tested independently. When the 3×3 HRA performance was studied with a single lock-up fault, the reduction of displacement was found to be a maximum of 14.34% and minimum in the presence of loose/short-circuit fault (11.13%). However, the reduction of force was recorded maximum (12.18%) in the presence of loose/short-circuit fault and minimum (10.95%) in the presence of a lock-up fault.

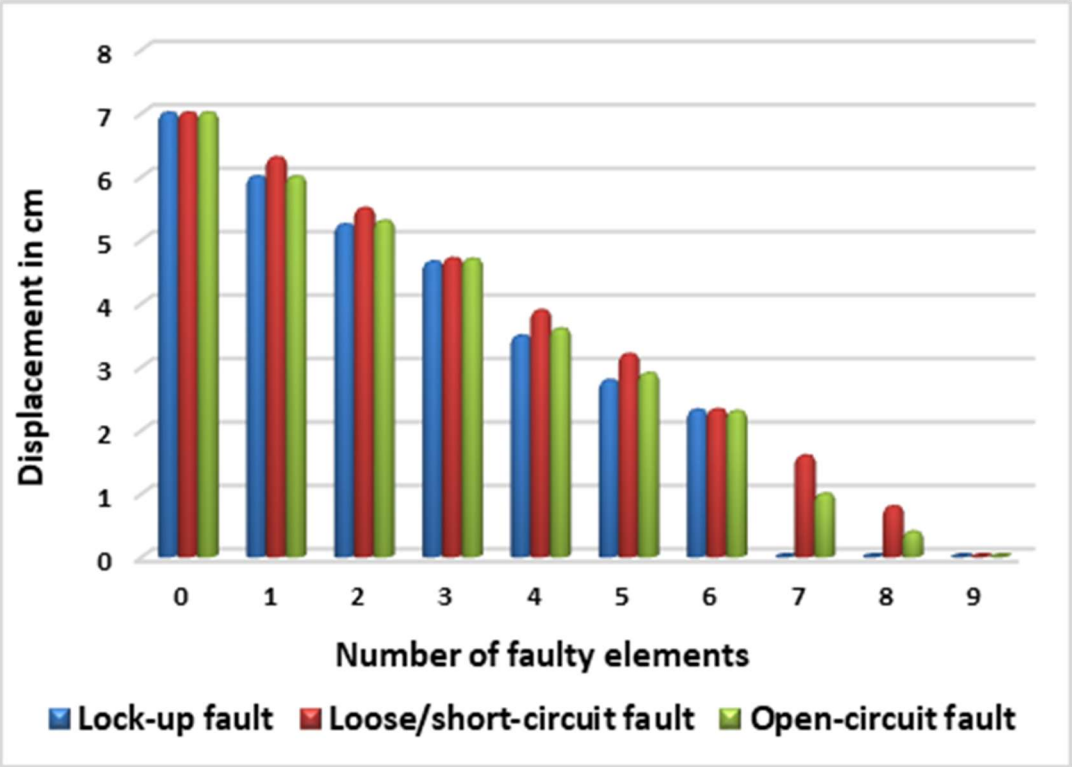

Figure 4.33. Comparison of displacements of a 3x3 HRA under the lock-up, open-circuit and short-circuit/ loose faults

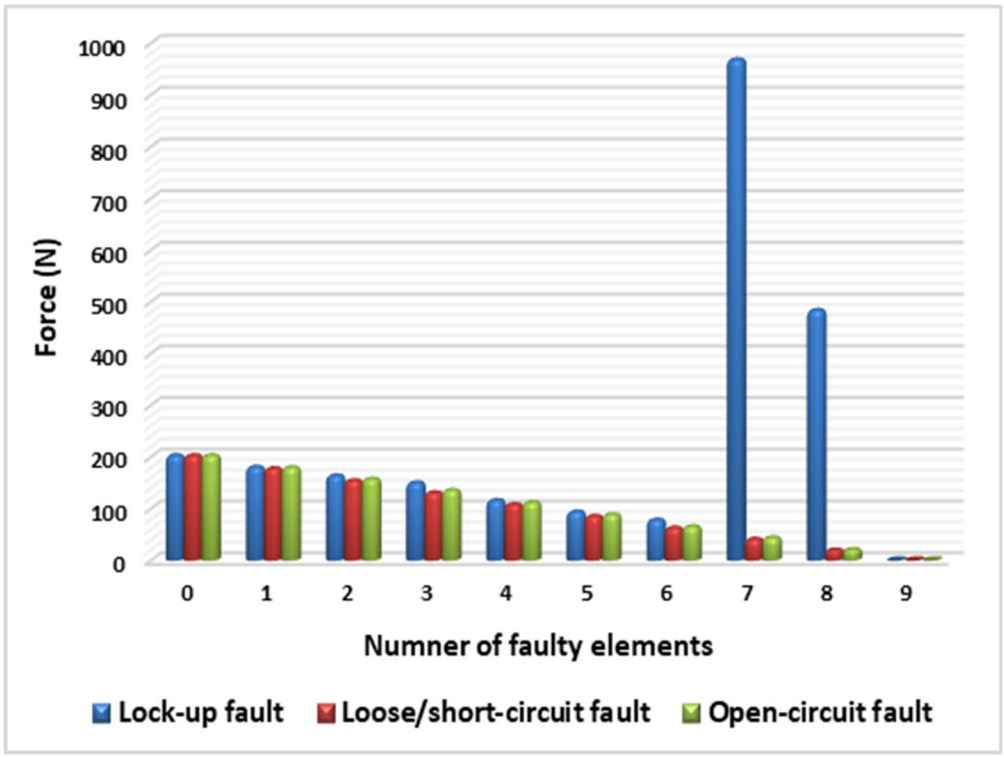

Figure 4.34 Comparison of forces of a 3x3 HRA under the lock-up, open-circuit and short-circuit/ loose faults

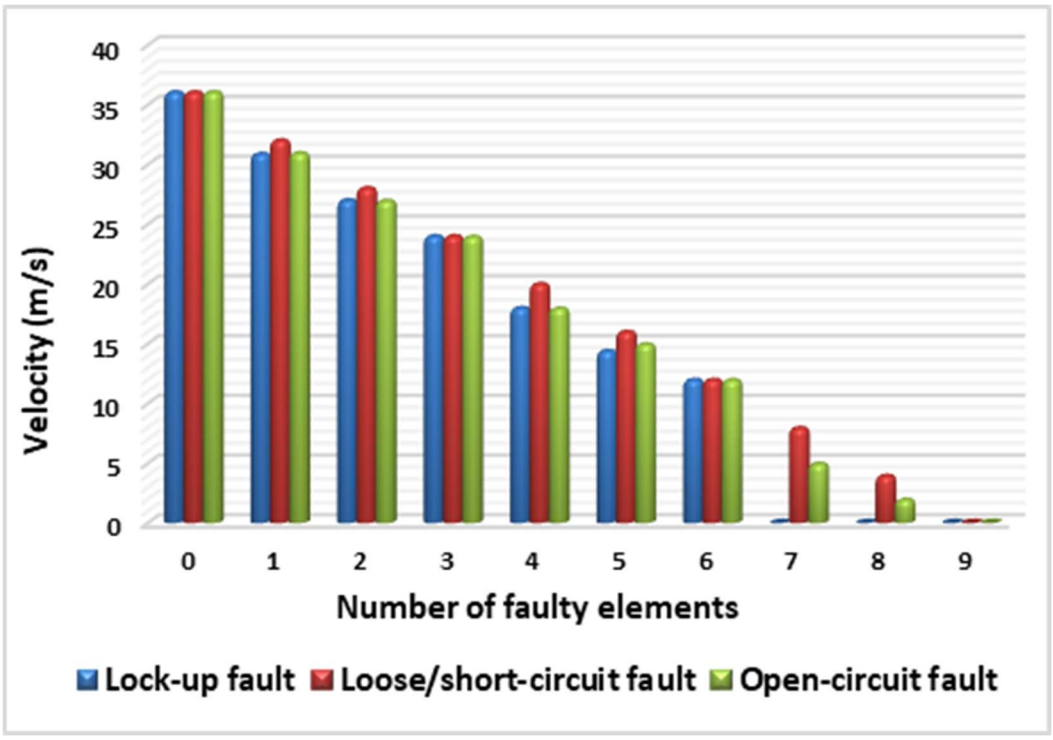

Figure 4.35. Comparison of velocities of a 3x3 HRA under the lock-up, open-circuit and short-circuit/ loose faults

The HRA was able to tolerate up to 6 faulty elements provided that at least one actuation element in each series is in healthy condition. The reduction in the performance of HRA depends on the number of faulty actuation elements, the type of fault and the position of the faulty actuation element in the configuration. However, the fault location in the configuration of the HRA is out of the scope of current work.

CHAPTER 5

EXPERIMENTAL SETUP OF A HRA

The concept of HRA was demonstrated with the help of an experimental setup that was custom designed and constructed to a lab scale. The installation was used for simulation model validation, and for conducting experiments to test the setup. This chapter explains the details of the electrical and mechanical components of the setup and an assembled 3×3 HRA with data acquisition to collect the required data. The first section discusses the details of the mechanical parts, which include lead-screw, aluminum hollow cylinder, roller ball bearings, aluminum housing of the EMA, and the linear ball bearings.

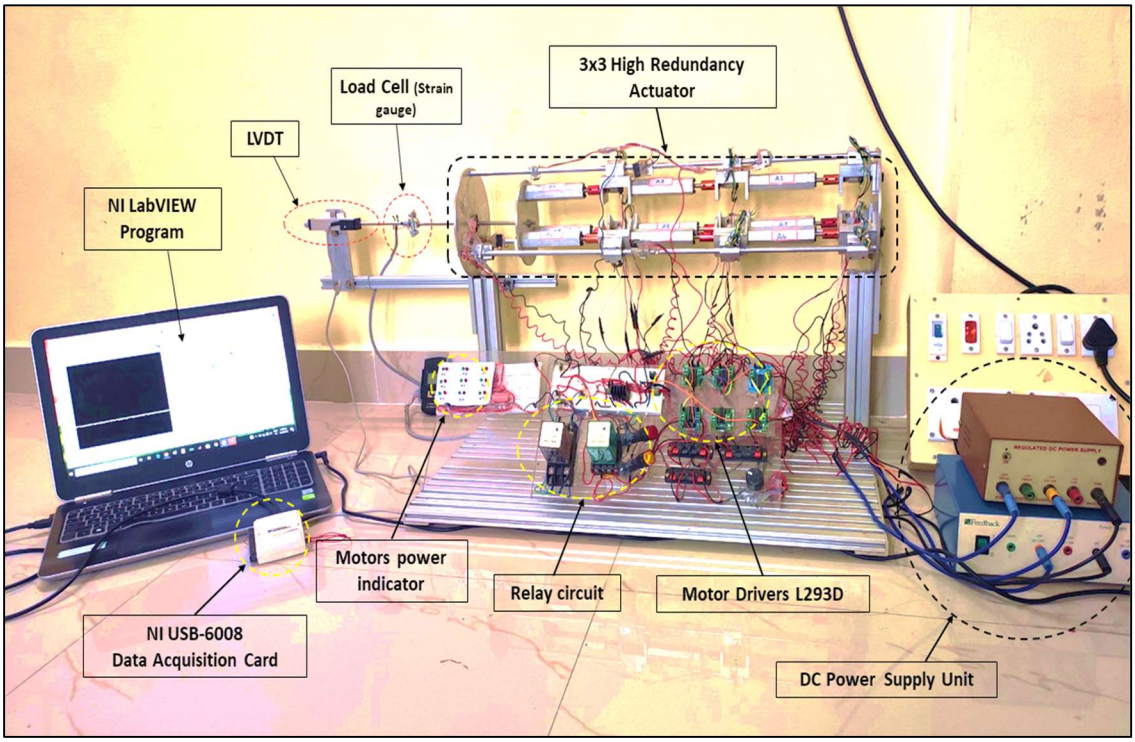

Figure 5.1 Experimental setup of a series-in-parallel 3×3 HRA

The second section discusses the electrical components, which include DC motor, motor drivers, voltage regulators, relays and limit switch circuit, and power supply unit. The last section in this chapter discusses the sensors, like the Linear Variable Differential

Transducer (LVDT), and the data acquisition module (DAQ), and ends with results the conclusions.

Figure 5.1 shows the actual experimental setup and figure 5.2 shows the block diagram of the experimental setup. From the block diagram, the circuit connection between all the components was made clear. The input for the HRA was from the motor driver circuit and the output forward and backward stroke of HRA was measured by using an LVDT with the aid of a NI hardware module USB-6008. The individual actuator positions were measured by sending the encoder signals from the individual actuators to the microcontroller Arduino board. The Arduino board and the NI module are connected to the laptop/PC to measure the displacement with the help of MATLAB and LABVIEW software programs. The limit switches are placed to limit the forward and backward stroke of the HRA and also to change the direction of motion by giving the signal to the relay circuit. The relay circuit will give the signal to the drivers to which the actuators of the HRA were connected. The DC power supply units with voltage regulators were used to power the electric components of the circuit. The load cell with a digital display which was connected to the HRA end effector rod will give the force that the HRA can apply. However, the displacement of the HRA was the main focus of the present work.

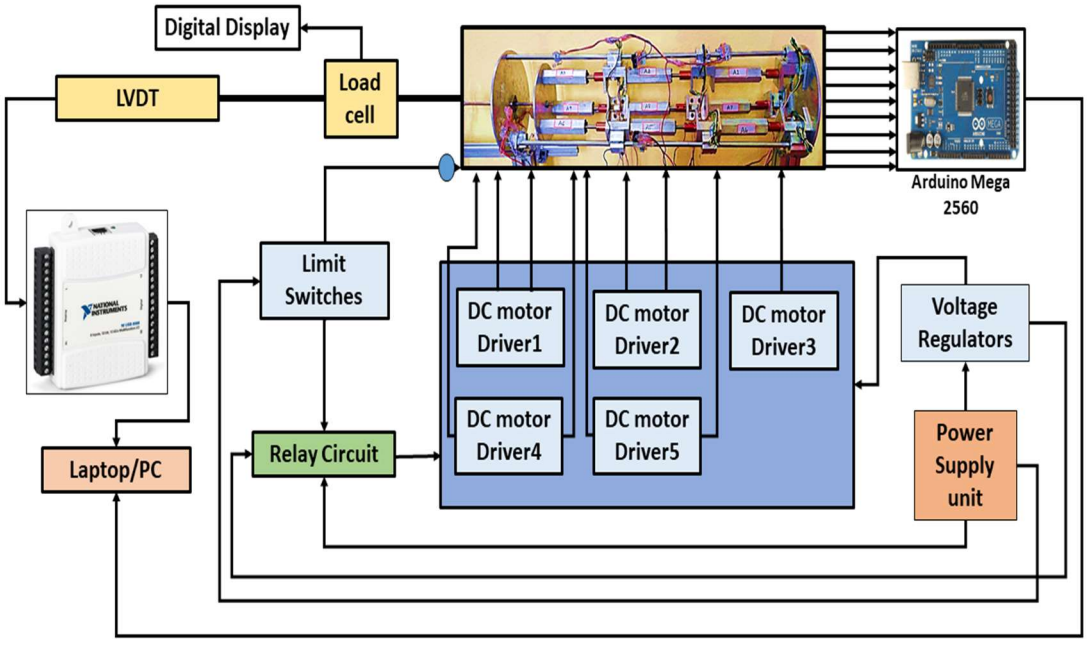

Figure 5.2 The block diagram of the experimental setup.

5.1 Mechanical Components

The mechanical parts of the EMA are very much essential to be rigid and custom-designed according to the requirement. In the present research work, the experimental setup was made to lab-scale for validation of the simulation results. Therefore, the mechanical parts are custom-designed to suit the particular DC motor. Also, the mechanical parts will allow the EMAs to connect in a series-in-parallel structure to form an HRA.

5.1.1 Lead screw

A lead screw or a power screw is a screw used as a linkage in a machine to translate rotary motion into linear motion. Because of the broad area of sliding contact between the screw and nut, screw threads have enormous frictional energy losses compared to other linkages. They are not typically used to carry high power, but more for intermittent use in low power actuator and positioner mechanisms. In general, lead screws are used in machine slides (such as in machine tools), linear actuators, presses, and jacks. Compared to lead screw ball screw or roller screw is more efficient for high end or precise applications. However, in the present work, a 3D printed stainless steel lead screw with a flange copper nut was used. Figure 5.3 shows the image of the lead screw, and table 5.1 gives the specifications of it.

Figure 5.3 Lead screw

Table 5.1 Specifications of the lead screw

S.NO.	Parameter	Value
1	Material	Stainless Steel screw, copper nut
2	Pitch	1mm
3	Lead of thread	6mm
4	Screw Diameter	6mm
5	Screw Length	100mm
6	Direction	Right-handed
7	Copper Nut Size	10x13x25mm

5.1.2 Aluminum hollow cylinder

The rotation of the screw will make the nut to move linearly forward and backward according to the direction of rotation of the screw. So, as the required linear motion for the actuation system was from the nut, a hollow aluminum cylinder was fixed to the nut placing the screw inside. This arrangement will make the hollow cylinder to move linearly when the screw rotates. Here in the present work, to an aluminum rod of hexagon shape, an 8mm trough hole was made to accommodate the screw, and the nut was fixed at one end of the cylinder. The front view and the top view of the aluminum cylinder line diagram with dimensions and the assembly of the lead screw and the nut arrangement were shown in figure 5.4.

5.1.3 Shaft coupling

The rotary motion generated by the motor must be transferred to the lead screw to achieve the linear motion of the actuator. So, there must be a rigid link connecting the motor shaft and the lead screw. There are so many ways to connect them, but in our particular case, they are connected with the help of a rigid shaft coupling. In the present work, the selected DC motor shaft diameter was 3mm, and the screw diameter was 6mm. To make it possible for connecting these two diameters, a shaft coupling of 3mm on one

side and 6mm on the other side has opted. Figure 5.5 shows the rigid shaft coupling with dimensions.

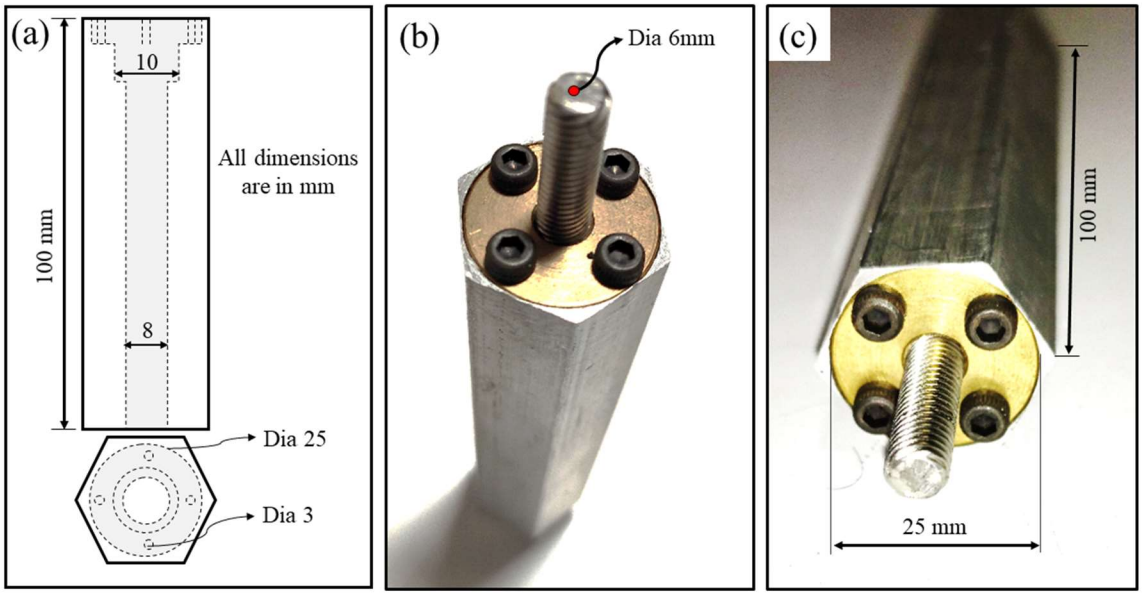

Figure 5.4 (a) Line diagram of hexagon cylinder (b) & (c) Lead screw with aluminum cylinder

Table 5.2 Specifications of shaft coupling

S.No.	Parameter	Value
1	Material	Aluminum alloy
2	Diameter (D)	12mm
3	d_1 & d_2	3mm & 6mm
4	Length (L)	25mm
5	Screws	M4

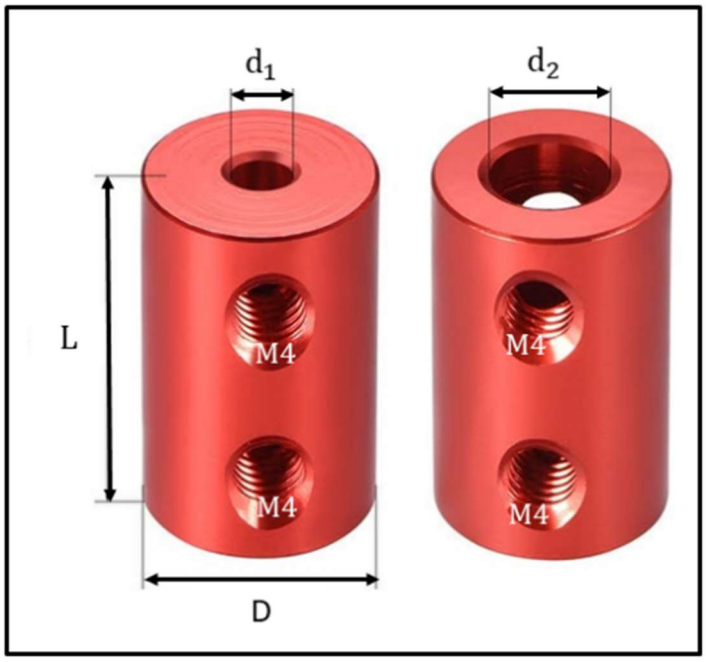

Figure 5.5 Rigid shaft couplings

5.1.4 Bearings

A bearing is a machine element that reduces the friction between the moving parts and makes a relative motion to only the desired action. The linear ball bearings provide a free linear movement of the moving part, and a ball roller bearing will offer a free rotational motion around a fixed axis. In the present work, ball bearings of inner diameter 3mm, outer diameter 10mm, and 5mm thickness were used for the motor shafts to be adequately aligned and fixed. These bearing will also make the motor shafts to rotate smoothly without any angular deviations. The present HRA consists of nine DC motors, so; nine ball bearings for all the nine motor shafts were fixed. Figure 5.6 (a) shows the ball bearing of an internal diameter of 3mm and an external diameter of 10mm.

The HRA consists of actuators having a fixed base and a movable base, as already discussed in the previous chapters. So, for attaining a movable base for the actuators, linear ball bearings with aluminum housing and a round stainless steel rod were used. The inner diameter of the bearing was 8 mm, and the outer housing dimensions are 30mm × 30mm, as shown in Figure 5.6 (b). The present HRA has nine actuation elements, out of which three are fixed to the base, and only six having the movable base. However, to avoid the

misalignment of the actuation elements when connected in series, all the nine actuation elements are provided with these linear ball bearings.

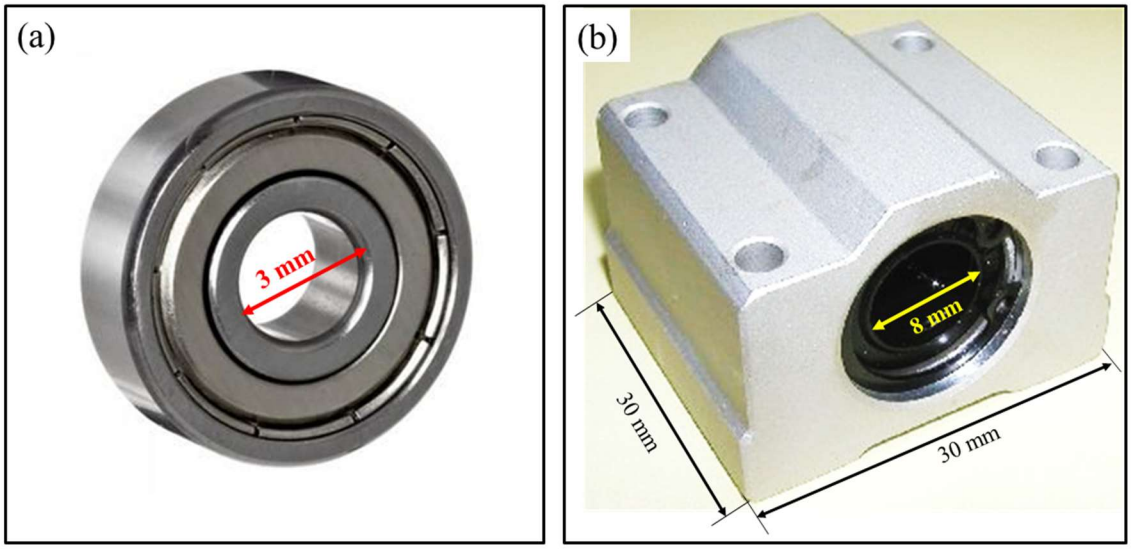

Figure 5.6 (a) Ball bearing (b) Linear ball bearing with aluminum housing

5.1.5 Slotted aluminum block

After getting all the mechanical components, there must be one main body of the actuation element to which all those mechanical components have to be attached. Considering an aluminum block of 55×40×40mm size, and a slot of 42mm length and 25mm depth was made to place the motor inside the slot. A through-hole of diameter 3mm at one side of the block at the center was made to insert the motor shaft. By making a circular groove of 10mm diameter and a depth of 5mm to insert ball bearing was made at the same center. Figure 5.7(a) shows the block with the ball bearing insert. At the bottom of the block, four holes of a 3mm diameter were made to fix the linear ball bearing. Figure 5.7(b) shows the motor attached in the groove, shaft position through the ball bearing, and the linear ball bearing fixed at the bottom of the block. Hence, this linear ball bearing enables the base of the slotted aluminum block movable along with the motor.

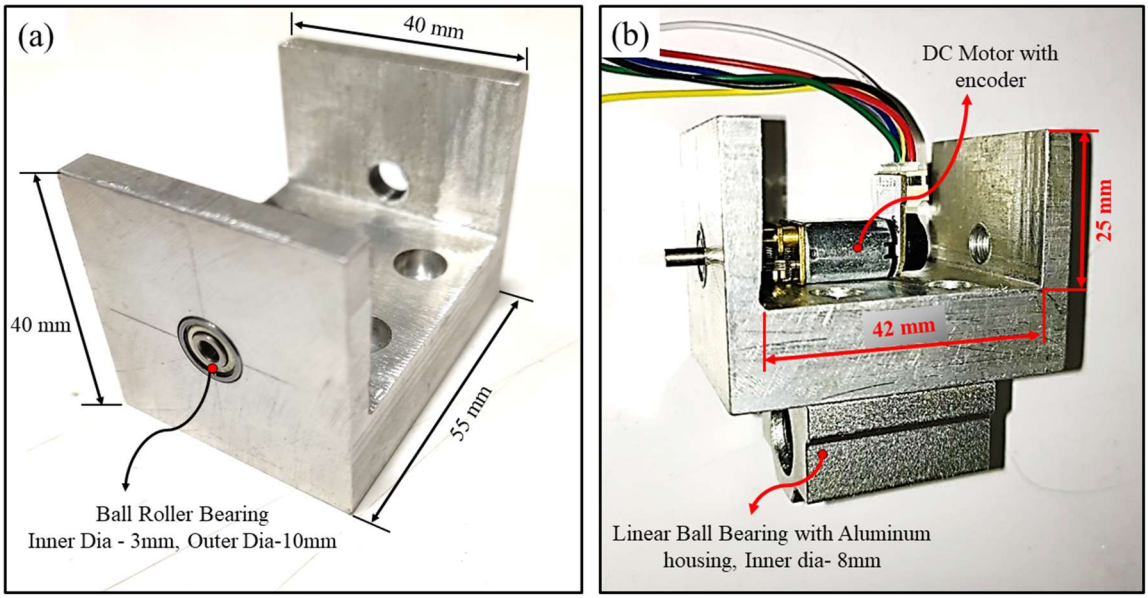

Figure 5.7 Slotted aluminum block

5.2 Electrical Components

5.2.1 Geared DC Motor with Rotary Encoder

A micro metal geared DC motor with an encoder was used to transmit the rotary motion to the lead-screw. The gearbox connected to the DC motor has a ratio of 380:1, which means per one revolution of the motor shaft the motor has to make 380 revolutions. The motor has two built-in Hall-effect encoders at the back end to measure the speed of the motor in real-time. The motor has a D profile metal output shaft of length 9.0 mm and diameter of 3.0 mm. The detailed specifications of the motor and the image of it are provided in table 5.4 and figure 5.8 respectively.

In the present work, the Hall Effect encoder has two Hall Effect sensors and six pins as shown in figure 5.8 (b). Out of six pins, two pins are for the input supply for the motor, two pins are for the input supply Vcc and ground of the encoder, and the other two are the output ports A-Phase and B-Phase of the encoder. The two-channel magnetic Hall effect encoder's Hall sensor requires an input voltage, Vcc, between 3.3V and 5V. The A and B outputs are square waves from 0 V to Vcc approximately 90° out of phase. The hall sensor has seven pole pairs, so the resolution of the encoder will be increased by sevenfold. The average number of output pulses can touch up to 7*2*380 pulses per revolution. The

direction of the motor can be known by the transitions and the speed of the motor can be known by the frequency of the transitions. The details regarding the linear measurement using the encoder were explained in section 5.4.

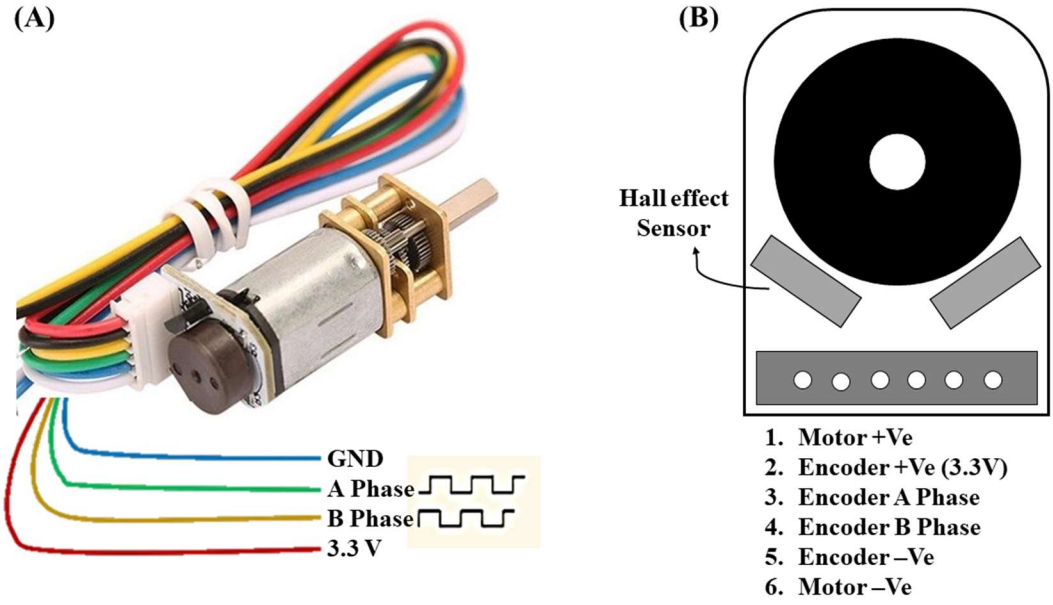

Figure 5.8 (A) DC geared Motor with encoder (B) Motor Interface (Hall effect sensor)

Table 5.3 Specifications of Geared DC motor with Encoder

S.NO.	Parameter	Value
1	Rated Voltage	6.0 V
2	Motor Speed	15000 RPM
3	Gear Reduction Ratio	380:1
4	Reducer Length	9.0 mm
5	No-Load Speed	41 rpm@6v
6	No-Load Current	60 mA
7	Rated Torque	2.5 kg.cm
8	Rated Speed	24 rpm@6V
9	Current Rating	170 mA
10	Instant Torque	<2.8kg.cm
11	Hall Feedback Resolution	5320
12	Weight	18g

5.2.2 Motor drivers

The motor driver is mainly used for driving the motor. Five L293D motor drivers were used to drive 9 motors which are connected to the mechanical lead-screw setup. Each motor driver has two channels and it is capable of driving two DC motors. So, five motor drivers were used to drive the actuation elements. A 5V DC supply voltage is used to power the motor driver. The motor driver accepts a voltage range of 0V to 12V to run the motor. Signals from the relay circuit to the driver will make the motor rotate clockwise or anticlockwise direction. The image of the motor driver which was used in the experimental setup was as shown in figure 5.9.

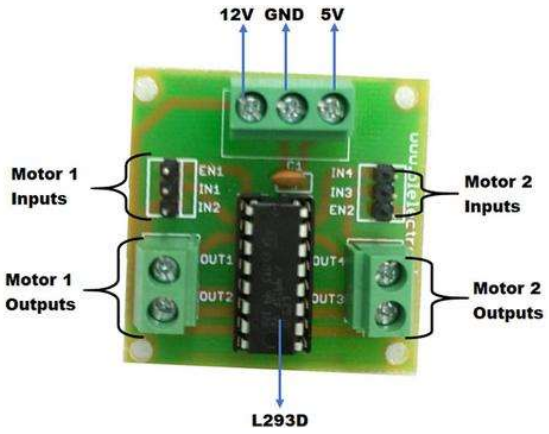

Figure 5.9 Motor Drives

5.2.3 Limit Switches and Relays

The forward and backward motion of the EMA will be occurred due to interchanging the input polarities of the actuator motor accordingly. This change in polarity has to happen when the lineae actuator reaches the extreme ends. So, the limit switches fixed at the extreme ends will trigger the relay which intern will change the polarity of the signal and send it to the motor drivers to which the actuator motors were connected. The circuit diagram of the two relays connected with a single motor driver and the limit switches are shown in figures 5.10 and 5.11.

5.2.3.1 When Normally Open limit switch is not active

Figure 5.10 shows the circuit diagram of one motor connected to the relay circuit when the NO limit switch was not active, but in the actual case, there are nine DC motors connected through five motor drivers in the same manner. Three voltage regulators and two LEDs which indicate the forward or backward movement of the actuator were used in the circuit. The latching of the relay-1 was done by connecting pins 2 and 3. When the Normally Open (NO) limit switch was not active, then the motor will rotate in the clockwise direction by receiving the signal from pins 4 and 5 of relay-2 through the motor driver. And throughout this time the yellow color LED will be glowing, which indicates the motor was rotating in the clockwise direction. So, the leadscrew attached to the motor will travel in the backward direction.

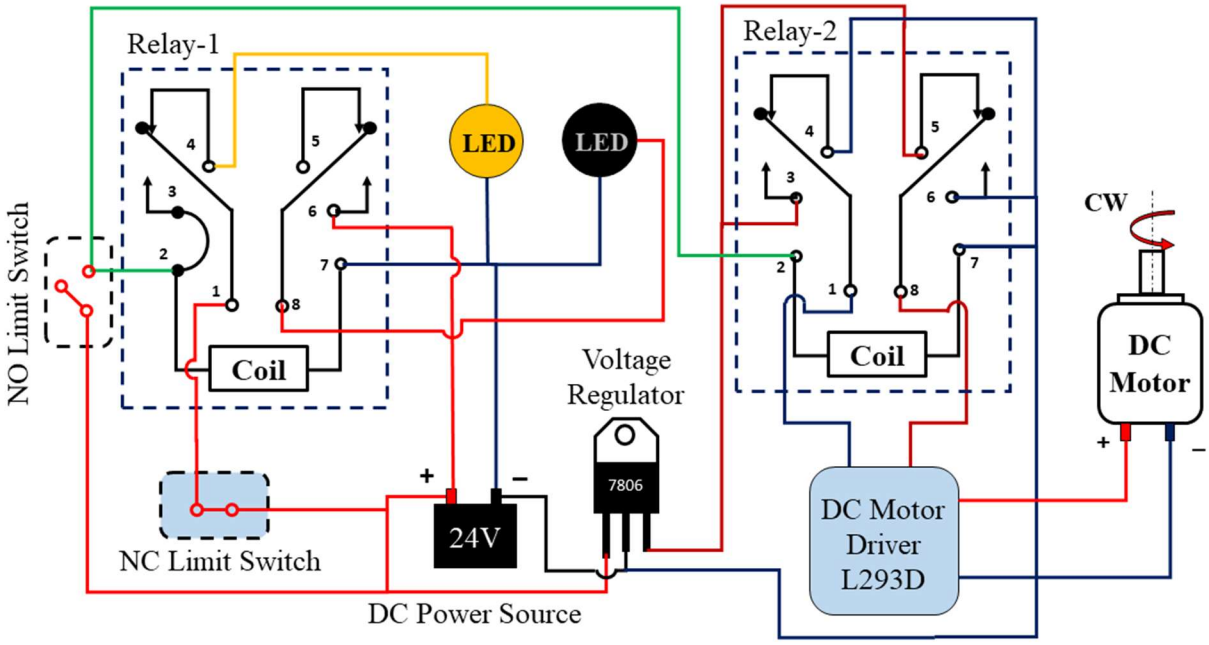

Figure 5.10 Relay circuit when the NO limit switch is not active

5.2.3.2 When Normally Open limit switch is active

When the Normally Open (NO) limit switch was active as shown in figure 5.11, then the coils of relay-1 and relay-2 both will get activated. The relay-1 makes the red color LED switch-on and yellow color LED to switch off. The relay-2 gives the signal to the motor to rotate in the anti-clockwise direction by giving the signal from pins 3 and 6

through the motor driver. And throughout this time the red color LED will be glowing, which indicates the motor was rotating in the anti-clockwise direction. So, the leadscrew attached to the motor will travel in the forward direction. The Normally Closed (NC) limit switch works as vise versa. The hardware setup of the relay circuit is shown in figure 5.12.

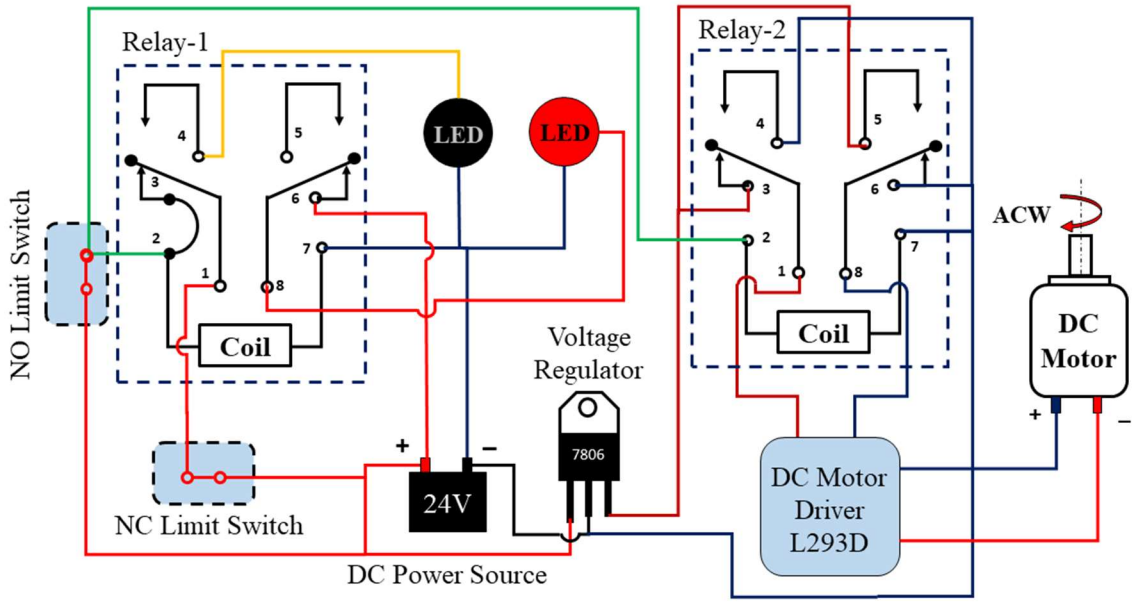

Figure 5.11 Relay circuit when the NO limit switch is active

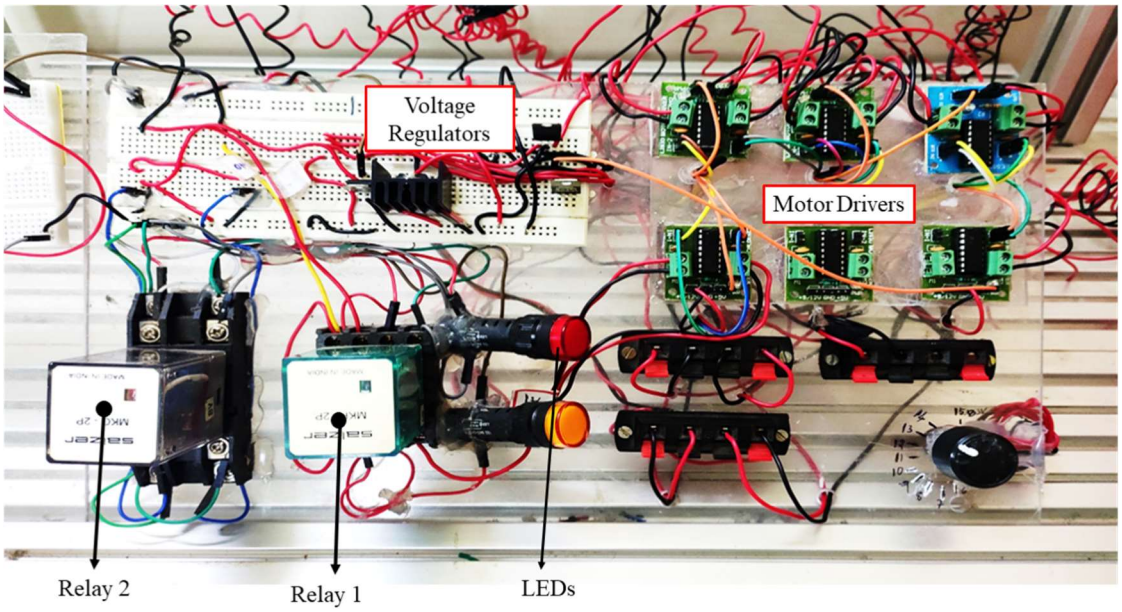

Figure 5.12 Hardware setup of the relay circuit

5.3 HRA Setup with 3×3 Series-In-Parallel Configuration

The HRA hardware setup was the assembly of all the mechanical components and the DC motor. In this section, the assembly of the single EMA and the assembly of the 3×3 HRA with series-in-parallel configuration were discussed in detail.

5.3.1 Assembly of Single Electromechanical Actuator

As discussed in the previous chapters, the EMAs are a combination of an electric motor (electrical system) and a mechanical gear-box (mechanical system). Figure 5.13 shows a single electromechanical actuator formed by assembling the slotted aluminum block, a geared DC motor with encoder, a rigid shaft coupling, a lead screw with an aluminum cylinder, and a linear bearing with a stainless steel rod. The DC motor will produce the rotational motion/torque upon supplying the electrical energy. The shaft coupling will transfer the generated torque from the DC motor to the lead-screw. Based on the direction of rotation of the lead-screw, the hollow cylinder attached to the nut will make through and flow motion linearly.

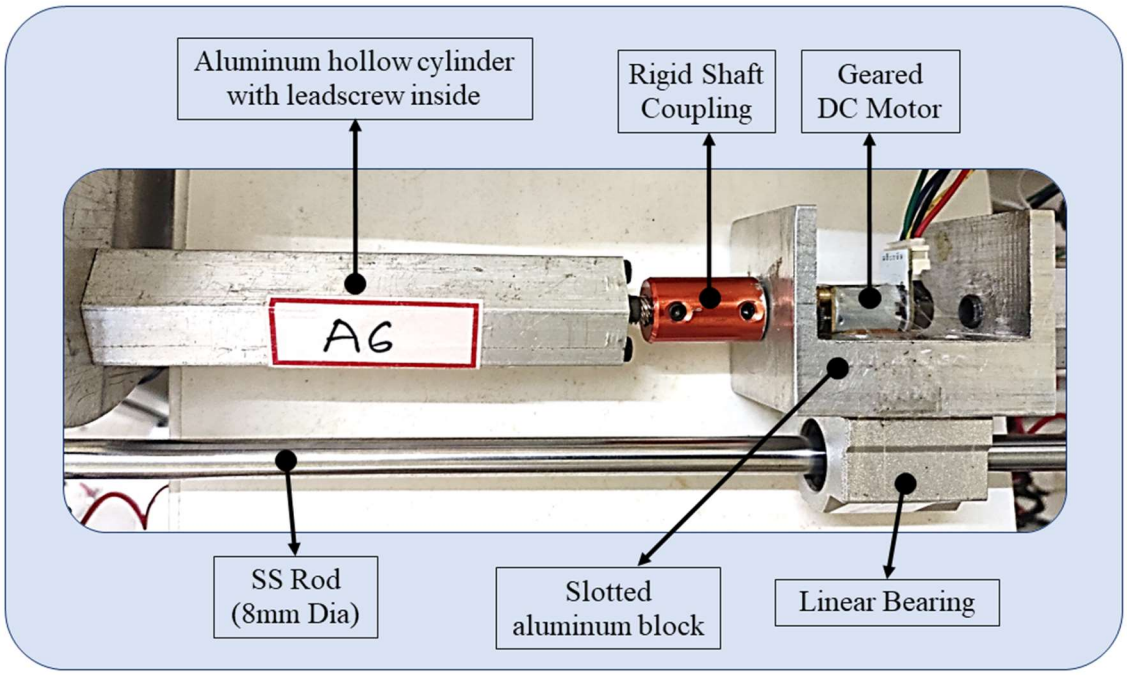

Figure 5.13 Single electromechanical actuator

5.3.2 Assembly of 3×3 HRA

The assembly of HRA consists of two circular plates of diameter 170mm rigidly fixed by the fixed supports at the extreme ends. The front circular disc has a linear flange bearing attached at its center through which the HRA rod making forward and backward motion. One end of the rod coming through the linear flange bearing was free and the other end of the rod was attached to the movable circular disc of diameter 130mm which was attached to the series of actuators arrangement. The 3×3 series-in-parallel attachment of the actuators was done by attaching the three individual EMAs back-to-back. Out of the three, one actuator was fixed to one of the fixed circular discs and the other two are moveable because of the attached linear bearing with the circular rod at the bottom of each actuator. The circular rods are fixed between the two circular fixed plates and passing through the linear bearings. Similarly, two more similar series arrangements are made and attached to the same fixed circular plates in parallel to the series arrangement to form the 3×3 series-in-parallel configuration. One end of the actuators in the series are attached to the fixed plate and the other ends are attached to the circular movable plate having a rod attached to its center. The limit switches for limiting the forward and backward strokes of the HRA are placed at the suitable positions as shown in figure 5.14.

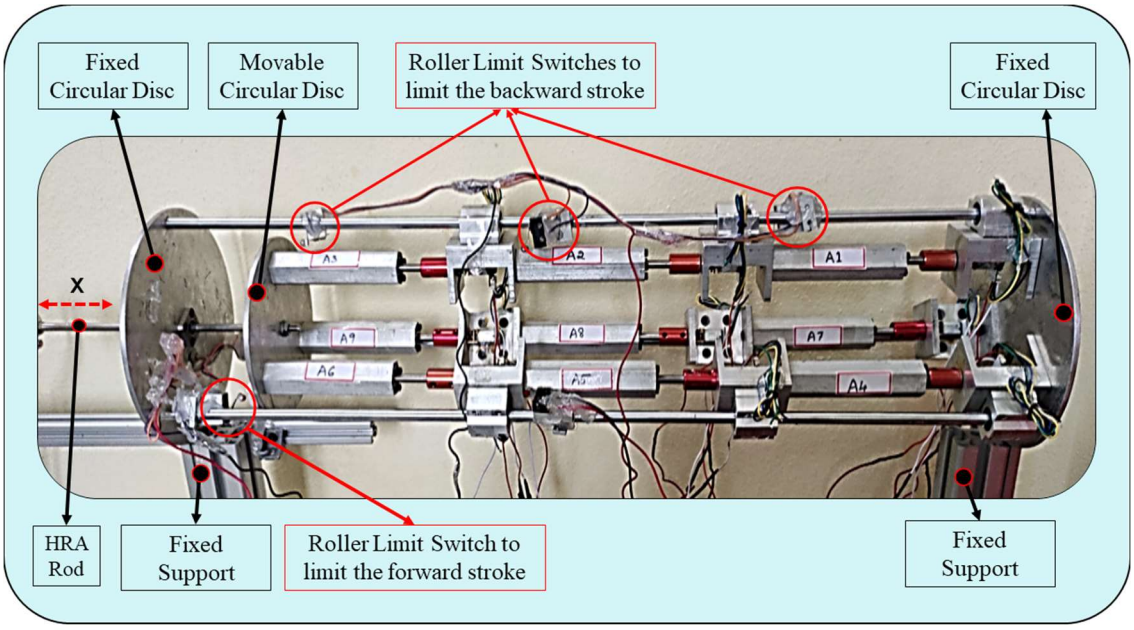

Figure 5.14 Hardware setup of an assembled 3×3 HRA

5.4 Measuring the Linear Position of the Actuator with Rotary Encoder

A rotary encoder is a type of position sensor which is used for defining the angular position of the shaft. The encoder produces either analog or digital signals when there is a movement of rotation of the shaft. Depending upon the output signal or sensing technology the encoders are classified into many types. In the present work, the DC motor was attached with an incremental rotary encoder. It is the simplest sensor to measure the rotary position of the shaft. The output of this encoder is a series of square wave pulses. And this encoder is also known as a quadrature encoder or relative rotary encoder.

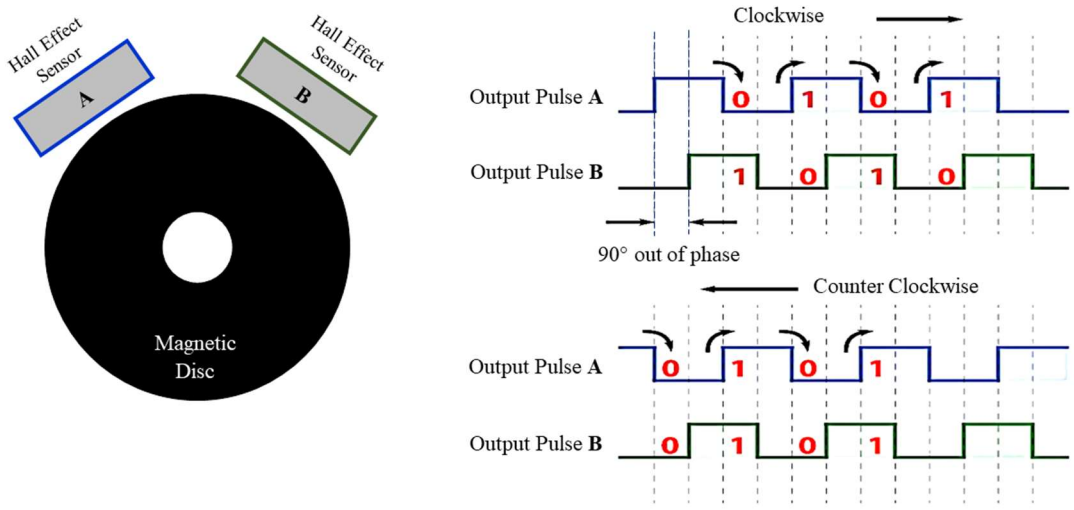

Figure. 5.15 Hall Effect Rotary Encoder and the encoder output waves

5.4.1 Hall Effect Encoder

A Hall Effect quadrature encoder was used in the present work. A Hall Effect encoder as shown in figure 5.15 is a non-contact type sensor that detects a magnetic field. The wear and tear are zero between any parts in the sensor as there is no physical contact between them. A Hall Effect encoder has a magnetic disc connected to the back-end of the motor shaft, and one or more Hall Effect sensors are placed near the magnet. As the magnet turns, the Hall Effect sensor detects the pole of the magnet as it comes next to the sensor. This produces a square wave pulse output from Encode pins A and B (Refer to figure 5.7). Any of the two encoder outputs, either A or B can be used for determining the rotary position of the shaft just by counting the number of pulses of the signal. However,

to determine the direction of rotation of the shaft both encoder outputs need to be considered. If both the encoder signals are considered at the same time, then the two output signals are displaced at 90 degrees out of phase from each other. If the encoder disc is rotating in the clockwise direction then output A will be ahead of output B as shown in figure 5.15. By counting the states each time the signal changes from high to low or from low to high and observing that at that particular time two output signals have opposite values. Similarly, if the encoder is rotating counterclockwise the output signals change from high to low or from low to high have equal values. So, by considering this the program can be made to read the encoder position and rotation direction. However, in the present case, the linear displacement made by the actuators lead-screw due to the rotation of the motor shaft has to be determined. This can be done by calculating the number of pulses per revolution which will be the same as the pulses per pitch length of the screw. To read the encoder pulses through an Arduino Mega 2560 microcontroller a MATLAB/Simulink block diagram logic has been used.

5.4.2 Encoder connection with the Microcontroller

In general, an encoder of this type is connected as shown in figure 5.16, the motor is powered by pins 1 and 6. The encoder outputs are 3 and 4, the Vcc pin of the encoder was feed with 3.3V from the Arduino board. The encoder output readings from the Arduino board are fed to the computer's MATLAB/Simulink program through a USB cable connected from the microcontroller to the computer. The main aim of this program is to measure the speed of the motor eventually to get the linear displacement of the actuator. So, the output from any one of the encoder phases either A or B is sufficient. The encoder output pins are connected to the digital input/output pins 31 and 32 of the Arduino board. A push-button was connected across pin 5 and pin 2 as it was important to reset the counts. This shows how an encoder connected to the Arduino mega, similar to all the nine actuator's encoders are connected to the other digital pins to measure the linear displacement of the actuators.

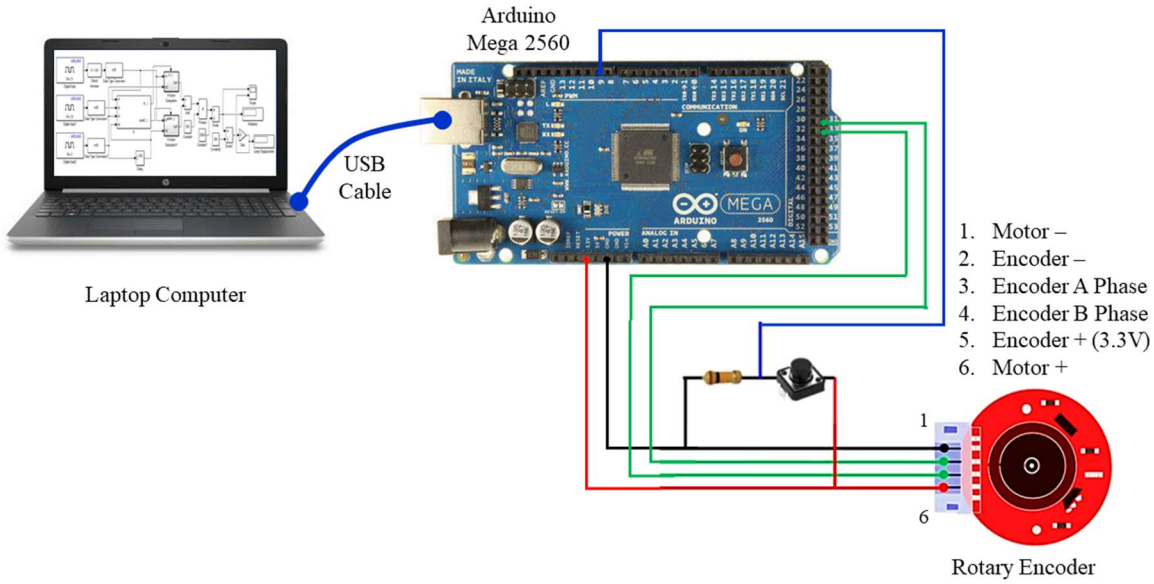

Figure. 5.16 Hall Effect rotary encoder connected with Arduino microcontroller

5.4.3 MATLAB/Simulink to read the encoder pulses

To read the pulses generated by the encoder through the microcontroller was done with the aid of MATLAB/Simulink program. A signal edge detection technique was used to count the pulses generated by the encoder. An edge of a signal is defined as the conversion of the signal from a high state to a low state or vice-versa. The three different types of signal edges depending upon the type of conversion are shown in figure 5.17.

- Rising edge: when the signal is converting its state from a low (0) to a high (1).
- Falling edge: when the signal is converting its state from a high (1) to a low (0).
- Either edge: when the signal is changing state, from low to high or from high to low.

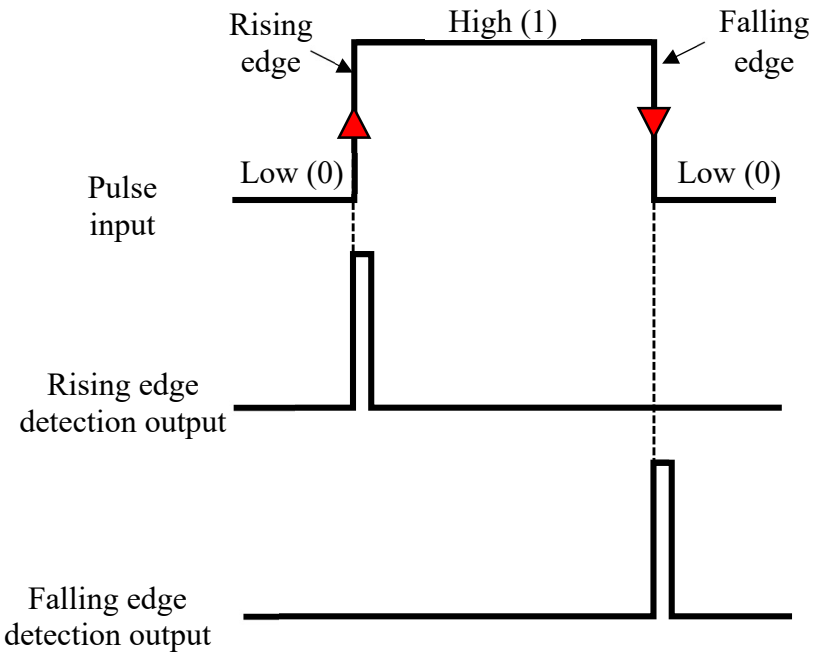

Figure 5.17 Square wave

In a square wave, the distance between the rising and falling edges is the pulse width of that square wave. From figure 5.15 it was observed that, during the clockwise rotation of the encoder, the output of signal-B is equal to zero at all the rising edges of signal-A. Similarly, for the anticlockwise rotation of the encoder, the output of signal-B is equal to one at all the rising edges of signal-A. Based on this logic the Simulink block diagram has been constructed to count the number of pulses of the encoder.

Figure 5.18 shows the Simulink block diagram was made with the Simulink support package for Arduino hardware. The digital input blocks were taken to read the output of the encoders which are connected to pin numbers 31 and 32 of the Arduino board and pin number 9 was used to reset the pulses. To detect the raised edge, a Detect Increase block was used to determines if the input is strictly greater than its previous value or not. If the input signal is greater than its previous value then the output is true (equal to 1) and if the input signal is less than or equal to its previous value then the output is false (equal to 0). To the detect increase block, a data type conversion block was used to convert the values into an integer. The ‘if statement block’ from the Simulink was used to determine the clockwise or anticlockwise rotation of the encoder shaft. The output was added and

multiplied with 360 to get the total number of pulses per revolution. The Hall Effect sensor will generate seven pulses per revolution of the encoder and the number of pulses generated for one revolution of the motor shaft is equal to 2660 because the gear ratio of the motor was 380:1. So, from this, the number of revolutions of the shaft can be observed but to calculate the linear displacement of the leadscrew which was attached to the shaft, the output number of revolutions was multiplied with the value six as the leadscrew will have a linear displacement of 6mm per revolution. Therefore the output will be the linear displace of the single actuator in millimeters. If the encoder shaft was rotating in the opposite direction then a negative value will be shown in the display. So, for the forward direction of the actuator moves the distance shown will be positive, and the backward direction will be negative. The same program was used for all the nine actuators to measure the displacements of forwarding and backward strokes.

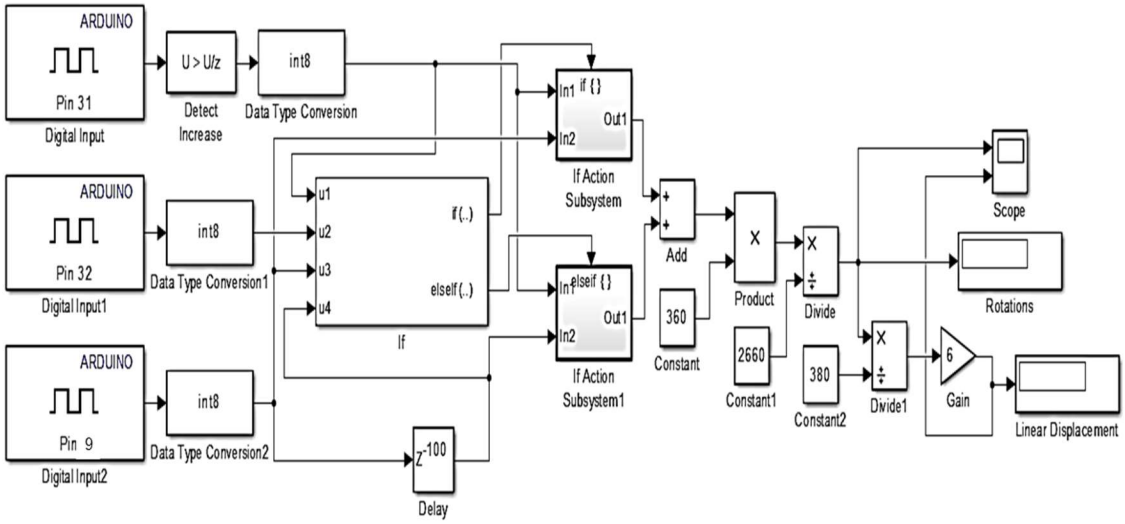

Figure 5.18 MATLAB/Simulink block diagram to measure the linear displacement of the actuator

5.5 Sensors and DAQ

5.5.1 Linear Position Sensor

A linear position transducer with restoring spring by Novotechnik, TR50 was used to measure the linear displacement of the actuator. The LVDT has three pins, the voltage input pin, the variable pin, and the ground pin. The variable pin on the middle varies the resistance with the ground pin then that voltage is going to come out when it's connected between 0 and 5 volts. The datasheet of the linear position transducer with all the specifications is attached in annex 2. The measurement of the linear position was made with the help of a NI USB-6008 data acquisition system. The data collected from the data card was plotted with the help of LABVIEW software.

Figure 5.19 Linear position transducers (Novotechnik, TR50)

5.5.2 Data Acquisition card

A DAQ is used to make measurements of physical phenomena and record them in some manner to analyze them. The USB-6008 is a multifunctional DAQ that offers analog I/O, digital I/O, and a 32-bit counter. The USB-6008 provides basic functionality for applications such as simple data logging, portable measurements, and academic lab experiments. The device features a lightweight mechanical enclosure and is bus-powered for easy portability. It is easy to connect sensors and signals to the USB-6008 with screw-terminal connectivity.

Figure 5.20 NI USB-6008 DAQ

5.5.3 Linear measurement of the HRA with sensor and DAQ

The basic data acquisition system using LabVIEW software and a USB-6008 hardware module was made to read the linear displacement from the LVDT which was connected to the end effector rod of the HRA. To acquire the voltage values from the DAQ, appropriate drivers need to be installed. LabVIEW then introduces the waveform data type which accumulates voltage values with time using loops and shift registers eventually writing that data to a file. Every voltage measurement is differential in nature, however, the negative terminal of the LVDT was connected to the ground. So, the positive terminal voltage with reference to the ground was measured.

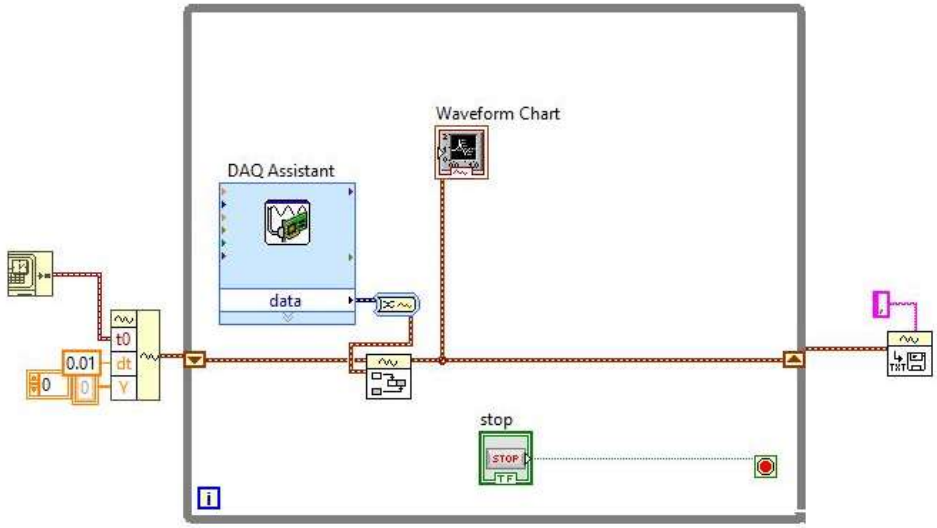

Figure 5.21 LABVIEW block diagram to read LVDT

The variable pin of the LVDT varies the resistance when the negative and positive terminals of it were connected to the ground and 5 volts pin of the USB-6008 NI module. And the variable pin of the LVDT was connected to an analog input port (Ai2) of the module. So, the voltage varies from 0 to 5 volts.

A DAQ assistant block was launched to create a new task, it is possible to edit the task of the DAQ at any time. The signal from the LVDT has to be measured continuously so, a while loop around the DAQ assistant was made in the LABVIEW. A control stop button was kept to stop the program which was running. A dynamic data type block was connected to the DAQ assistant to convert the dynamic data type into numeric Boolean, waveform, and array data type. From the dynamic data use a block called build waveform and connect that to the data out. A waveform is made up of three things, T0 which was the initial time when data collections start happening, DT which was the time step between samples that it took, and Y are the actual voltage values. So Y was an array of all the voltages that DAQ collected. By adding the waveform chart to the front panel which is going to plot the waveform.

5.6 Results and Discussion

This chapter has explained in detail the experimental setup used to collect experimental data. The components of all three main parts: the mechanical part; the electrical part and the data acquisition part have been discussed in detail. The present work is mainly focused on the fault tolerant displacement of the actuation system so, the results related to the displacement of the individual actuator and the HRA were provided.

Firstly the displacement of the single physical EMA was validated with the derived mathematical model. The physical EMA position was measured with the help of the rotary encoder which was attached at the back end of the shaft. The comparison of actual EMA position with the derived mathematical model was shown in the figure 5.22. The actual displacement of the actuator was following the same path as the model with an insignificant deviation. The maximum displacement of the mathematical model and the actual in the forward stroke is reaching up to 1.7cm.

The displacement of the HRA model with the actual are compared both under the open and closed loop circuit. Under open loop circuit, the displacement of the actual HRA

was very much deviated from the model because of the uncontrolled input signal. Because of this signals, the variations in the velocities/displacements of the actuators was occurred, but under the closed loop circuit, where the negative positional feedback signal was given to the actual HRA through a PI controller. The displacement plots under open loop was shown in Figures 5.23 and under closed loop was shown in figures 5.24.

The displacement plots of the actual HRA under healthy and faulty conditions are compared with the mathematical model plots as shown in the figure 5.25 and figure 5.26. It is difficult to introduce the motor faults in the physical model for testing so, only the mechanical lock-up fault and loose faults are introduced. The lock-up fault was introduced by making input of the particular actuator to zero so that the movement of the actuator was restricted. The loose fault of the actuator was introduced by ditching the motor shaft with the shaft coupling so that there was no applied force by that particular actuator. The results are observed with single lock-up fault and double lock-up faults and single loose fault and double loose fault independently. The combination of both faults simultaneously has not investigated in the present work.

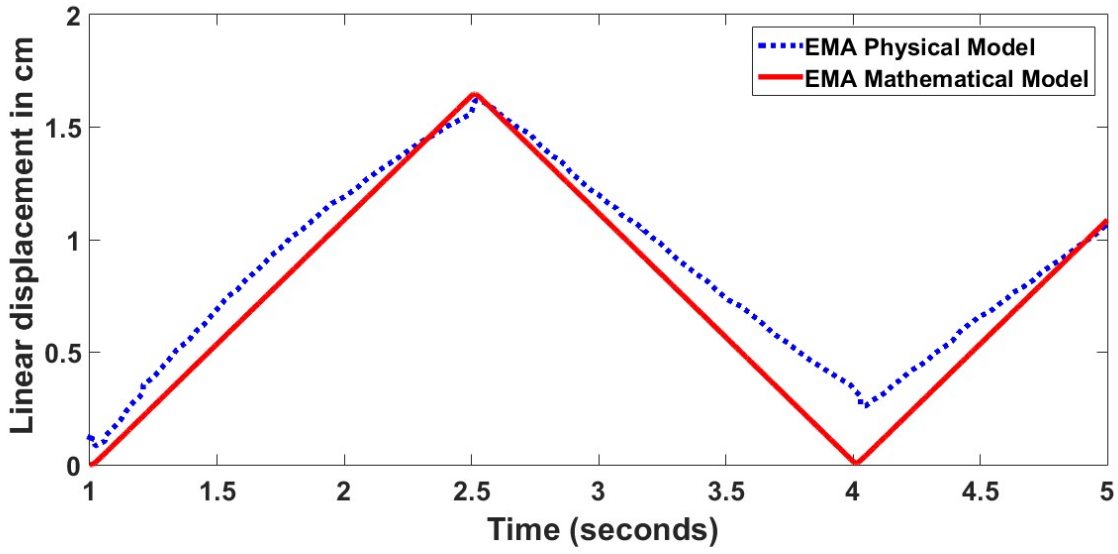

Figure 5.22 Linear displacement of single EMA physical model and mathematical model

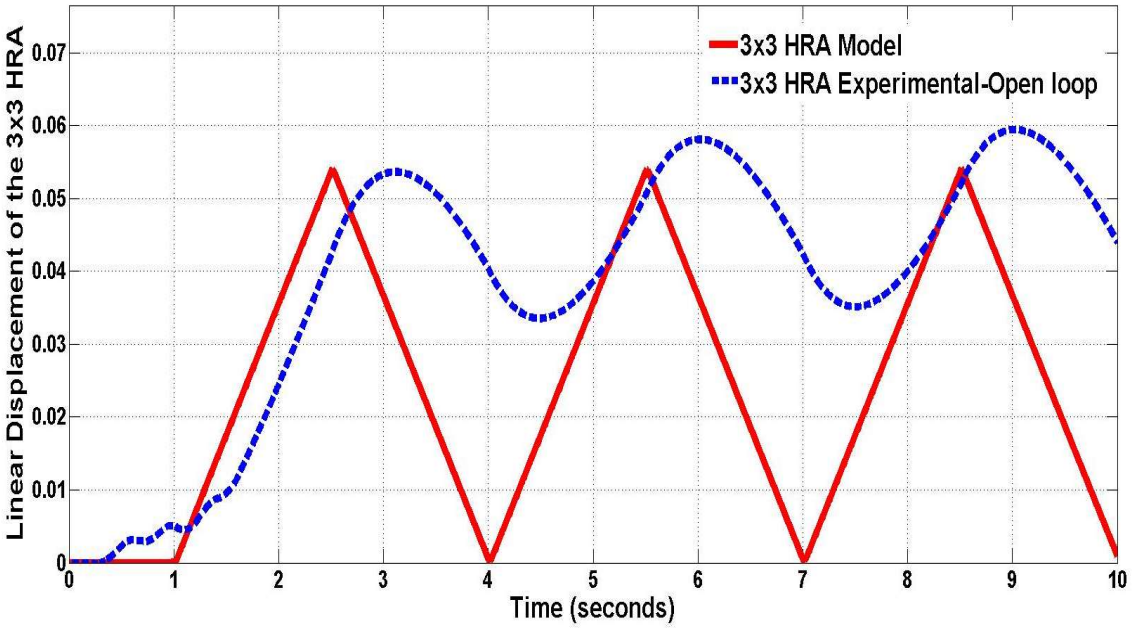

Figure 5.23 Linear displacement of 3×3 HRA mathematical model and physical model under open loop

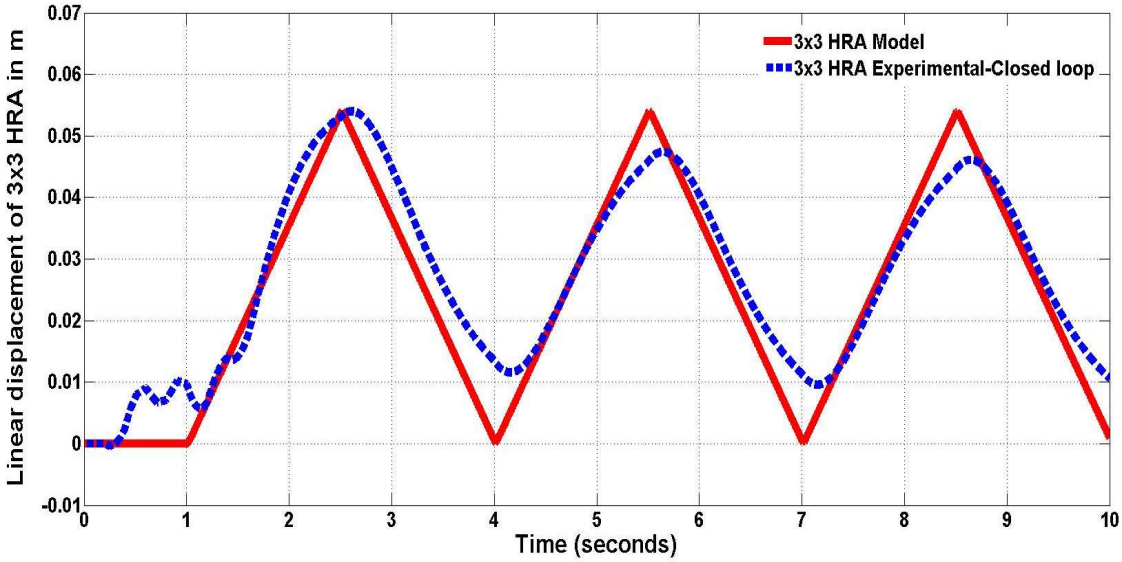

Figure 5.24 Linear displacement of 3×3 HRA mathematical model and physical model under closed loop

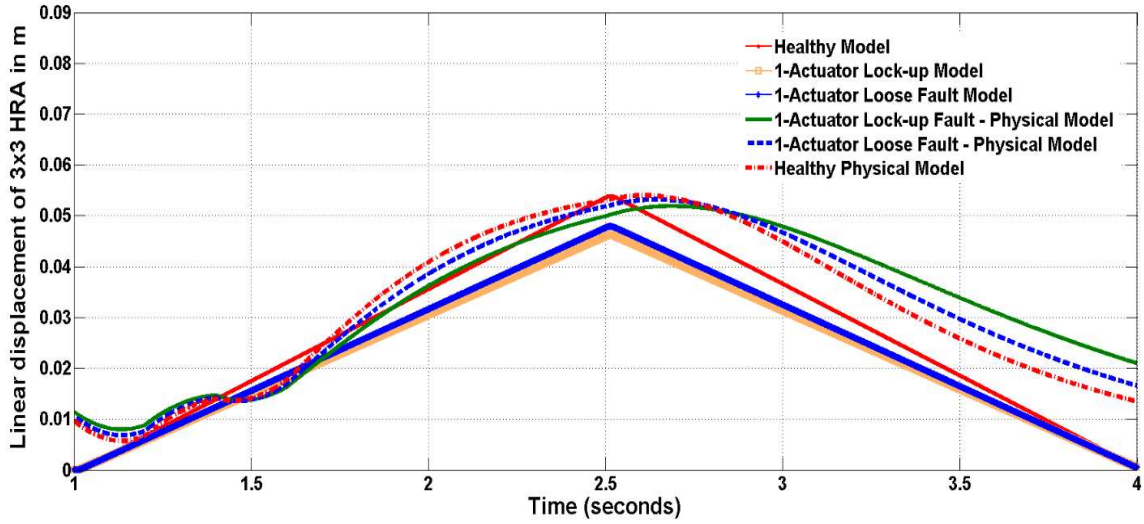

Figure 5.25 The linear position of the HRA under healthy and single faulty conditions compared with mathematical model faults

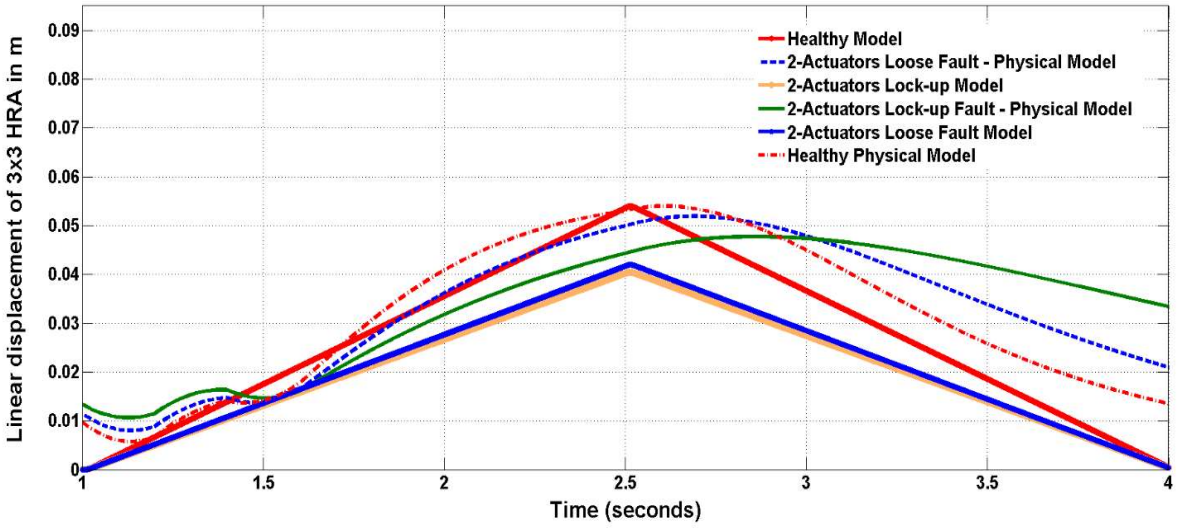

Figure 5.26 The linear position of the HRA under healthy and double faulty conditions compared with mathematical model faults

5.7 Conclusion

This chapter gives the specifications of all the mechanical components, and the details of all the electric components including sensors and DAQ used in the experimental setup of the HRA. The individual mechanical components are assembled to form a single EMA and all the nine individual actuators are assembled with the help of the SS rods,

aluminum sheet, and linear bearings to form the 3×3 HRA. The assembly was made in such a way that the arrangement of actuators is in a 3×3 series-in-parallel configuration. LVDT and rotary encoders are used to measure the linear displacement of the HRA and individual actuators respectively.

The derived mathematical model of the single EMA and the 3×3 HRA was validated with the physical model. The performance of 3×3 high redundancy actuation system was studied and it was able to achieve the positional fault tolerance up to a satisfactory level. Even after the failure of two actuation elements the actuation system is able to achieve the required displacement approximately instead of complete failure.

CHAPTER - 6

CONCLUSIONS AND SCOPE OF FUTURE WORK

6.1 Conclusions

In this thesis, research work related to a highly redundant and fault-tolerant actuator has been presented. The high redundancy actuation is an approach to achieve fault-tolerant actuation. This provides fault-tolerance by using a large number of small actuation elements which are assembled in matrix (parallel and series) arrangement to form a single intrinsic fault-tolerant actuator.

Firstly, a literature review on the previous works associated with the high redundancy actuator was done and based on that it was concluded that the high redundant actuation system based on electromechanical actuation elements could be expanded.

The reliability of HRA configurations was discussed and presented in chapter-3. The equations were derived and expanded for both series-in-parallel and parallel-in-series arrangements. The reliabilities of required travel and force capabilities of both the configurations were analyzed under element fault probability and it was observed that,

- The selection of the best suitable configuration has a significant influence on the reliability of HRA, even though the number of elements is the same in the same two-dimensional configuration.
- The force capability of parallel-in-series structure for low fault probabilities is superior by nearly a factor of two. So, for a particular application, if force is the major required consideration then the best HRA configuration was parallel-in-series configuration.
- The travel capability of series-in-parallel structure for low fault probabilities is superior by nearly a factor of two. So, for a particular application, if travel is the major required consideration then the best HRA configuration was series-in-parallel configuration.

By selecting the travel capability as the major requirement, the series-in-parallel arrangement was considered as the HRA configuration for further analysis. The first half of the chapter-4 presents the mathematical modelling of a single DDEMA and the multiple actuators with two elements in series and two elements in parallel. Then it was extended to a 3×3 HRA system. The second half of chapter-4 presents the 3D model of a single direct driven EMA and a 3×3 HRA with direct driven EMAs. Electric motor faults (Open circuit and short circuit faults) and mechanical faults (lock-up and loose faults) were modeled and introduced into the mathematical model and 3D model and by simulating using MATLAB/Simulink software. The following results were obtained,

- The series arrangement increases the travel capability and the parallel arrangement increases force capability above the capability of an individual element.
- In the presence of faults, there is no sudden failure of the actuator but a gradual decrease in the performance was observed and it can be concluded that the ability of the actuation system to tolerate the faults was improved.
- The pure series configuration of three actuation elements showed that the travel capability improved by three times (i.e. from 2.323 cm to 7.027 cm) and the pure parallel configuration of 3 actuation elements showed an increased force capability by almost three times (i.e. from 26.8 N to 80.39 N).
- The system with three actuators in a series configuration can tolerate the lock-up fault, open-circuit fault, and short-circuit/loose fault as long as the failure is limited to 2 actuation elements, the system remains to perform with graceful degradation.
- The force capability of pure series actuators under loose/short-circuits fault is nearly 18% less than the other types of faults. Although the pure parallel system was able to tolerate the loose/short-circuit fault with graceful degradation of 33.4%, it failed to perform with the other two faults.
- The 3×3 HRA performance was studied with a single lock-up fault, the reduction of displacement was found to be a maximum of 14.34% and minimum in the presence of loose/short-circuit fault (11.13%). The reduction of force was recorded maximum (12.18%) in the presence of a loose/short-circuit fault and minimum (10.95%) in the presence of a lock-up fault.

The experimental setup of the HRA was presented in chapter-5, where the fabricated HRA setup with nine actuation elements was given. Details of all the mechanical, electrical, and data acquisition of the HRA were provided. The obtained results are,

- The displacement performance of the experimental HRA has been validated with the simulation model.
- This HRA can achieve nearly 100% fault-tolerance even after the failure of two actuation elements of the system.

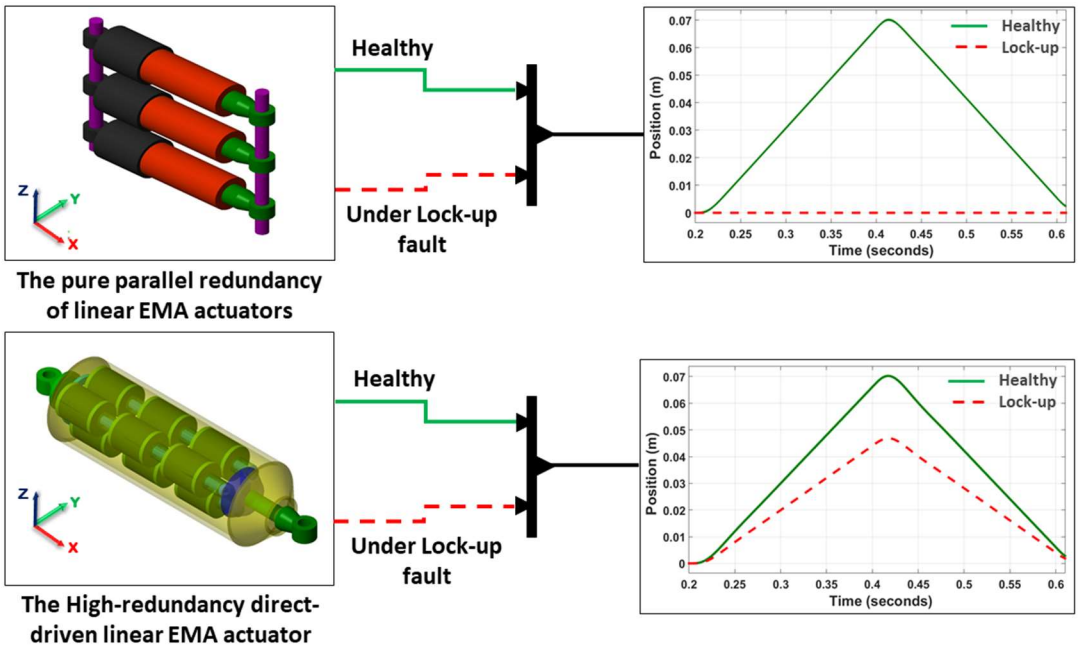

Figure 6.1 The general comparison between the parallel redundancy and HRA

6.2 Scope of Future Work

The research work on high redundancy actuator presented in this thesis has provided significant contribution but still, some more works are required to be done before the concept of HRA can be implemented in the real industry. The performance of the HRA under different possible combinations of faults must be studied. The fabricated experimental setup described within this thesis was meant for laboratory testing. So, to implement it for a particular application like an aircraft aileron it will be very big which can be implemented in a real industry. On the other hand, this HRA concept can be

implemented with micro-actuators which are based on piezoelectric actuators or micro-electromechanical systems (MEMS).

REFERENCES

[1] M. Venables, “Let intelligent robots take the strain [automobile industry],” Manufacturing Engineer, vol. 85, no. 2, pp. 34{35, April 2006.

[2] S. Jensen, “Flight test experience with an electromechanical actuator on the F-18 systems research aircraft,” Proceedings of Digital Avionics Systems Conference, vol. 1, no. 19, pp. 1-10, 2000.

[3] Bemment, Samuel D.Goodall, Roger M.Dixon, Roger Ward, Christopher P. “Improving the reliability and availability of railway track switching by analysing historical failure data and introducing functionally redundant subsystems”. Proceedings of the Institution of Mechanical Engineers, Part F: Journal of Rail and Rapid Transit, PP 1-18, 2017

[4] M. Sghairi, A. D. Bonneval, Y. Crouzet, J. Aubert, and P. Brot, Challenges in Building Fault-Tolerant Flight Control System for a Civil Aircraft," International Journal of Computer Science, IAENG, vol. 35, no. 4, pp. 1-5, 2008.

[5] R. J. Patton, \Fault-tolerant control system : The 1997 situation,"SAFE-PROCESS '97, IFAC Symposium on fault detection, supervision and safety, pp. 1033-1054, 1997.

[6] S. Wang, M. Tomovic, and H. Liu, Commercial Aircraft Hydraulics Systems. Elsevier Inc., 2016.

[7] S. Kwon, J.-M. Cheon, J. Lee, C.-K. Kim, and S.-J. Kim, A design and implementation of a fault-tolerant rod control system for nuclear power plants," in Industrial Electronics, 2006 IEEE International Symposium on, vol. 3, July 2006, pp. 1933-1936.

[8] Andrighetto, P. L., Valdiero, A. C., and Carlotto, L. (2006). Study of friction behavior in industrial pneumatic actuators, ABCM Symposium series in Mechatronics, 2, pp. 369- 378.

[9] Hesselroth, T., Sarker, K., Van der Smagt, et al., (1994). Neural network control of a pneumatic robot arm. IEEE International Conference on Systems, Man, and Cybernetics, 24, (1) pp. 28-38.

[10] G.Qiao, G.Liu, Z.Shi et al. A review of electromechanical actuators for More/All Electric aircraft systems, Proceedings of the Institution of Mechanical Engineers, Part C: Journal of Mechanical Engineering Science, Issue 127, Year 2017.

[11] J.Li, Z.Yu, Y.Huang et al. A review of electromechanical actuation system for more electric aircraft. AUS 2016 - 2016 IEEE/CSAA International Conference on Aircraft Utility Systems, pp 490-497, 2016.

[12] D. Briere, C. Favre, and P. Traverse, “A family of fault tolerant systems: electrical flight controls from airbus a320/a330/a340 to future military transport aircraft,” Microprocess Microsyst, vol. 19, no. 2, pp. 75-82, 1995.

[13] H. Antong, R. Dixon, C. Ward, Modelling and building of experimental rig for high redundancy actuator, Int. Conf. Control. 2014 (2014) 384–388.

[14] X. Du, R. Dixon, R.M. Goodall, A.C. Zolotas, Mechatronics modelling and control of a high redundancy actuator, Mechatronics 20 (2010) 102–112.

[15] R. Dixon, T. Steffen, J. Davies, R.M. Goodall, A.C. Zolotas, J. Pearson, X. Du, HRA intrinsically fault tolerant actuation through high redundancy, IFAC Proc. (2009) 1216–1221.

[16] T. Steffen, F.Schiller, M.Blum et al. Analysing the reliability of actuation elements in series and parallel configurations for high-redundancy actuation. International Journal of Systems Science, Volume 7721, Issue April 2013, pp 1-18, 2012.
[17] Blanke, M., Staroswiecki, M., and Wu, N.E. (2001), 'Concepts and Methods in Fault-tolerant Control', in Proceedings of the American Control Conference '01, Arlington, pp. 2606–2620.
[18] Antong, Hasmawati, Dixon, Roger, Ward, Christopher P, High Redundancy Actuator with 12 Elements: Open- and Closed-loop Model Validation, FAC-Papers OnLine, volume 49, issue 21, pp 254-259, 2016.
[19] R.J. Patton, Fault detection and diagnosis in aerospace systems using analytical redundancy, Comput. Control Eng. 8 (1991) 127–136.
[20] Davies, Jessica, Steffen, Thomas et al., Modelling of high redundancy actuation utilising multiple moving coil actuators, IFAC Proceedings Volumes (IFAC-PapersOnline), Volume 17, Issue I part 1, pp 3228-3233, 2008.
[21] M. M. Mahmoud, J. Jiang, and Y. Zhang, Active Fault Tolerant Control Systems: Stochastic Analysis and Synthesis. Springer-Verlag, 2003.
[22] M. S. Shaker, Doctoral Thesis: Active Fault-Tolerant Control of Non-linear System with Wind Turbine Application. University of Hull, 2012.
[23] L. Jiang, Doctoral Thesis: Sensor Fault Detection and Isolation using System Dynamics Identification Techniques. The University of Michigan, 2011.
[24] S. Reece, S. Roberts, C. Claxton, and D. Nicholson, Multi-sensor fault recovery in the presence of known and unknown fault types," in Information Fusion, 2009. FUSION '09. 12th International Conference on, 2009, pp. 1695-1703.
[25] G. Heredia, A. Ollero, M. Bejar, and R. Mahtani, Sensor and actuator fault detection in small autonomous helicopters," Mechatronics, vol. 18, pp. 90-99, 2008.
[26] T. Steen, F. Schiller, M. Blum, and R. Dixon, Increasing the reliability of high redundancy actuators by using elements in series and parallel," SAFECOMP 2009, pp. 270-282, 2009.
[27] T. Steen, R. Dixon, R. Goodall, and A. Zolotas, Requirements Analysis for High Redundancy Actuator: Technical Report. Loughborough University, 2007.
[28] H. Antong, R. Dixon, C. Ward, Modelling and building of experimental rig for high redundancy actuator, Int. Conf. Control. 2014 (2014) 384–388,
[29] R. J. Patton, Fault detection and diagnosis in aerospace systems using analytical redundancy," Computing Control Engineering Journal, vol. 2, no. 3, pp. 127{136, 1991.
[30] A. Avizienis, Fault-tolerance: The survival attribute of digital systems,"Proceedings of the IEEE, vol. 66, no. 10, pp. 1109{1125, Oct 1978.
[31] M. Blanke, M. Staroswiecki, and N. E. Wu, Concepts and methods in fault-tolerant control," Proceedings of the American Control Conference, 2001.
[32] A. Singh and S. Murugesan, Fault-tolerant sytems," computer, vol. 23, no. 7, pp. 15-17, July 1990.
[33] R. Pillay, S. Chandran, and S. Punnekkat, Optimizing resources in real-time scheduling for fault tolerant processors," in Parallel Distributed and Grid Computing (PDGC), 2010 1st International Conference on, Oct 2010, pp. 101-106.

[34] I. Koren and C. Krishna, Fault Tolerant Systems. Morgan Kaumann Publications, 2007.
[35] T. Steen, F. Schiller, M. Blum, and R. Dixon, Increasing the reliability of high redundancy actuators by using elements in series and parallel," SAFECOMP 2009, pp. 270-282, 2009.
[36] M. Landau, Redundancy, rationality, and the problem of duplication and overlap," Public Administration Review, vol. 29, no. 4, pp. 346-358, 1969.
[37] R. Dixon, T. Steffen, J. Davies, R.M. Goodall, A.C. Zolotas, J. Pearson, X. Du, HRA –intrinsically fault tolerant actuation through high redundancy, IFAC Proc. (2009) 1216–1221.
[38] J. Downer, When Failure is an Option: Redundancy, reliability and regulation in complex technical systems. Center for Analysis of Risk and Regulations, 2009.
[39] T. Way, Redundancy in aviation," http://www.wayforward.net/ redundancy.html, 2008, accessed: 15/05/2015.
[40] \Redundant power supply," http://www.computerhope.com/jargon/r/redunpow.htm, accessed: 15/05/2015.
[41] R. J. Patton, Fault-tolerant control system : The 1997 situation,"
[42] SAFE-PROCESS '97, IFAC Symposium on fault detection, supervision and safety, pp. 1033-1054, 1997.
[43] D. R. Ryder, Redundant Actuator Development Study: Contractor Report. Boeing Commercial Airplane Company, 1973.
[44] J. Davies, Doctoral Thesis: Modelling, Control and Monitoring of High Redundancy Actuation. Loughborough University, 2009.
[45] E. Balaban, P. Bansal, P. Stoelting, A. Saxena, K. Goebel, and S. Curran, \A diagnostic approach for electro-mechanical actuators in aerospace systems," in Aerospace conference, 2009 IEEE, 2009, pp.1-13.
[46] J. Davies, T. Steffen, R. Dixon, R.M. Goodall, A.A. Zolotas, J.Pearson, Modeling of high redundancy actuation utilising Multiple moving coil actuators, IFAC Proceedings volume 17 (2008) 3228-3233.
[47] J. Davies, T. Steen, R. Dixon, and R. M. Goodall, \Modelling of high redundancy actuator utilising multiple moving coil actuators," 17th IFAC World Congress, Korea, pp. 3228-3233, 2008.
[48] T. Steen, J. Davies, R. Dixon, R. Goodall, and A. Zolotas, Using a series of moving coils as a high redundancy actuator," in Advanced intelligent mechatronics, 2007 IEEE/ASME international conference on, 2007, pp. 1-6.
[49] X. Du, R. Dixon, R.M. Goodall, A.C. Zolotas, Mechatronics modelling and control of a high redundancy actuator, Mechatronics 20 (2010) 102–112,
[50] R. Dixon, T. Steffen, J. Davies, R.M. Goodall, A.C. Zolotas, J. Pearson, X. Du, HRA intrinsically fault tolerant actuation through high redundancy, IFAC Proc. (2009) 1216–1221,
[51] J. Davies, H. Tsunashima, R.M. Goodall, R. Dixon, T. Steffen, Fault detection in High Redundancy Actuation using an interacting multiple-model approach, IFAC Proc. (2009) 1228–1233,
[52] J. Davies, T. Steffen, R. Dixon, R. Goodall, A. Zolotas, Active versus passive fault tolerant control of a High Redundancy Actuator, Eur. Control Conf. (2009) 3671–3676,

[53] David Arriola, Frank Thielecke, Model-based design and experimental verification of a monitoring concept for an active-active electromechanical aileron actuation system, Mechanical Systems and Signal Processing 94 (2017) 322–345
[54] Blanke, M., and Thomsen, J.S. (2006), 'Electrical Steering of Vehicles – Fault-tolerant Analysis and Design', Microelectronics and Reliability, 46, 1421–1432.
[55] Ribeiro, R.L.A., Jacobina, C.B., da Silva, E.R.C., and Lima, A.M.N. (2004), 'Fault-tolerant Voltage-fed PWM Inverter AC Motor Drive Systems', IEEE Transactions on Industrial Electronics, 51, 439–446.
[56] James Li, Reliability Comparative Evaluation of Active Redundancy vs. Standby Redundancy. International Journal of Mathematical, Engineering and Management Sciences Vol. 1, No. 3, 122–129, 2016, ISSN: 2455-7749
[57] Blanke, M., Staroswiecki, M., and Wu, N.E. (2001), 'Concepts and Methods in Fault-tolerant Control', in Proceedings of the American Control Conference '01, Arlington, pp. 2606–2620.
[58] Jakub Podivinsky, Ondrej Cekan, Marcela Simkova, Zdenek Kotasek, The evaluation platform for testing fault-tolerance methodologies in electro-mechanical applications. Microprocessors and Microsystems 39 (2015) 1215–1230
[59] George Vachtsevanos Frank Lewis Michael Roemer. Intelligent Fault Diagnosis And Prognosis For Engineering Systems, JOHN WILEY & SONS, INC, 2006.
[60] Blanke, M., Kinnaert, M., Lunze, J., and Staroswiecki, M.(2006), Diagnosis and Fault tolerant Control, Berlin: Springer.
[61] Blanke, M., Staroswiecki, M., and Wu, N.E. (2001), 'Concepts and Methods in Fault tolerant Control', in Proceedings of the American Control Conference '01, Arlington, pp. 2606–2620.
[62] Blanke, M., and Thomsen, J.S. (2006), 'Electrical Steering of Vehicles – Fault-tolerant Analysis and Design', Microelectronics and Reliability, 46, 1421–1432.
[63] Du, X., Dixon, R., Goodall, R.M., and Zolotas, A.C. (2006), 'Assessment of Strategies for Control of High Redundancy Actuators', Proceedings of the ACTUATOR 2006, Bremen, June.
[64] Du, X., Dixon, R., Goodall, R.M., and Zolotas, A.C. (2007), 'LQG Control for a High Redundancy Actuator', in Proceedings of the 2007 IEEE/ASME International Conference on Advanced Intelligent Mechatronics, Zurich, September.
[65] Frank, P.M. (1990), 'Fault Diagnosis in Dynamic Systems using Analytical and Knowledge-based Redundancy – A Survey and Some New Results', Automatica, 26, 459–474.
[66] Heidergott, B., Olsder, G.J., and van der Woude, J. (2005), Max Plus at Work: Modeling and Analysis of Synchronized Applications, Princeton: Princeton University Press.
[67] Jenab, K., and Dhillon, B.S. (2006), 'Assessment of Reversible Multi-state k-out-of-n: G/F/Load-Sharing Systems with Flow-graph Models', Reliability Engineering & System Safety, 91, 765–771.
[68] Jiang, B., Yang, H., and Shi, P. (2010), 'Switching Fault Tolerant Control Design via Global Dissipativity', International Journal of Systems Science, 41, 1003–1012.
[69] Oppenheimer, M.W., and Doman, D.B. (June, 2006), 'Control Allocation for Overactuated Systems', in Proceedings of the 14th Mediteranean Conference on Control and Automation, Ancona.

[70] Pham, H. (2003), Handbook of Reliability Engineering, New York: Springer.
[71] Ribeiro, R.L.A., Jacobina, C.B., da Silva, E.R.C., and Lima, A.M.N. (2004), 'Fault-tolerant Voltage-fed PWM Inverter AC Motor Drive Systems', IEEE Transactions on Industrial Electronics, 51, 439–446.
[72] Shammas, N.Y.A., Withanage, R., and Chamund, D. (2006), 'Review of Series and Parallel Connection of IGBTs', IEE Proceedings Circuits, Devices and Systems, 153, 34–39.
[73] Steffen, T. (2005), Control Reconfiguration of Dynamical Systems: Linear Approaches and Structural Tests, Lecture Notes in Control and Information Sciences, Berlin: Springer.
[74] Steffen, T., Davies, J., Dixon, R., Goodall, R.M., Pearson, J., and Zolotas, A.C. (2008), 'Failure Modes and Probabilities of a High Redundancy Actuator', in Proceedings of the 17th IFAC World Congress, Seoul, July, pp. 3234–3239.
[75] Steffen, T., Davies, J., Dixon, R., Goodall, R.M., and Zolotas, A.C. (2007), 'Using a Series of Moving Coils as a High Redundancy Actuator', in Proceedings of the 2007 IEEE/ASME International Conference on Advanced Intelligent Mechatronics, September, Zurich.
[76] Steffen, T., Schiller, F., Blum, M., and Dixon, R. (2009), 'Increasing the Reliability of High Redundancy Actuators by Using Elements in Series and Parallel', in Proceedings of the The 28th International Conference on Computer Safety, Reliability and Security SAFECOMP 2009, eds.
[77] B. Buth,G. Rabe, and T. Seyfarth, Hamburg: Springer, pp. 270–282.
[78] Thomas Steffen, Frank Schiller, Michael Blum et al. Increasing Reliability by Means of Efficient Configurations for High Redundancy Actuators. Proceedings of the 7th IFAC Symposium on Fault Detection, Supervision and Safety of Technical Processes Barcelona, Spain, June 30 - July 3, 2009
[79] Marco Muenchhof, Mark Beck, Rolf Isermann Technische, Fault-tolerant actuators and drives Structures, fault detection principles and applications. Annual Reviews in Control 33 (2009) 136–148.
[80] G. J. J. Ducard, Fault-tolerant Flight Control and Guidance Systems. Springer-Verlag, 2009.
[81] J. D. Schierman, D. G. Ward, J. R. Hull, and N. Gandhi, \Integrated adaptive guidance and control for re-entry vehicles with
ight-test results," AIAA Journal of Guidance, Control and Dynamics, vol. 27, no. 6, pp. 975{988, Nov 2004.
[82] G. Ducard, Doctoral Thesis: Fault-Tolerant Control and Guidance Systems for a Small Unmanned Aerial Vehicle. Swiss Federal Institute of Technology, 2007.
[83] D. Enns and T. Keviczky, Dynamic inversion based fight control for autonomous rmax helicopter," in American Control Conference, 2006, June 2006, pp. 3916{3923.
[84] R. Adams, J. M. Bungton, A. G. Sparks, and S. S. Banda, Robus Multivariable Floght Control. Springer-Verlag, 1994.
[85] J. F. Magni, S. Bennani, and J. Terlouw, Robust Flight Control: A Design Challenge. Springer-Verlag, 1997.
[86] S. I. AlSwailem, Doctoral Thesis: Application of Robust Control In Unmanned Vehicle Flight Control System Design. Craneld University, 2004.

[87] K. A. Wise, J. S. Brinker, A. J. Calise, D. F. Enns, M. R. Elgersma, and P. Voulgaris, Direct adaptive reconfigurable fight control for a tailless advanced fighter aircraft," International Journal of Robust and Nonlinear Control, vol. 9, pp. 999{1012, 1999.
[88] J. S. Brinker and K. A. Wise, Flight testing of reconfigurable control law on the x-36 tailless aircraft," AIAA Journal of Guidance, Control and Dynamics, vol. 24, no. 5, pp. 903-909, 2001.
[89] J. Buffington, P. Chandler, and M. Pachter, On-line system identification for aircraft with distributed control effectors," International Journal of Robust and Nonlinear Control, vol. 9, pp. 1033-1049, 1999.
[90] P. L. Fontenrose and C. E. H. Jr., Development and flight testing of quantitative feedback theory pitch rate stability augmentation system," AIAA Journal of Guidance, Control and Dynamics, vol. 19, no. 5, pp. 1109-1115, 1996.
[91] S. Rasmussen and C. H. Houpis, Development and flight testing of quantitative feedback theory pitch rate stability augmentation system," International Journal of Robust and Nonlinear Control, vol. 7, pp. 629-642, 1997.
[92] S. Bennani, R. van der Sluis, G. Schram, and J. A. Mulder, \Control law reconfiguration using robust linear parameter varying control," pp. 977, 1999.
[93] G. Papageorgiou and R. A. Hyde, Analysing the stability of ndi-based fliight controllers with lpv methods," AIAA Guidance, Navigation and Control Conference and Exhibit, pp. 1{, 2001.
[94] M. E. Campbell, J. W. Lee, and E. Scholte, Simulation and flight test of autonomous aircraft estimation, planning, and control algorithms," AIAA Journal of Guidance, Control and Dynamics, vol. 30, no. 6, pp. 1597-1609, 2007.
[95] M. L. Steinberg and A. B. Page, Nonlinear adaptive flight control with generic algorithm design optimization," International Journal of Robust and Nonlinear Control, vol. 9, pp. 1097-1115, 1999.
[96] S. Singh, M. Steinberg, and A. Page, Nonlinear adaptive and sliding mode flight path control of f/a-18 model," IEEE Transaction on Aerospace and Electronic Systems, vol. 39, no. 4, pp. 1250-1262, Oct 2003.
[97] H. Alwi and C. Edwards, Fault tolerant control of a civil aircraft using a sliding mode based scheme," in Proceedings of IEEE Control and Decision Conference, and European Control Conference, Dec 2005, pp. 1011-1016.
[98] M. Corradini, G. Orlando, and G. Parlangeli, A fault tolerant sliding mode controller for accommodating actuator failures." in Proceedings of IEEE Control and Decision Conference, and European Control Conference, Dec 2005, pp. 3091-3096.
[99] G. Schram, G. Copinga, P. Bruijn, and H. Verbruggen, \Failuretolerant control of aircraft: a fuzzy logic approach," in Proceedings of the IEEE American Control of Aircraft, vol. 4, Jun 1998, pp. 2281-2285.
[100] Y. Zhang and J. Jiang, Integrated design of reconfigurable fault tolerant control systems," in AIAA Journal of Guidance, Control and Dynamics, vol. 24, no. 1, 2000, pp. 133-136.
[101] Y. M. Zhang and J. Jiang, Active fault-tolerant control system against partial actuator failure," in IEEE Proceedings in Control Theory Application, 2001, pp. 95-104.

Appendix A

1. Outline drawing of the geared DC motor used in the experimental setup

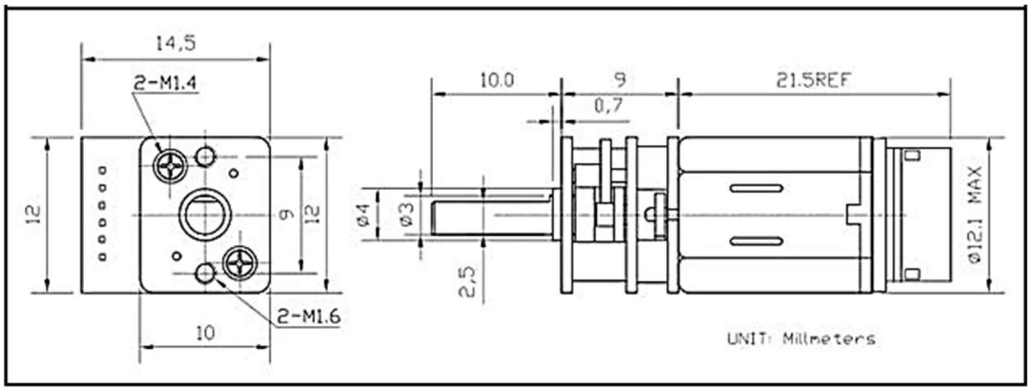

2. Pin configuration and functions of the DC motor Driver (L293D)

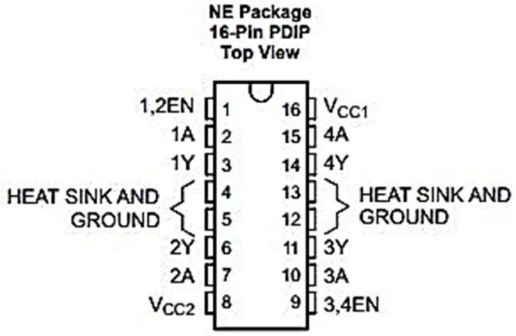

Pin Functions

PIN		TYPE	DESCRIPTION
NAME	NO.		
1,2EN	1	I	Enable driver channels 1 and 2 (active high input)
<1:4>A	2, 7, 10, 15	I	Driver inputs, noninverting
<1:4>Y	3, 6, 11, 14	O	Driver outputs
3,4EN	9	I	Enable driver channels 3 and 4 (active high input)
GROUND	4, 5, 12, 13	—	Device ground and heat sink pin. Connect to printed-circuit-board ground plane with multiple solid vias
V_{CC1}	16	—	5-V supply for internal logic translation
V_{CC2}	8	—	Power VCC for drivers 4.5 V to 36 V